Interaction between two bacteriophytochromes and their signal transduction in *Agrobacterium fabrum*

Zur Erlangung des akademischen Grades eines

DOKTORS DER NATURWISSENSCHAFTEN

(Dr. rer. nat.)

von der KIT-Fakultät für Chemie und Biowissenschaften

des Karlsruher Instituts für Technologie (KIT)

genehmigte

DISSERTATION

von

Peng Xue

aus

Anhui, China

Dekan: Prof. Dr. Reinhard Fischer

Referent: Prof. Dr. Tilman Lamparter

Korreferent: Prof. Dr. Reinhard Fischer

Tag der mündlichen Prüfung: 22.07.2019

Die vorliegende Dissertation wurde am Botanischen Institut des Karlsruhe Instituts für Technologie (KIT), Lehrstuhl 1 für Molekulare Zellbiologie, im Zeitraum von September 2015 bis Juli 2019 angefertigt.

Hiermit erkläre ich, dass ich die vorliegende Dissertation, abgesehen von der Benutzung der angegebenen Hilfsmittel, selbständig verfasst habe.

Alle Stellen, die gemäß Wortlaut oder Inhalt aus anderen Arbeiten entnommen sind, wurden durch Angabe der Quelle als Entlehnungen kenntlich gemacht.

Diese Dissertation liegt in gleicher oder ähnlicher Form keiner anderenPrüfungsbehörde vor.

Zudem erkläre ich, dass ich mich beim Anfertigen dieser Arbeit an die Regeln zur Sicherung guter wissenschaftlicher Praxis des KIT gehalten habe, einschließlich der Abgabe und Archivierung der Primärdaten, und dass die elektronische Version mit der schriftlichen übereinstimmt.

Karlsruhe, im Juli 2019

Peng Xue

Publications

Ausdieser Arbeit sind folgende Publikationen entstanden:

Xue, P., Bai Y., Rottwinkel G., Averbukh E., Ma Y., Roeder T., Scheerer, P., Krauß, N., and Lamparter, T. (2019). Phytochrome mediated responses in *Agrobacterium fabrum*: growth, swimming, plant infection and interbacterial competition. (In preparation).

Xue, P., El kurdi, A., Kohler, A., Ma, H., Kaeser, G., Ali, A., Fischer, R., Krauß, N., and Lamparter, T. (2019). Evidence for weak interaction between two phytochromes Agp1 and Agp2 from *Agrobacterium fabrum*. *FEBS letters*. **593**, 926-941.

Weitere Publikation, die nicht direkt mit dem Thema dieser Arbeit verknüpft sind:

Xue, P., and Wen, B. (2018). Desiccation tolerance of intermediate pomelo (*Citrus maxima* 'Mansailong') seeds following rapid and slow drying. *Seed Science and Technology* **46**, 511-519.

Ma, H., Zhang, F., Ignatz, E., Suehnel, M., Xue, P., Scheerer, P., Essen, L.O., Krauß, N., and Lamparter, T. (2017). Divalent cations increase DNA repair activities of bacterial (6-4) photolyases. *Photochemistry and Photobiology* **93**, 323-330.

Abbreviations

Agp1	*Agrobacterium fabrum* phytochrome 1
Agp2	*Agrobacterium fabrum* phytochrome 2
BV	biliverdin
CFU	colony forming units
D	darkness
DTT	dithiothreitol
EDTA	ethylenediaminetetraacetic acid
FP	forward primer
GUS	β-glucuronidase
HK	histidine kinases
IPTG	isopropyl- β-D-1-thiogalaktopyranosid
Kan	kanamycin
L	white light
LC	liquid chromatography
M	mutant
MS	mass spectrum
MUG	4-Methylumbelliferyl-β-D-glucuronide hydrate
NDPK2	nucleotide diphosphate kinase 2
OUT	operational taxonomic unit
PAPP5	phytochrome-associated protein phosphatase 5
PCM	photosensory core module
PDB	protein data bank
PIFs	phytochrome-interacting factors
PKS1	phytochrome kinase substrate 1
Pr	phytochrome red absorbing
Pfr	phytochrome far-red absorbing
R	relaxase
RP	reverse primer

SEC	size exclusion chromatography
TCEP	tris (2-carboxyethyl) phosphine
TEAB	triethylammonium bicarbonate
T4CP	type IV coupling protein
T4SS	type IV secretion system
T6SS	type VI secretion system
TMT	tandem mass tags
UPLC	ultra high-Performance liquid chromatography
VeA	velvet A
WT	wild type
X-Gluc	5-bromo-4-chloro-3-indolyl glucuronide

Contents

Zusammenfassung

Agrobacterium fabrum ist ein nicht photosynthetisch aktives, gramnegatives, stäbchenförmiges Bodenbakterium welches die Bildung von Wurzelhalsgallentumoren in mindestens 140 Arten von Dikotyledonen und Gymnospermen auslösen kann. Die Tumorbildung wird durch den Transfer der T-DNA, einem Bereich auf dem Ti-plasmid, in das Pflanzengenom initiiert. Für diesen Transfer von DNA wird das sogenannte Typ-IV-Sekretionssystem verwendet.

Frühere Ergebnisse unserer Gruppe zeigten, dass weißes Licht die Infektion des Stamms der Gurkenpflanzen (*Cucumis sativus*) mit *A. fabrum* unterdrückt. Lichtwahrnehmung wird über Photorezeptor-Proteine wie z.B. Phytochrome ermöglicht. Von diesen Rotlichtrezeptoren gibt es zwei in *Agrobacterium fabrum*, genannt Agp1 und Agp2. Auch die Konjugation, ein ähnlicher Prozess bei dem einzelsträngige Plasmid-DNA an benachbarte Bakterien weitergegeben wird, sowie auch die Bewegung von *A. fabrum* zeigen eine Phytochrom-abhängige Regulation. Neben dem Typ-IV-Sekretionssystem besitzt *A. fabrum* auch noch das Typ-VI-Sekretionssystem, welches für die interbakterielle Kompetition nötig ist. Das T6SS dient hierbei der Übertragung von toxischen Proteinen an benachbarte Bakterien.

In dieser Arbeit wurden Wildtyp- und Phytochrom-Mutanten Stämme von *A. fabrum* genutzt, um die Funktion der beiden Phytochrome näher zu bestimmen. Es wurde herausgefunden, dass sowohl die Mutanten ohne Phytochrom, als auch die Mutanten mit nur einem Phytochrom schneller wachsen als der Wildtyp. Die gleichen Stämme wurden auch dafür verwendet, den Einfluss von Phytochrom auf die Infektion der Stämme und Blätter von *Nicotiana Benthamiana* in Dunkelheit und unter kontinuierlichem Rotlicht bei Raumtemperatur zu untersuchen. Die Phytochrom-Doppelmutante zeigte einen negativen Einfluss auf die Infektion. Zudem konnte ein Agp1 inhibierender, sowie ein Agp2 fördernder Effekt von Rotlicht gefunden werden.

Um herauszufinden, ob es eine Interaktion zwischen den Phytochromen Agp1 und Agp2 gibt, wurden verschiedene Experimente, darunter

Größenausschlusschromatographie, Photokonversion, Dunkelreversion, Autophosphorylierung und Messungen bezüglich der Chromophorassemblierungskinetik, durchgeführt. In allen Ansätzen zeigten die von den Mixturen der beiden Phytochrome erhaltenen Daten Unterschiede gegenüber den unter der Annahme einer fehlenden gegenseitigen Beeinflussung der beiden Phytochrome erwarteten Einzelmessungen und deuten dadurch darauf hin, dass es eine direkte Interaktion *in vitro* gibt. Diese Interaktion legt ein *in vivo* Zusammenwirken der beiden Phytochrome nahe.

Die Quantifizierung der Expressionslevel des Proteoms in WT *A. fabrum* und der Phytochrom-Doppelmutante zeigt, dass bei Anwesenheit von Phytochrom die Expression des für die Konjugation notwendigen Proteins traA (Atu5111) begünstigt wird. Zusätzlich konnten Einflüsse auf das an der Chemotaxis beteiligte Protein mcpC (Atu0872), das Flagellenprotein motC (Atu0570) und des Pilusprotein (Atu0220) nachgewiesen werden. Zudem wurden Effekte auf das Hämolysin-coregulierte Protein (Atu4345) und das Toxin Atu4347 des T6SS beobachtet. Es wurden Kompetitionsexperimente mit Wildtyp *A. fabrum* bzw. mit der Phytochrome-Doppelmutante durchgeführt, indem sie mit Bodenbakterien inokuliert, die DNA extrahiert und anschließend die hypervariable Region V2 der 16S rRNA analysiert wurde, um die Zusammensetzung der Bakterienmixtur herauszufinden. Zusammengefasst legen die Ergebnisse der Proteomuntersuchung und der Kompetitionsexperimente nahe, dass das Vorhandensein von Phytochromen die interbakterielle Konkurrenzfähigkeit verbessert und dadurch die Überlebensrate von *A. fabrum* erhöht.

Summary

Agrobacterium fabrum is a non-photosynthetic, gram-negative, rod-shaped soil bacterium that causes the formation of tumours known as the crown gall disease in at least 140 species of dicotyledons and gymnosperms. The tumour formation is initiated by the transfer of the so-called T-DNA of the Ti plasmid from bacteria into the genome of plants. For this transfer of DNA the Type IV secretion system (T4SS) is utilized.

Previous results from our group showed that white light suppresses the infection of cucumber (*Cucumis sativus*) stems with *A. fabrum*. Light perception is accomplished by photoreceptor proteins like *e.g.* the red light photoreceptors called phytochrome. *A. fabrum* contains two phytochromes, termed Agp1 and Agp2. Conjugation, a similar process in which single stranded plasmid DNA is transferred to adjacent bacteria, was shown to be regulated by the presence of phytochrome. The movement is also controlled by phytochrome. Additionally, *A. fabrum* contains the type VI secretion system (T6SS) for competition against other bacteria. The T6SS can be used to transfer toxic proteins to adjacent bacteria.

In this work, *A. fabrum* wild type (WT) and phytochrome mutant strains were used to determine the function of both phytochromes. It was found that both single and double phytochrome mutants grow faster than the WT. The same strains were also used to check for an effect on the infection of the stem and the leaves of *Nicotiana benthamiana* in darkness and under continuous red light irradiation at room temperature. The double phytochrome mutants showed a negative effect on the infection. Moreover, red light could inhibit the effect of Agp1 and promote the influence of Agp2.

In order to study whether there is an interaction between the phytochromes Agp1 and Agp2, multiple experiments, including size exclusion chromatography, photoconversion, dark reversion, autophosphorylation and measurements of the chromophore assembly kinetics, were performed. In all assays, the data obtained from mixtures of the two phytochromes show differences to the data that were predicted based on the assumption that one phytochrome does not affect the respective other, indicating

that there is a direct interaction *in vitro*. This interaction partially explain a coaction of both phytochromes *in vivo*.

Quantification of the expression levels of the proteome in WT *A. fabrum* and the double mutant strain showed that phytochromes could promote the expression of the protein traA (Atu5111) necessary for conjugation. Additionally, there were influences on the chemotaxis protein mcpC (Atu0872), the flagellar protein motC (Atu0570) and the pilus protein (Atu0220). Moreover, an effect on the haemolysin coregulated protein (Atu4345) and the protein toxin Atu4347 of the T6SS was observed. Competition assays with either *A. fabrum* WT or double phytochromes mutant inoculated together with soil bacteria followed by analysis of the hypervariable region V2 of the 16S rRNA gave insight into the composition of bacteria after letting them compete for a given time. Taken together, the results from proteomics and competition assays suggest that the presence of phytochromes could improve the interbacterial competitiveness and therefore the survival rate of *A. fabrum.*

Introduction

1. Phytochromes

The photoreceptor phytochrome was first found in plants. Later, proteins of the phytochrome were discovered in fungi and bacteria (Beattie et al., 2018). The common feature among phytochromes is photoconversion between two conformational states, the Pr form (red absorbing) and Pfr form (far-red absorbing). A typical phytochrome consists PAS domain (Aravind and Ponting, 1999), a GAF domain (Aravind and Ponting, 1997) and PHY domain at N-terminal, which are combined to become a photosensory core module (PCM). At the C-terminus, it contains a histidine kinase module (Figure 1) (Buchberger and Lamparter, 2015; Lamparter et al., 2017; Rockwell et al., 2006).

Phytochromes regulate light effects in plants at many developmental stages such as germination of seeds, seedling de-etiolation or flowering (Kendrick and Kronenberg, 1994; Li et al., 2011). In fungi, conidia germination, stress response and the balance between sexual and vegetative development are controlled by phytochromes (Bayram et al., 2010; Igbalajobi et al., 2019; Yu et al., 2016; Yu and Fischer, 2018). Phytochromes of some photosynthetic bacteria control pigments and proteins related to photosynthesis (Giraud et al., 2002; Giraud et al., 2004). In non-photosynthetic bacteria, phytochromes regulate the conjugation and DNA transport to plant cells (Bai et al., 2016; Oberpichler et al., 2008). As typical dimeric proteins, phytochromes consists of two identical subunits. Heterodimers formation is found in organisms with several phytochromes. For example, in the model plant *Arabidopsis thaliana* with five different phytochromes phyA to phyE, heterodimers can be formed between phyB, phyC, phyD and phyE (Sharrock and Clack, 2004). In plants, many phytochrome interacting proteins are known, for example, phytochrome-interacting factors (PIFs) (Kami et al., 2012; Ni et al., 1998), phytochrome-associated protein phosphatase 5 (PAPP5) (Ryu et al., 2005), phytochrome kinase substrate 1 (PKS1) (Fankhauser et al., 1999; Lariguet et al., 2006; Schepens et al., 2008), the cytosolic proteins nucleotide diphosphate kinase 2 (NDPK2) (Choi et al., 1999; Shen et al., 2005; Tanaka et al., 1998) or other related proteins (Al-Sady et al., 2006; Castillon

et al., 2007; Kircher et al., 1999). In fungi, phytochrome modulated the signal transmission through interacting with velvet A (VeA) and the blue light receptor system (LreA/LreB) (Igbalajobi et al., 2019; Purschwitz et al., 2008; Yu et al., 2016). Gene activation by the phytochrome-interacting transcription factor PpsR is triggered during phytochrome signal transmission in *Rhodopseudomonas palustris* and *Bradyhizobium spec.* (Jaubert et al., 2004; Penfold and Pemberton, 1994). Most bacterial phytochromes are histidine kinases, therefore, the phytochromes might have signal transmitting function (Esteban et al., 2005; Lamparter et al., 2002). The typical mechanism of a histidine kinase is that after autophosphorylation at a conserved His residue, phosphate is transferred from the His to a conserved Asp on a response regulator protein. For response regulator of bacterial phytochrome, the roles are still unclear and also the other interaction partners have not yet been discovered. In a given organism, knowing interaction partners and the interaction modes are a necessity to uncover the mechanism of signal transduction.

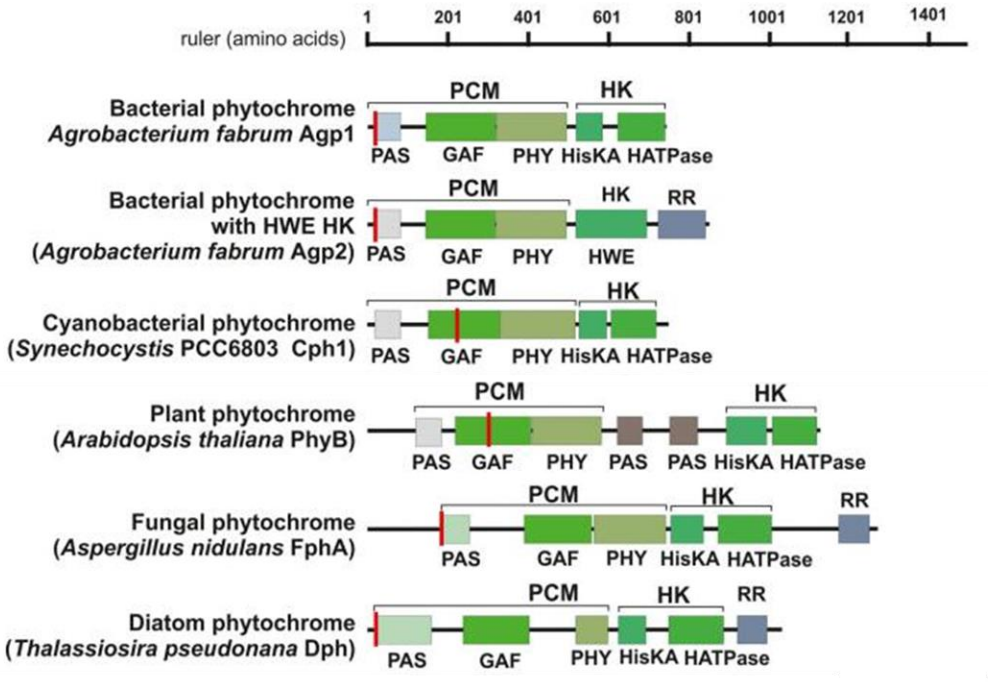

Figure 1. Domain structures of different phytochromes. Vertical red lines indicate the position (Cys residues) of bilin attachment. Modified figure from (Lamparter et al., 2017).

2. Soil bacterium *Agrobacterium fabrum*

Agrobacterium fabrum is a non-photosynthetic, gram-negative and rod-shaped bacterium that causes the crown gall (tumor) disease (Figure 2A) in at least 140 species of dicotyledons or gymnosperms to utilize nutrients from the plants (Moore et al., 1997). It usually lives in the soil, preferably in cultivated fields with loose soil (Smith and Townsend, 1907). The bacterial movement is provided by four to six flagella on the side of cell (Figure 2B) (Chesnokova et al., 1997; Shaw et al., 1991).

Figure 2. Crown gall (A) caused by *Agrobacterium fabrum* (B) in *Platanus orientalis*. Figure B from Alyssa Collins.

2.1 Conjugation

Conjugation is a mechanism of horizontal gene transfer and therefore, it is very important for adapting to the environment or for gaining a selectional benefit, and then that it is also in *A. fabrum*. For example, it is responsible for the transfer of the Ti (tumour inducing) plasmid between *A. fabrum* strains (Holmes and Jobling, 1996a, b; Pan et al., 1995; Ray and Ryan, 2004). In *A. fabrum*, TraA proteins are supposed to initiate the process of conjugation through nicking double stranded DNA at the *oriT* position and covalently binding to the single stranded DNA (Cho and Winans, 2007). The transfer of DNA – protein adduct to the recipient cell is facilitated via the Type 4 secretion system (T4SS). Three TraA homologs have been found in *A. fabrum*, which are encoded by the Ti-plasmid, the At-plasmid, and the linear chromosome, respectively (Cho and Winans, 2007; Goodner et al., 2001; Wood et al., 2001). Donor cells without a Ti-plasmid have a lower conjugation rate than strains with (Krieger et al., 2008), meaning that the Ti encoded TraA protein may promote the conjugation predominantly. A lower conjugation rate is observed in single *agp1* or *agp2* gene mutant donor cells as compared to the wild type cells. Moreover, there is no conjugation in the double *agp1* and *agp2* gene mutant cells. Therefore, I speculate that both phytochromes Agp1 and Agp2 can interact with each other and also with TraA protein to regulate the conjugation. Here I tested whether there was an interaction between Agp1 and Agp2 *in vitro*.

2.2 Plant infection

Under natural conditions, *A. fabrum* is chemotactically attracted to wounds of plants producing compounds such as L-arabinose, pyrogallic acid, vanillin and acetyl syringone that function as chemoattractants and inducers of the toxic region of virulence genes on the Ti plasmid that encode the virulence proteins in *A. fabrum* (Ashby, 1988; Gelvin, 2000; Morris and Morris, 1990; Parke et al., 1987). The soil bacterium causes the tumors by transmission and subsequent insertion of the T-DNA, which contains genes like the onc-genes and the ops-genes originating from the Ti plasmid into the genome of plant cells (Figure 3). The onc-genes encode proteins which can induce additional growth by increasing the auxin and cytokinine levels locally, while the ops-genes encode for opsin. The T4SS is necessary for the T-DNA transfer (Alvarez-Martinez and Christie, 2009; Chilton et al., 1977; Gelvin, 2003; Nester, 2015). The tumors form optimally at 22 °C. However, a significant decrease in tumor formation at higher temperature or white light is observed in plants (Dillen et al., 1997; Oberpichler et al., 2008).

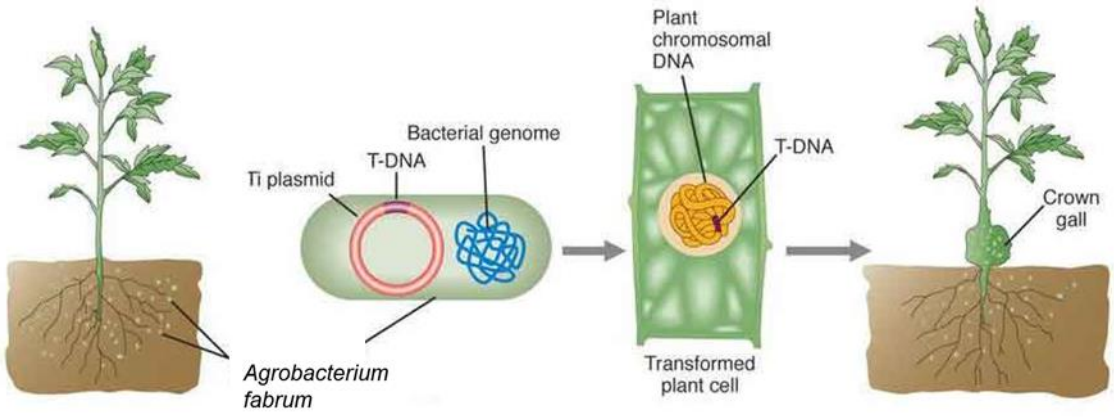

Figure 3. Plant infection model of *Agrobacterium fabrum*. Modified figure is from Steven M. Carr and Griffiths.

2.3 Type IV secretion system

The T4SS transports Ti and At plasmids during the process of conjugation to the recipient cell. Moreover, *A. fabrum* can use the T4SS to deliver T-DNA into plant cells and finally to cause the crown gall formation. The T4SS is composed of the proteins VirB1-11 and VirD4 (Figure 4) and therefore, it is also named VirB / VirD4 T4SS (Alvarez-Martinez and Christie, 2009; Beijersbergen et al., 1994; Shirasu et al., 1990; Ward et al., 1988). VirD2, a relaxase, initiates the infection process by nicking the *oriT* position of pTi plasmid and then helicase covalently binds with single stranded T-DNA (Yanofsky et al., 1986). The process of the delivery of T-DNA-protein complexes via T4SS is driven by ATPases (VirD4, VirB4 and VirB11) which can also interact with each other (Atmakuri et al., 2004; Ripoll-Rozada et al., 2013).

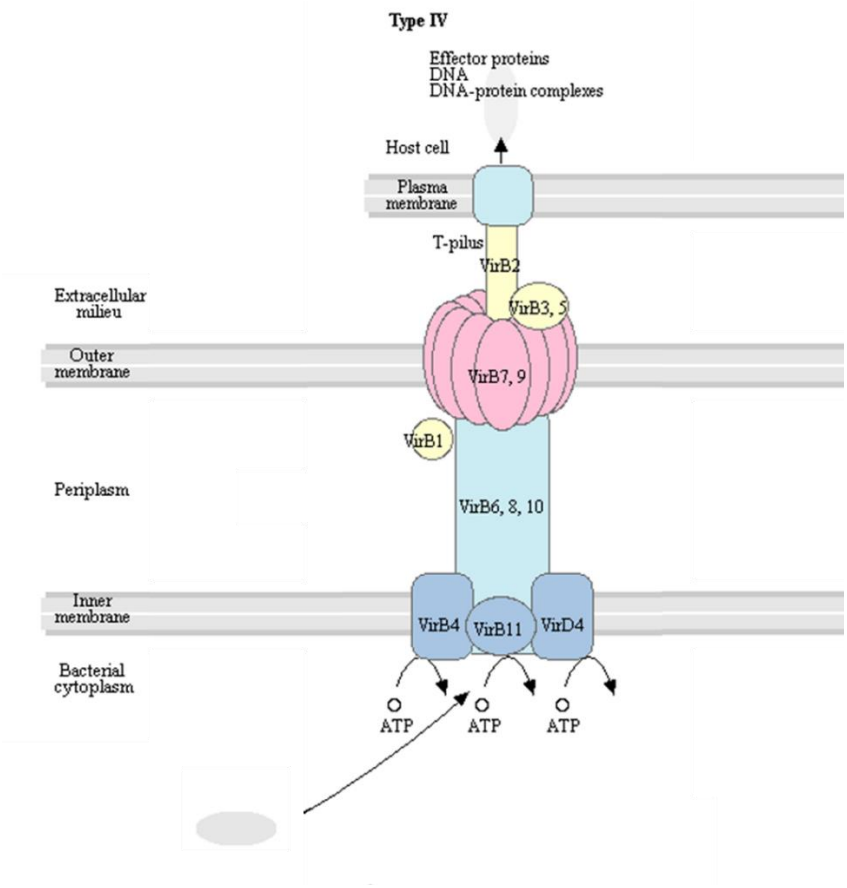

Figure 4. Type IV secretion system model of *Agrobacterium fabrum*. Modified figure from Kanehisa Laboratories (https://www.kegg.jp/kegg-bin/show_pathway?atu03070).

2.4 Type VI secretion system

On the basis of abundant extracellular accumulation of haemolysin-coregulated protein (Hcp, Au4345) induced by pH 5.5, the type VI secretion system (T6SS) (Figure 5) of *A. fabrum* was detected (Lassalle et al., 2011; Wu et al., 2008). In the *A. fabrum* T6SS gene cluster, there are three operons, *imp*, *hcp* and *vgrG* which encode 14 genes (*atu4343* to *atu4330*), 9 genes (*atu4344* to *atu4352*) and 5 genes (*atu3642* to *atu3638*), respectively (Lin et al., 2013). During interbacterial competition, T6SS of *A. fabrum* C58 launches DNase effectors into *Escherichia coli* DH10B cells to ultimately kill them, whereas the injection of effectors can cause the counteroffensive by *Pseudomonas aeruginosa in vitro*. However, in plant, competition between *A. fabrum* and *P. aeruginosa* would be won by *A. fabrum*. There are three prospective toxin / immunity pairs (Atu4350 / Atu4351, Atu3640 / Atu3639 and Atu4347 / Atu4346 proteins) of T6SS in *A. fabrum*. DNase activity was observed in the Atu4350 and Atu3640 proteins, and Atu4347 could be a peptidoglycan amidase. *A. fabrum* can used the toxin protein to kill other bacterium (English et al., 2012; Ma et al., 2014). Similarly, for a competitive *in soil A. fabrum* could also have advantage provided by the T6SS and the effectors.

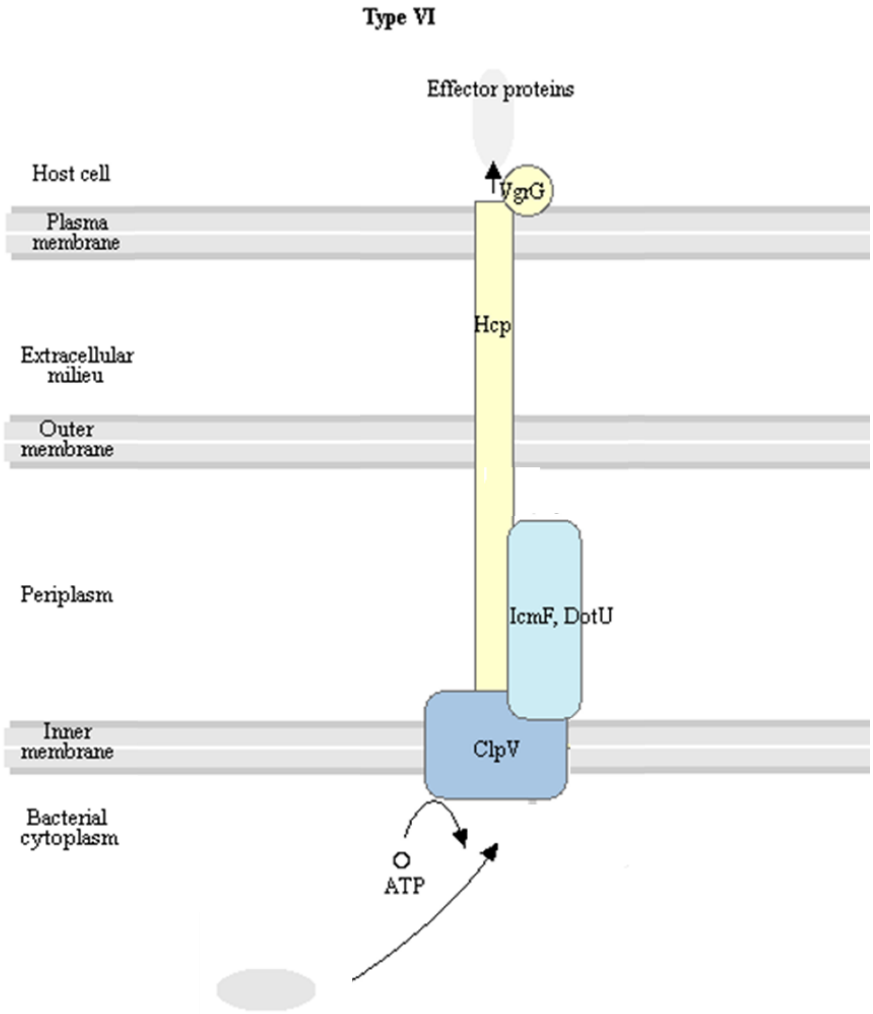

Figure 5. Type VI secretion system model of *Agrobacterium fabrum*. Modified figure from Kanehisa Laboratories (https://www.kegg.jp/kegg-bin/show_pathway?atu03070).

3. Phytochromes from *A. fabrum*

Plants and cyanobacterium use phytochromobilin (Rüdiger and Thümmler, 1994) and phycocyanobilin (Hübschmann et al., 2001; Wu et al., 1997) as a chromophore, respectively. For fungal or bacterial phytochromes, biliverdin (BV) is used as a chromophore (Bhoo et al., 2001). The first prokaryotic phytochrome was found in cyanobacterium *Synechocystis* (Hughes et al., 1997). Later, in *A. fabrum* phytochromes Agp1 and Agp2 were discovered (Goodner et al., 2001; Karniol and Vierstra, 2003; Lamparter et al., 2002; Wood et al., 2001). The covalent binding sites of Agp1 and Agp2 for BV are localized at the cysteine (Cys)-20 and -13, respectively (Karniol and Vierstra, 2003; Lamparter et al., 2004; Lamparter et al., 2002). In darkness, Agp1 is in the Pr form and Agp2 is in the Pfr form (Karniol and Vierstra, 2003; Rottwinkel et al., 2010). Agp1 is a classical histidine kinase which has a conserved Phe residue, whereas Agp2 belongs to the HWE HK type which has a conserved histidine residue, a Trp-X-Glu motif and no recognizable "F box" (Bhoo et al., 2001; Karniol and Vierstra, 2004). Response regulator of Agp1 is a separate protein (Esteban et al., 2005; Lamparter et al., 2002), whereas Agp2 response regulator is found at the phytochrome C-terminus which is also found in fungal and bacterial phytochromes. In the chromophore pocket of phytochromes, the chromophore interacts with amino acid residues, which can determine the spectral properties. Protein-protein interaction or environmental changes can also influence the UV-vis spectra which in turn indicate changes within this pocket. Moreover, the phytochrome spectrum is pH dependent (van Thor et al., 2001; Zienicke et al., 2013). Temperature effects spectral properties of Agp1 and other phytochromes (Njimona and Lamparter, 2011; Njimona et al., 2014). For Agp2, spectral changes could be caused by the cell extract of *Agrobacterium agp1/2*$^{-}$ double knockout mutant (Krieger et al., 2008).

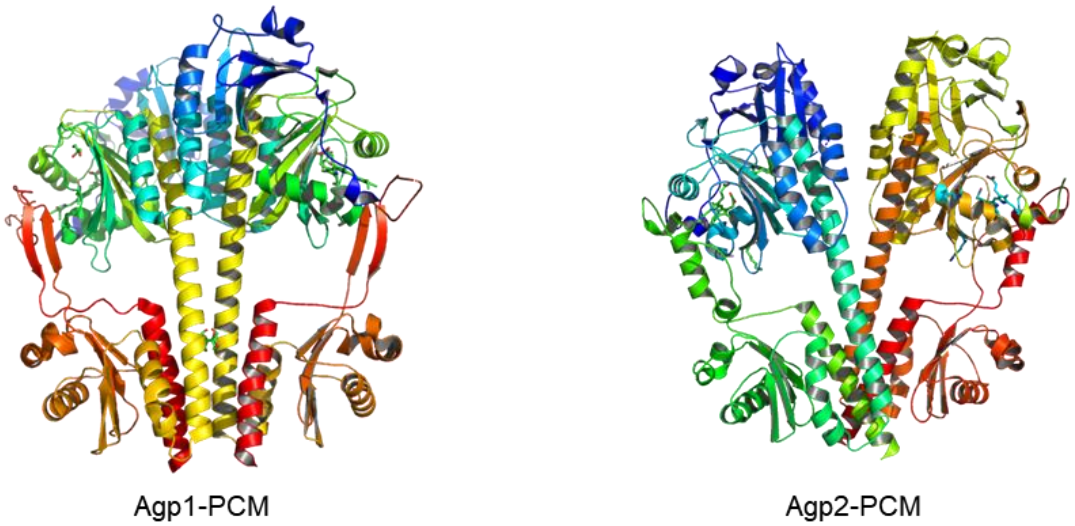

Figure 6. The structure of Agp1-PCM and Agp2-PCM. PCM: photosensory core module. Figures were constructed by PyMOL using the protein data bank (PDB) codes (Agp1-PCM: PDB code 5I5L; Agp2-PCM: PDB code 6G1Y) (Nagano et al., 2016; Schmidt et al., 2018).

4. Aim of this project

Researchers have mainly studied the biological functions of phytochromes in plants, fungi and photosynthetic bacteria, whereas little information is available on non-photosynthetic bacteria. Here phytochromes Agp1 and Agp2 of non-photosynthetic bacterium *A. fabrum* was studied. I investigated the phytochrome roles by *A. fabrum* phytochrome single and double mutants. For their molecular mechanisms, tandem mass tags (TMT) based quantitative proteomics was used to study the differentially expressed proteins of white light and dark grown *A. fabrum* wild type and double *agp1 / agp2*$^{-}$ knockout mutants. Moreover, the possibility of protein interaction between the phytochromes Agp1 and Agp2 from *A. fabrum* was also tested *in vitro*. I performed size exclusion, photoconversion, dark reversion, phosphorylation and BV assembly kinetics with purified, recombinant Agp1 and Agp2 in mixed solutions in comparison with single proteins.

Results

1 Distribution of phytochromes Agp1 and Agp2 in genus *Agrobacterium*

Phytochromes are widely distributed among bacteria, whereas there are also many species without a phytochrome gene (Lamparter, 2004). The distribution among relatives can provide additional information about a function. The genes for the phytochromes Agp1 and Agp2 are from *Agrobacterium fabrum* C58, the first *Agrobacterium* strain that has been sequenced (Goodner et al., 2001; Wood et al., 2001). Meanwhile, genomes of a large number of closely related strains and species are known. Here both Agp1 and Agp2 homologs were searched in 22 genomes of *Agrobacterium* or *Radiobacter*, the closest species found in NCBI database searches. Quite interestingly, 21 strains contained the Agp2 homolog, and only four the Agp1 homolog (Table 1). Agp2 of *A. fabrum* and related phytochromes from *Rhizobiaceae* belong to the bathy phytochromes which have a Pfr dark state and absorb in the larger wavelength range, and I suppose that the Agp2 homologs identified here are also bathy phytochromes. The distribution results showed that the long wavelength range could be even more closely related to survival and evolution of *Agrobacterium*.

Table 1. Distribution of Agp1, Agp2 and their homologs in *Agrobacterium*. Source of the secuqnces is from NCBI database searches.

Genus *Agrobacterium*	Agp1	Agp2	reference
Agrobacterium fabrum	+	+	(Goodner et al., 2001; Wood et al., 2001)
Agrobacterium deltaense	+	+	unknown
Agrobacterium salinitolerans	+	+	unknown
Agrobacterium sp. YIC 4121	+	-	unknown
Agrobacterium albertimagni	-	+	(Trimble et al., 2012)
Agrobacterium arsenijevicii	-	+	(Kuzmanović et al., 2015)
Agrobacterium bohemicum	-	+	(Zahradník et al., 2016)
Agrobacterium larrymoorei	-	+	unknown
Agrobacterium rhizogenes	-	+	(Franco et al., 2016; Kajala et al., 2014)
Agrobacterium rosae	-	+	unknown
Agrobacterium rubi	-	+	(Davis II et al., 2016)
Agrobacterium vitis	-	+	(Slater et al., 2009)
Agrobacterium genomosp. 13	-	+	unknown
Agrobacterium sp. FDAARGOS_525	-	+	unknown
Agrobacterium sp. 10MFCol1.1	-	+	unknown
Agrobacterium sp. CNPSo 2736	-	+	unknown
Agrobacterium sp. LAD9	-	+	unknown
Agrobacterium sp. MS2	-	+	unknown
Agrobacterium sp. NCPPB 925	-	+	unknown
Agrobacterium sp. RS6	-	+	unknown
Agrobacterium sp. RZME10	-	+	unknown
Agrobacterium sp. SUL3	-	+	unknown

2 Analysis of functions of phytochromes Agp1 and Agp2

2.1 The effect of Agp1 and Agp2 on growth

To test the effects of phytochromes Agp1 and Agp2 on growth of *A. fabrum*, the growth rates of wild type (WT) and phytochrome single (*agp1*$^-$ or *agp2*$^-$) and double (*agp1/2*$^-$) knockout mutants were assayed at different temperatures and light conditions. In earlier reports (Oberpichler et al., 2006), there was no significant difference between WT and *agp1*$^-$ or *agp2*$^-$ single mutants after growth at 28 ℃ for 6 h. But longer times were not tested. After measurement of the growth in darkness at 28 ℃ for 51 h, I observed that growth rates of both single and double mutants had higher than that of WT (Figure 7). Therefore, phytochromes Agp1 and Agp2 have a negative impact on growth in *A. fabrum*.

In order to investigate the impacts of light on the growth at 28 ℃, I compared the growth rates under darkness, white light, red light in which phytochromes Agp1 and Agp2 absorb (Karniol and Vierstra, 2003; Lamparter et al., 2002) or blue light. No significant differences were found in the growth rates of WT and mutants under darkness, white light and red light. However, blue light did promote their growth as compared to the other light condition (Figure 8). In *A. fabrum*, there are two blue light photoreceptor photolyases PhrA and PhrB which repair the UV damaged DNA (Oberpichler et al., 2011; Zhang et al., 2013). I assume that blue light could led to increased growth via the photolyases.

In a similar way like the conjugation research of *A. fabrum* WT and phytochrome mutants at various temperatures (Bai et al., 2016), the growth rates of WT and mutants were also studied at the same temperature range from 20 ℃ to 37 ℃ in darkness. The results showed that the bacterial growth rates at 25 ℃ had a maximum. From 20 ℃ to 32 ℃ all mutants had greater growth rates than WT, whereas at 37 ℃, growth rates of *agp2*$^-$ mutant and *agp1/2*$^-$ double mutant were lower than that of WT. Furthermore, there was no significant different between WT and *agp1*$^-$ mutant (Figure 9). These results indicate that at higher temperature 37 ℃ the Agp2 could play an important role in the promotion of growth under dark.

Similar to the experiments at 28 ℃ (Figure 8), the effects of different light conditions on the growth rates at 37 ℃ were also performed in darkness, white light, red light or blue light. Again, the promotion of growth by blue light was observed in WT and mutants when incubation temperature was 37 ℃. At 37 ℃ growth of WT and *agp1*$^{-}$ or *agp2*$^{-}$ single mutants was promoted by white light but inhibited by red light (Figure 10), which were opposed to the results (at 28 ℃ incubation temperature) that white and red light could not impact the growth rate as compared to the control darkness (Figure 8).

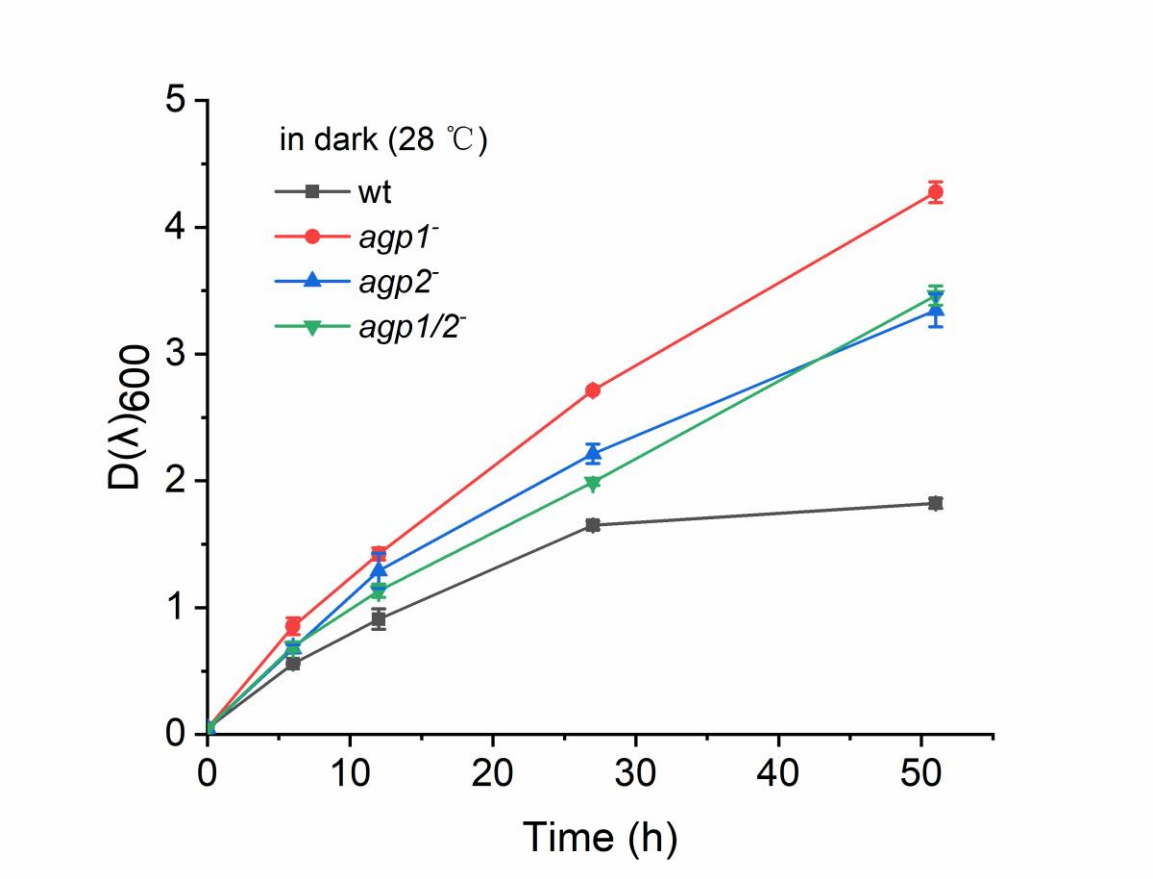

Figure 7. Growth curves of WT and mutants of *A. fabrum*. The cell concentration was measured as OD_{600} after 0, 6, 12, 27 or 51 h. Values are means ± SE of 3 replicates.

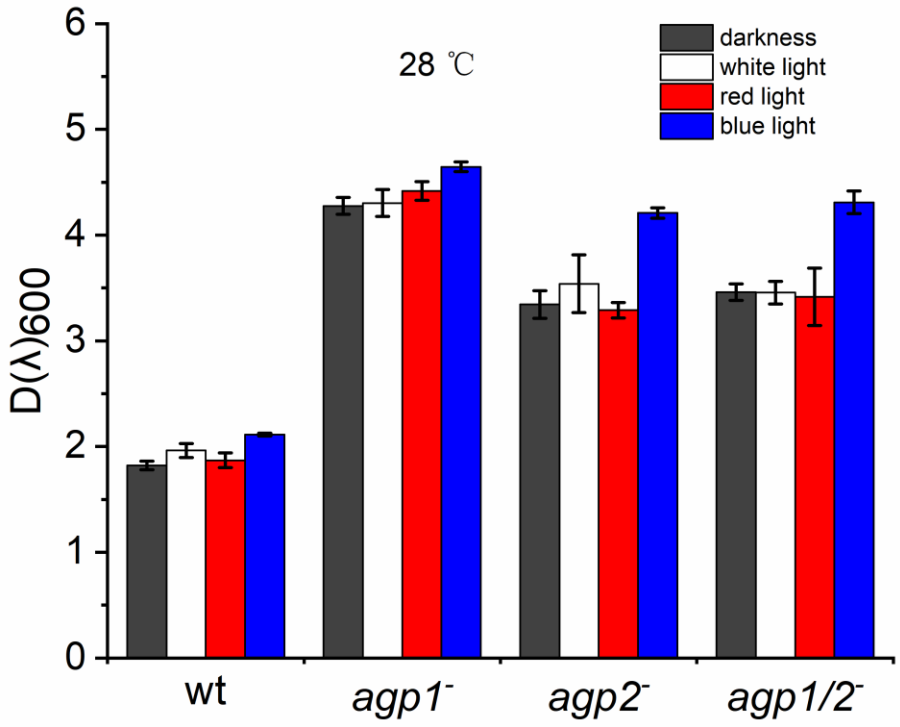

Figure 8. Effects of white, red and blue light on growth of *A. fabrum* at 28 ℃. The cell concentration was measured as OD_{600} after 51 h. Values represent means ± SE of 3 replicates.

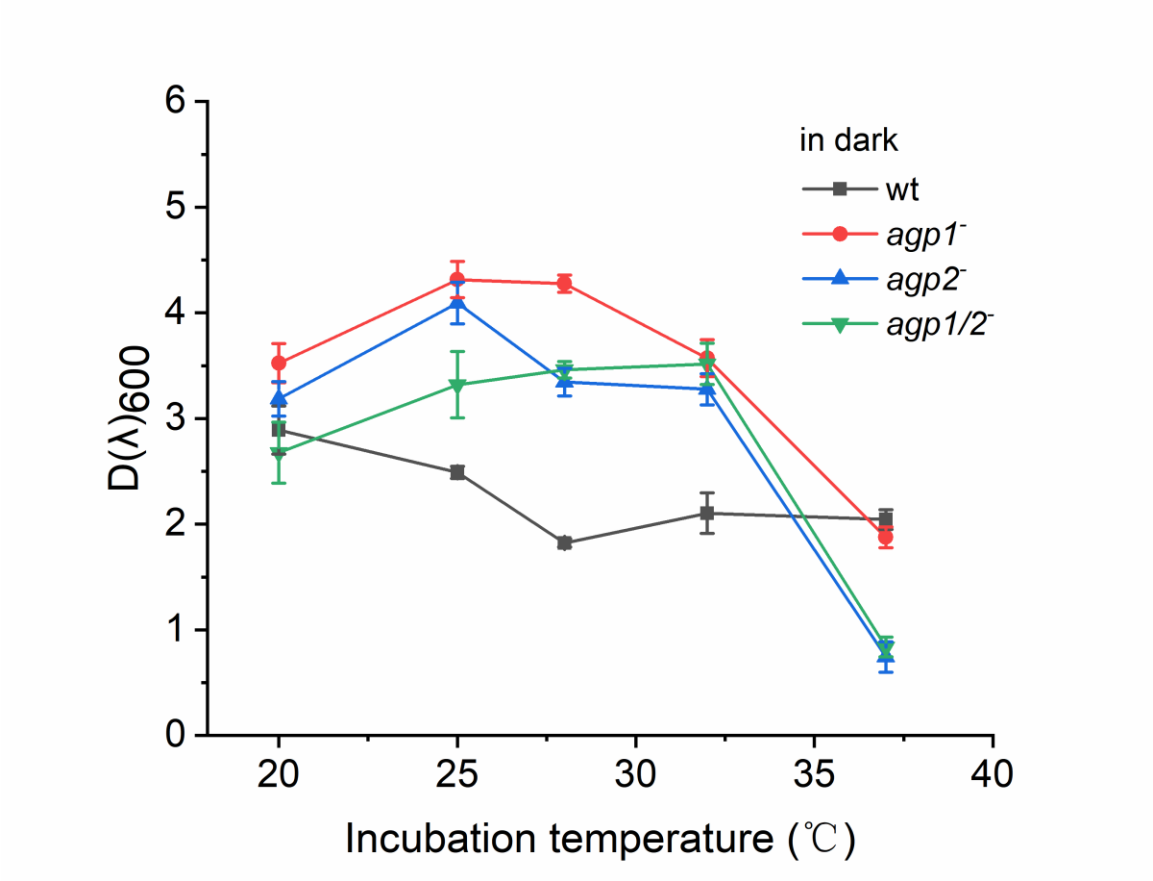

Figure 9. Effects of temperature on growth of *A. fabrum*. The cell concentration was measured after 51 h as OD_{600}. Incubation temperatures were 20, 25, 28, 32, and 37 °C. Mean values ± SE of 3 replicates.

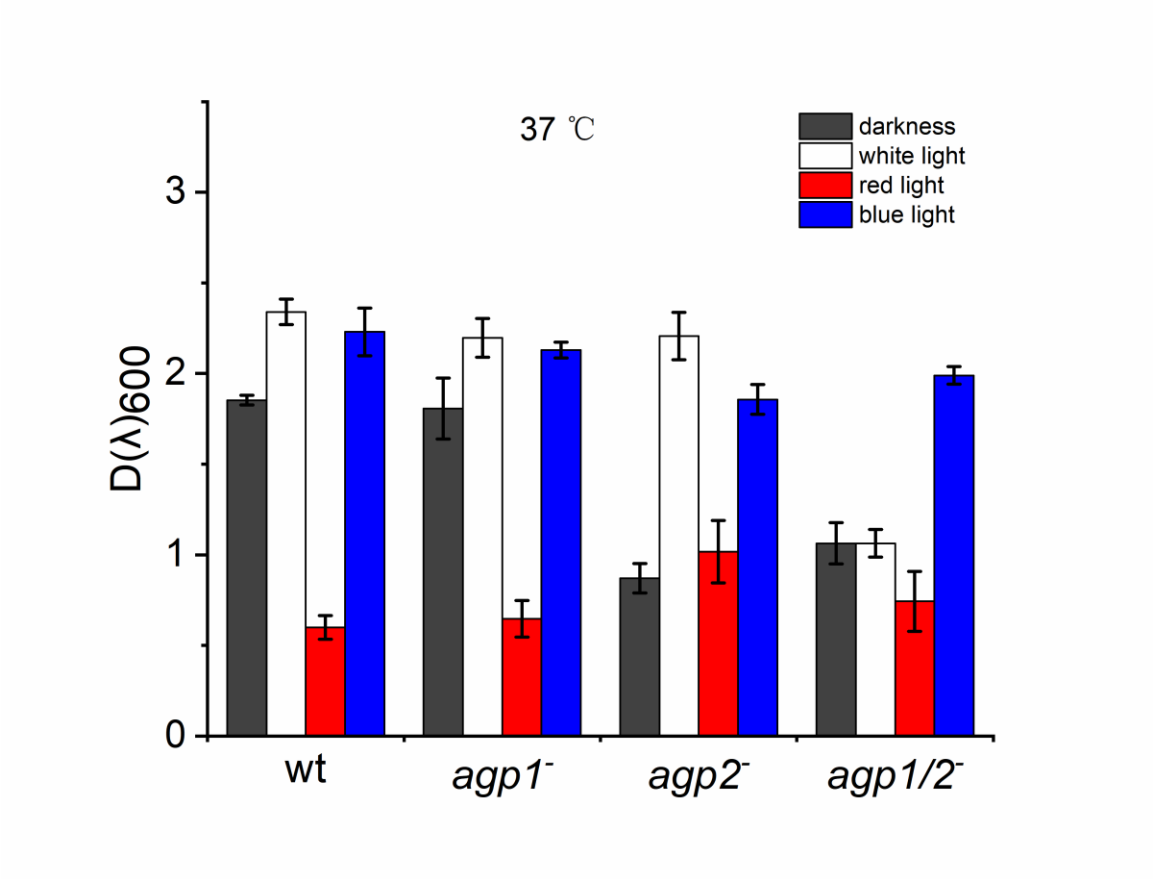

Figure 10. Effects of white, red and blue light on growth of *A. fabrum* at 37 ℃. The cell concentration was measured as OD_{600} after 51 h. Values represent means ± SE of 3 replicates.

2.2 The effect of Agp1 and Agp2 on the plant infection

Previous results from our group showed that white light suppressed the infection of cucumber (*Cucumis sativus*) stems with *A. fabrum* (Oberpichler et al., 2008). The question whether photoreceptor phytochromes Agp1 and Agp2 control the infection was addressed. In this research, I mainly used the WT, *agp1*$^{-}$, *agp2*$^{-}$ and *agp1/2*$^{-}$ *A. fabrum* to infect the stems and leaves of *Nicotiana benthamiana* in darkness and red light at room temperature, respectively. Elisabetha Averbukh contributed to the experiments of plant infection.

In the stem study, tumors were not observed in the plants infected by *agp1/2*$^{-}$ *A. fabrum* under darkness or red light, whereas tumors were observed in the plants infected by WT, *agp1*$^{-}$or *agp2*$^{-}$ *A. fabrum* under same light condition. In addition, I found that after infection by WT or *agp2*$^{-}$ *A. fabrum* in darkness tumors of the stems were bigger than those induced in red light. In contrast, the tumors caused by *agp1*$^{-}$ *A. fabrum* in darkness were smaller than in red light (Figure 11).

For the plant infection, the leaves were used as infected tissue. The β-glucuronidase (GUS) activity of infected leaves was estimated by staining and fluorometric assays. If the ability of infection was stronger, more *GUS* gene from *A. fabrum* carrying a pBIN-GUS plasmid could be transformed into the leaves, therefore the higher GUS activity would be observed in the infected leaves. After reaction with 5-bromo-4-chloro-3-indolyl glucuronide (X-Gluc, Thermo Fisher), apparent blue stains were just found in the transgenic leaves infected by WT or *agp2*$^{-}$ *A. fabrum* in darkness or by *agp1*$^{-}$ *A. fabrum* in red light (Figure 12). To compare the difference in GUS activity between the transgenic leaves, we used the fluorometric GUS assay. There was no significant difference in the leaves having the apparent blue stains (Figure 13).

Finally, I conclude that phytochromes Agp1 and Agp2 play a positive impact on infection in *A. fabrum*. Red light could inhibit the Agp1 but promote the Agp2.

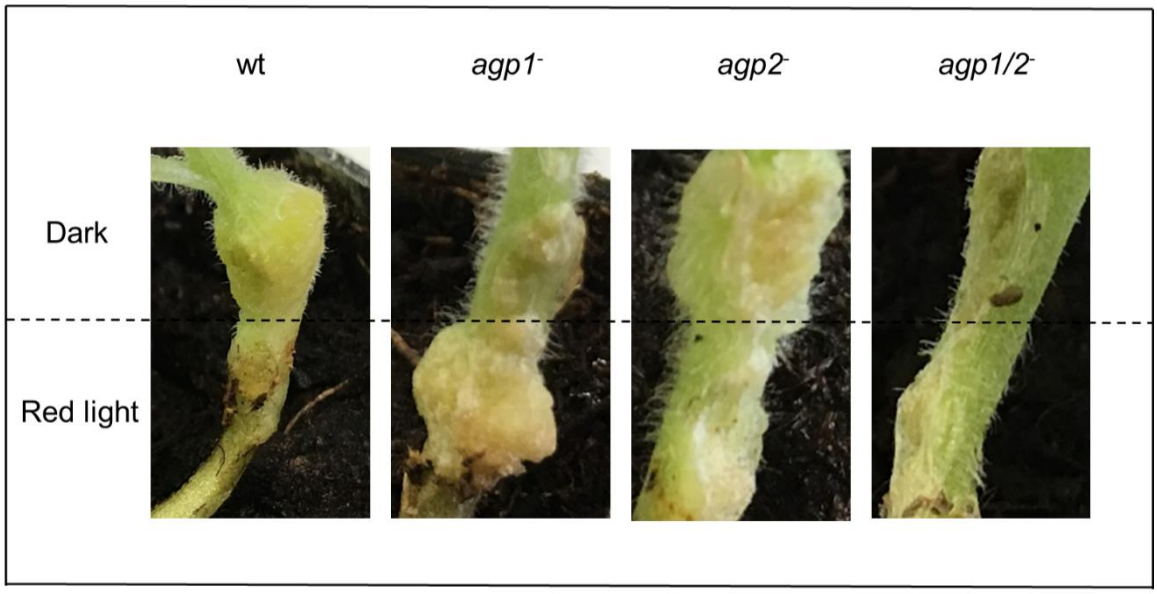

Figure 11. Comparison of WT and phytochrome mutants *A. fabrum* virulence in dark and red light. 6 weeks old *Nicotiana benthamiana* stems were infected with WT and phytochrome mutants (*agp1*$^{-}$, *agp2*$^{-}$ and *agp1/2*$^{-}$) *A. fabrum* collected from LB agar plates at room temperature. 3 independent infected stems with *A. fabrum* WT or the mutants. For the stem infection of *A. fabrum* WT and double mutant *agp1/2*$^{-}$, Elizaveta Averbukh has done similar experiment in her master thesis before me (Averbukh, 2018).

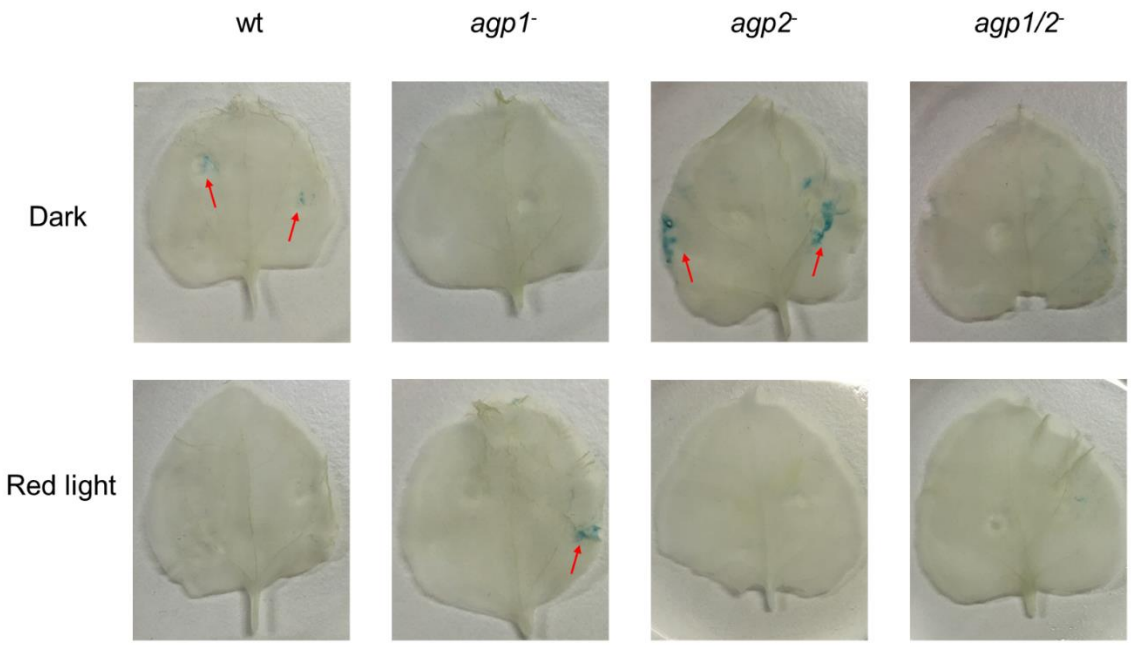

Figure 12. Virulence of WT and phytochrome mutants *A. fabrum* in dark and red light. WT and phytochrome mutants (*agp1*$^{-}$, *agp2*$^{-}$ and *agp1/2*$^{-}$) *A. fabrum* containing pBIN-GUS plasmid were used to infect 6 weeks old *Nicotiana benthamiana* leaves at room temperature. Blue β-glucuronidase (GUS) stains were indicated by red arrows. 3 independent infected leaf with *A. fabrum* WT or the mutants. For the leaf infection of *A. fabrum* WT and double mutant *agp1/2*$^{-}$, Elizaveta Averbukh has done similar experiment in her master thesis before me (Averbukh, 2018).

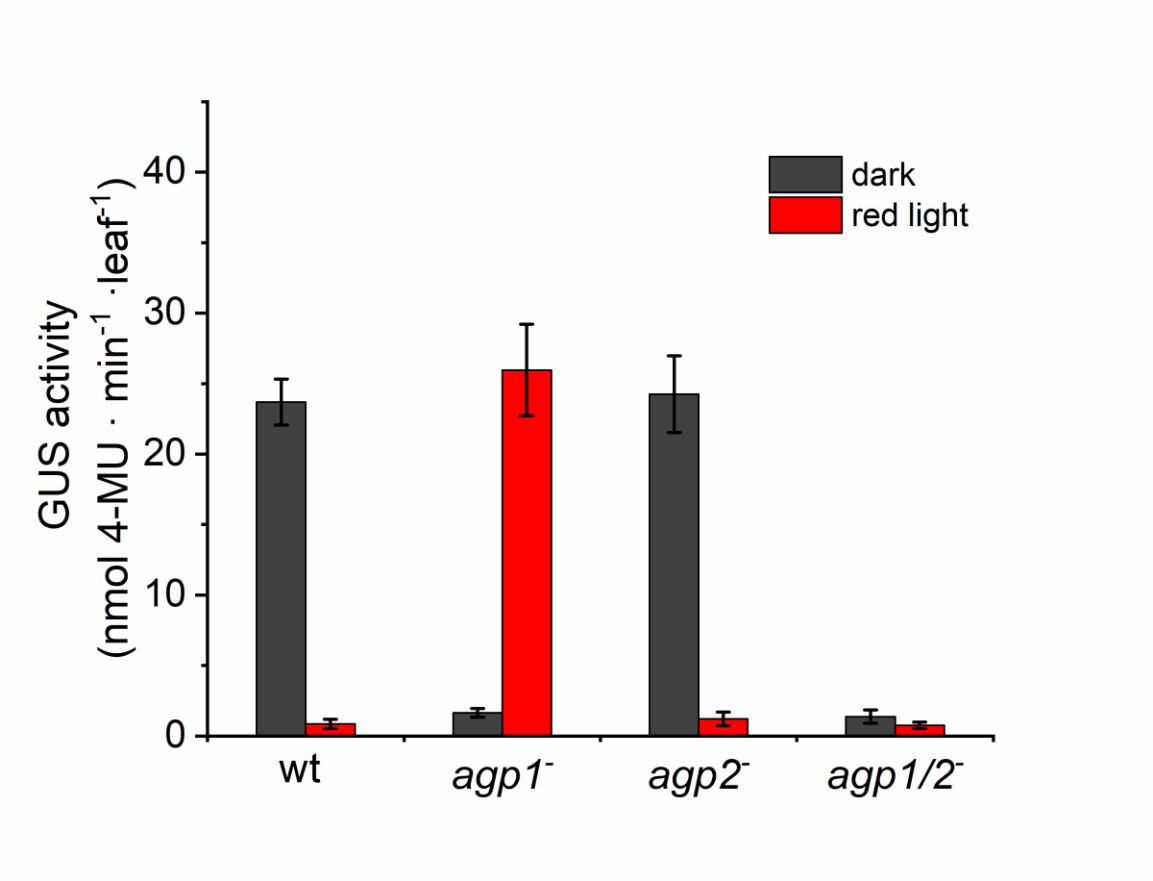

Figure 13. Fluorescent quantitative analysis of β-glucuronidase (GUS) activity of *Nicotiana benthamiana* leaves infected by WT and phytochrome mutants *A. fabrum* in dark and red light. Mean values of 3 independent infected leaves ± SE.

3 Evidence for weak interaction between Agp1 and Agp2 proteins

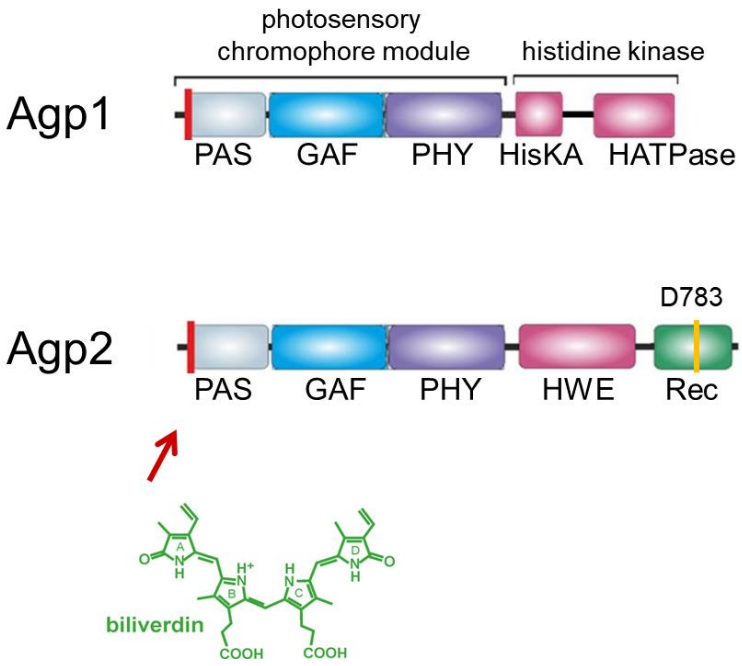

Figure 14. Domain structures of phytochromes Agp1 and Agp2. The PAS, GAF and PHY domains are included in the photosensory chromophore module. The red lines indicate BV binding sites (cysteines). In the response regulator of Agp2, the phosphoaccepting Asp residue (D783) indicated by an orange line was mutated to Ala or Asn.

3.1 Size exclusion chromatography

The possible protein – protein interaction could directly affect the size exclusion chromatography (SEC) pattern. Because the rate of protein movement may be inhibited by the interaction with the other phytochrome protein in the SEC column. Therefore, SEC profiles of Agp1 and Agp2 alone were compared with those of a mixture sample of Agp1 and Agp2. I tested all four different combinations. Each profile had one dimer peaks (260 kDa in Agp1, 280 kDa in Agp2) and three oligomer peaks (443 kDA to void volume) (Figure 15). The formation of oligomer was only observed in slow separations (0.1 ml / min flow rate). However, at high flow rate of 0.5 ml / min, only one dimer peak was observed, as in earlier studies (Noack et al., 2007). Therefore, the difference between low flow rate and high flow rate could be caused by the reduction of NaCl in the gel.

As compared with dimer peak of Agp1, that of Agp2 was always broader with longer elution times (Figure 15A-D), showing that a fraction of Agp2 eluted as monomer. I compared SEC profiles of Agp1 and Agp2 mixtures with those of mathematical addition between Agp1 and Agp2. A shift of Agp1 and Agp2 dimer peaks to earlier elution times would be caused by their stronger interaction. The dimer peaks of Agp1 and Agp2 were always observed at identical elution times. However, at elution times corresponding to the Agp2 monomer, the absorbances of the mixture were lower than those of added profiles, indicating that there could be an interaction between Agp2 monomer and Agp1. Each separation was repeated three times. A difference was found in all six runs when Agp2 was Pr form (Figure 15F and H, replicates). When Agp2 was Pfr form, I also observed that there was a difference in 4 out of 6 runs (Figure 15E and G, replicates). According to the SEC profiles, there could be a weak interaction between Agp1 and Agp2, especially with Pr form of Agp2.

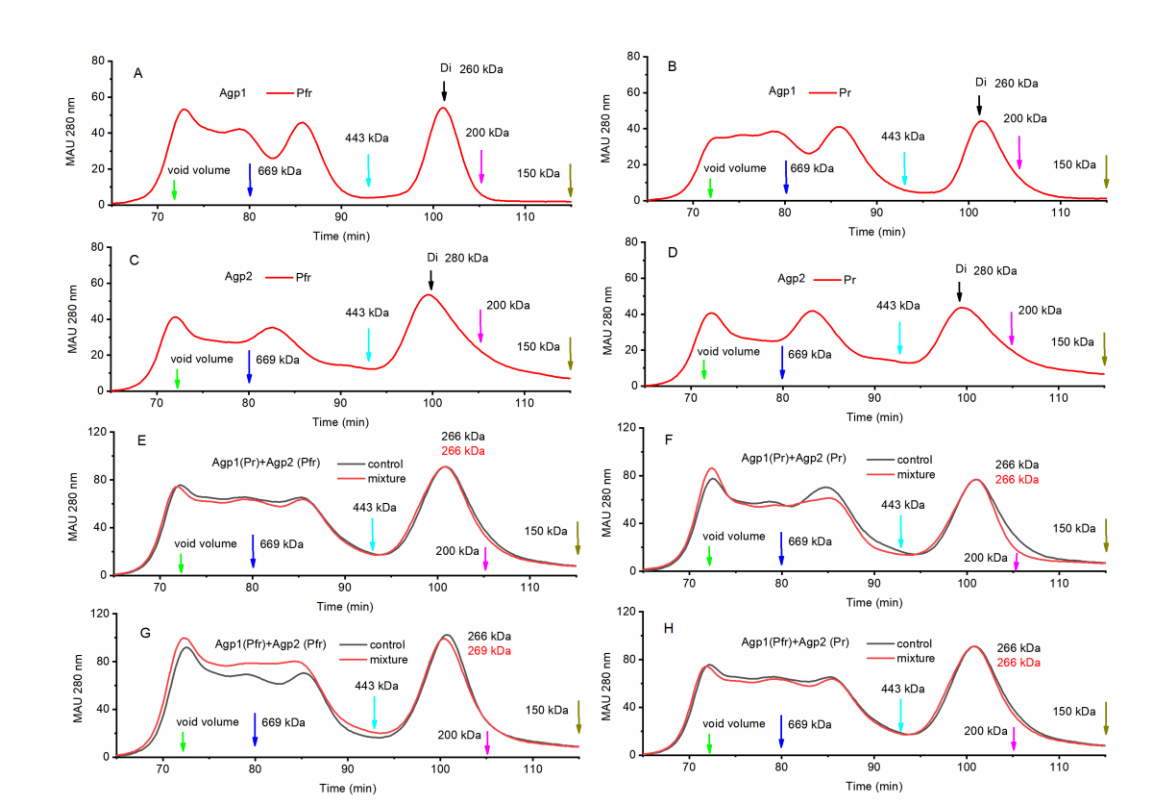

Figure 15. Size exclusion chromatography of Agp1 (A, B), Agp2 (C, D) and comparison between mixture profiles of Agp1 / Agp2 samples (mixture, red lines) and profiles of added Agp1 and Agp2 (control, black lines) (E, F, G, H). For Pfr of Agp1 and Pr of Agp2, the samples of dark states were irradiated with 2 min red or far-red light before the mixing, respectively. Either 200 µl mixture (4 µM Agp1, 4 µM Agp2) or as single Agp1 (4 µM) or Agp2 (4 µM) was used to the SEC column. The absorbance was measured at 280 nm. The elution times of marker proteins are indicated by arrows.

3.2 Dark conversion and UV/vis spectra

To test whether the possible interaction between Agp1 and Agp2 could affect their dark conversion, I compared the dark conversion of Agp1 or Agp2 with their mixture. The experiments were performed by mixing basic buffer or Agp2 with red irradiated Agp1 and then with time course measurements at 700 nm. Similarly, far-red irradiated Agp2 was measured at 750 nm after mixing with basic buffer or Agp1. Triexponential decay functions could be used to fit all dark reversion kinetics (Figure 16 and Table 2). Compared with control (far-red irradiated Agp2 and basic buffer), time constants t1, t2 and t3 of the mixture (far-red irradiated Agp2 and Agp1) were smaller. For the assay with red irradiated Agp1, the t1 and t2 of the mixture were smaller than those of the control (Agp1 alone), whereas there was no difference between their t3.

UV/vis spectra could also be affected by the possible protein–protein interaction. Therefore, the difference spectra between far-red or red irradiated Agp1 / Agp2 mixture and the dark states was compared with mathematically added control. For the experiments of far-red irradiation, Agp2 was mainly influenced, whereas the effect of Agp1 was small. There was a clear difference between the mixture and added samples. In the range of 700 nm, the difference spectrum of mixture was positive, whereas that of the control was negative (Figure 17A). Moreover, a maximum at ~700 nm is observed in the double difference spectrum which looks like a Pr spectrum from 600 nm to 800 nm.

For the similar experiments with red light, the a major extent of Agp1 conversion from Pr to Pfr and a minor extent of Agp2 Pfr to Pr conversion were caused by red light. Also, the difference between difference spectra of Agp1/Agp2 mixture and that of added was observed (Figure 17B). A shoulder at ~750 nm with maximum at ~700 nm is found in a double difference spectrum which resembles a Pfr spectrum from 600 nm to 800 nm. Both dark conversion and UV/vis spectra show protein – protein interactions between phytochromes Agp1 and Agp2.

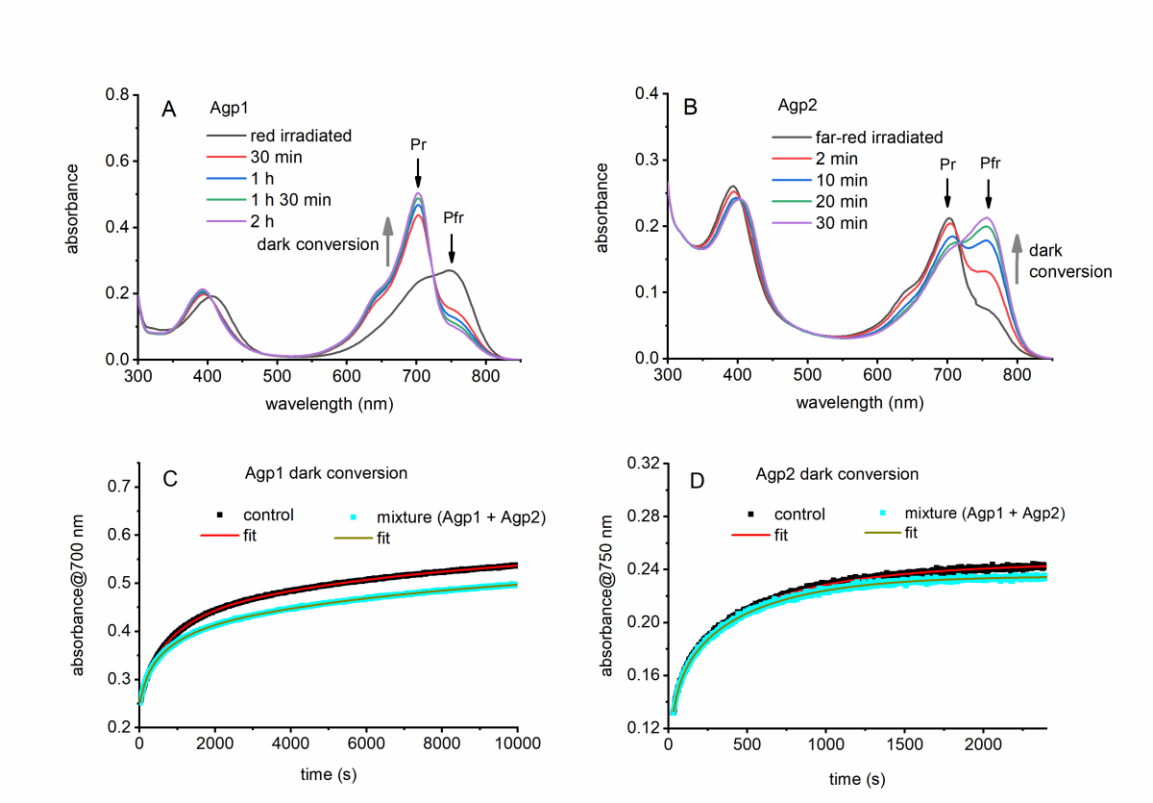

Figure 16. Dark conversion of red irradiated Agp1 (A), without and with Agp2, recorded at 700 nm (Pr increase) (C). Dark reversion of far-red irradiated Agp2 (B), without and with Agp1, measured at 750 nm (Pfr increase) (D). Samples were irradiated before mixing. Three replicates were performed in the experiments. In Table 2, the method of curves fitted to the experimental data is shown.

Table 2. Exponential fit for dark conversion of Agp1 and Agp2. t1, t2, t3: time constants; A1, A2, A3: amplitudes. All error values are obtained from the fit. Here one example is shown, which similar to results of the other two repetitions.

Equation: y = -A1*exp(-x/t1) - A2*exp(-x/t2) - A3*exp(-x/t3) + y0				
	Agp1		**Agp2**	
	in buffer	**in Agp2**	**in buffer**	**in Agp1**
A1	0.042 ± 0. 002	0.051 ± 0.002	0.046 ± 0.002	0.034 ± 0.003
A2	0.13 ± 0.002	0.094 ± 0.001	0.041 ± 0.004	0.029 ± 0.003
A3	0.16 ± 0.0004	0.15 ± 0.0005	0.057 ± 0.005	0.069 ± 0.002
t1 (s)	208 ± 9	160 ± 6	45 ± 3	34 ± 6
t2 (s)	870 ± 20	790 ± 20	250 ± 30	130 ± 20
t3 (s)	7500 ± 200	7700 ± 200	790 ± 50	540 ± 10
R-Square	0.99985	0.9997	0.99854	0.99799

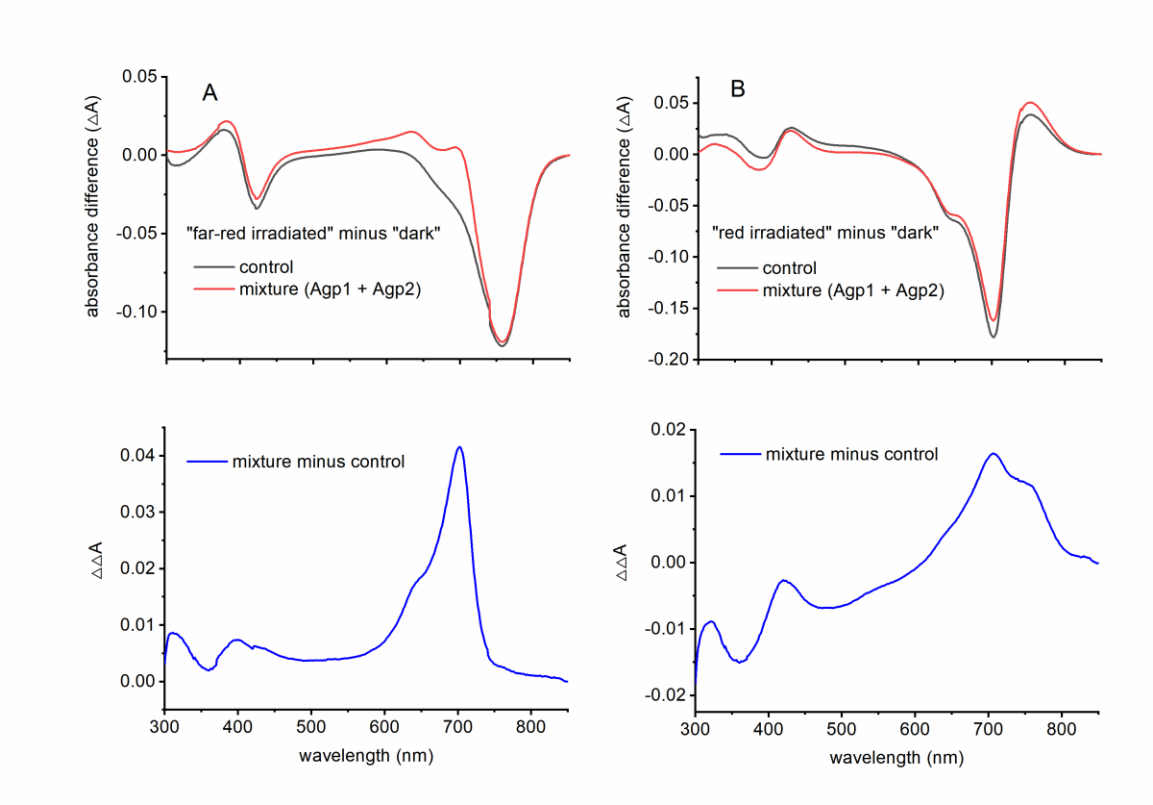

Figure 17. Difference absorbance spectrum of "far-red (A)" or "red (B) irradiated" minus "dark" state (above) and the double difference absorbance spectrum of "mixture" (Agp1 and Agp2) minus "control" (added; below). The final concentrations of agp1 and agp2 were 5 µM. Mixture and control are shown by red and black lines, respectively. The spectrum is also found in the other two replicates.

3.3 Histidine kinase autophosphorylation

Both Agp1 and Agp2 have a histidine kinase domain, and, an additional response regulator was found at C-terminus of Agp2 (Karniol and Vierstra, 2003; Lamparter et al., 2002). I tested whether their phosphorylation activities could be influenced by possible protein interaction. For Agp1, several phosphorylation studies has been performed in our group (Lamparter et al., 2002; Njimona and Lamparter, 2011), whereas agp2 phosphorylation has not yet been performed before. Here a weak phosphorylation band was just observed in the Agp2 sample with residual ammonium sulfate, but in the sample

without ammonium sulfate, no autophosphorylation band was detected (Figure 18A). For this observation of Agp2, I speculated that a fast transphosphorylation and dephosphorylation was catalyzed by the response regulator which was an example for another histidine kinase (Immormino et al., 2016) and this turnover would be suppressed by ammonium sulfate. Therefore, Agp2 mutants of response regulator at Asp783 were used to test the hypothesis. Homology analysis of response regulators indicated that the phosphate would be accepted by the Asp783 from His residue in the His kinase (Karniol and Vierstra, 2003). For the mutant Agp2_D783A, the autophosphorylation signal was higher as compared to WT Agp2. Moreover, the highest signal was observed in Agp2_D783N mutant (Figure 18B). Free phosphate would be detected if there was a ATP turnover in the proteins. Therefore, an assay of malachite green was chosen to detect free phosphate. After incubation of Agp1 (Pr), Agp2 (Pfr), Agp2_D783A (Pfr) or Agp2_D783N (Pfr) protein with ATP, I have not detected free phosphate (Figure 19). Therefore, the assumption of dephosphorylation was rejected. There was an obvious mobility differences of proposed dimers between Agp2 WT and the mutants according to their SEC results. The apparent molecular mass of Agp2, Agp2_D783A and Agp2_D783N were 280 kDa, 292 kDa and 318 kDa, respectively (Figure 20). These significant differences indicate that the Agp2 form is significantly influenced by the protein mutations. When the negatively charged amino acid of Asp is changed to neutral amino acids of Ala and Asn, there will be ionic interactions. The Agp2 mutant of Asn has biggest phosphorylation signal and also the maximum impact on SEC, which is positively related to the fact that Asn acid residue can play roles of donor or acceptor of hydrogen bonds. Finally, I suppose that the response regulator domain of Agp2 protein screens the histidine of HWE module, resulting in the inhibition of autophosphorylation, and that the reduction of ionic interactions of mutations can cause detached response regulator. For the Asn783 of Agp2_D783N, the side chain maybe maintain an obviously different structure as compared with Agp2_D783A.

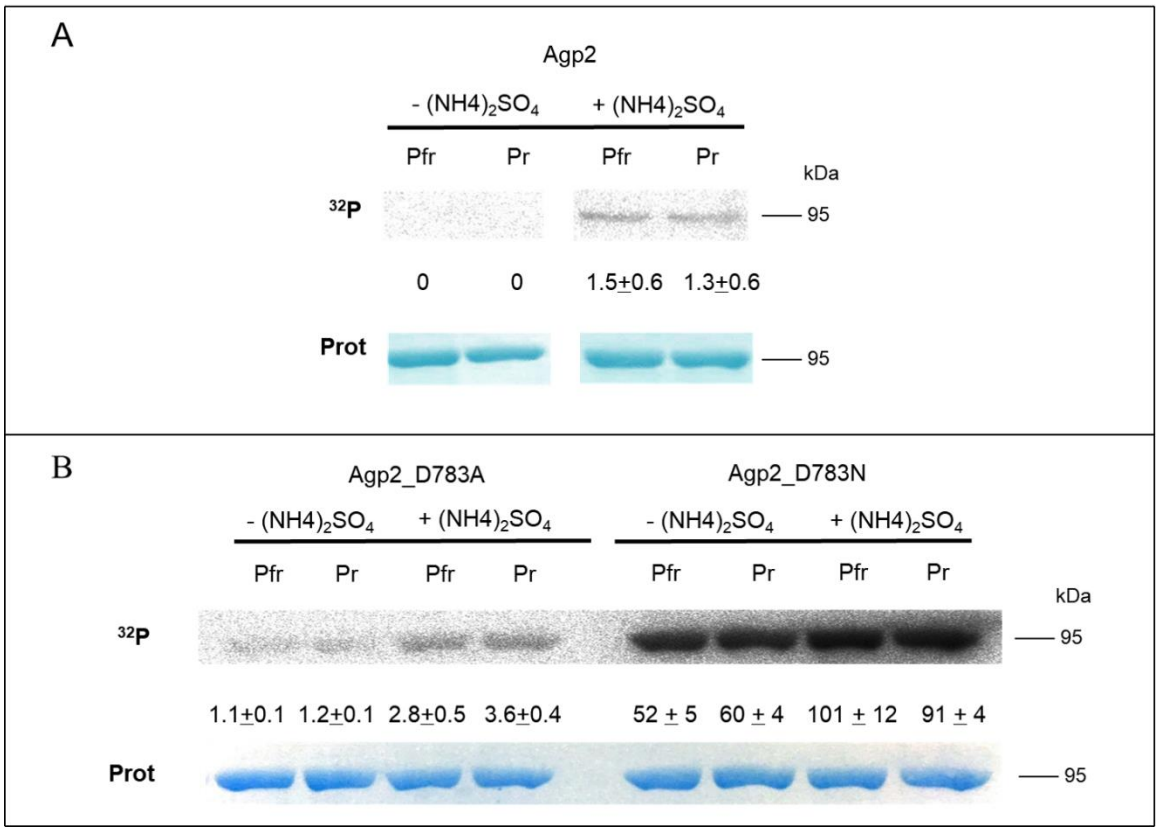

Figure 18. Phosphorylation of wild type Agp2 (A) and the mutants D783A and D783N (B). In (A, B) the concentration of $(NH_4)_2SO_4$ was always 50 mM. Typical autoradiograms are shown in above panels. In the rectangle area including a stained band, the whole pixel intensity without background was expressed as means ± SE of 5 replicates (staining intensities). All proteins were always incubated with ATPγ^{32}P for 20 minutes and films were exposed for 20 hours. The below panels show Coomassie stains.

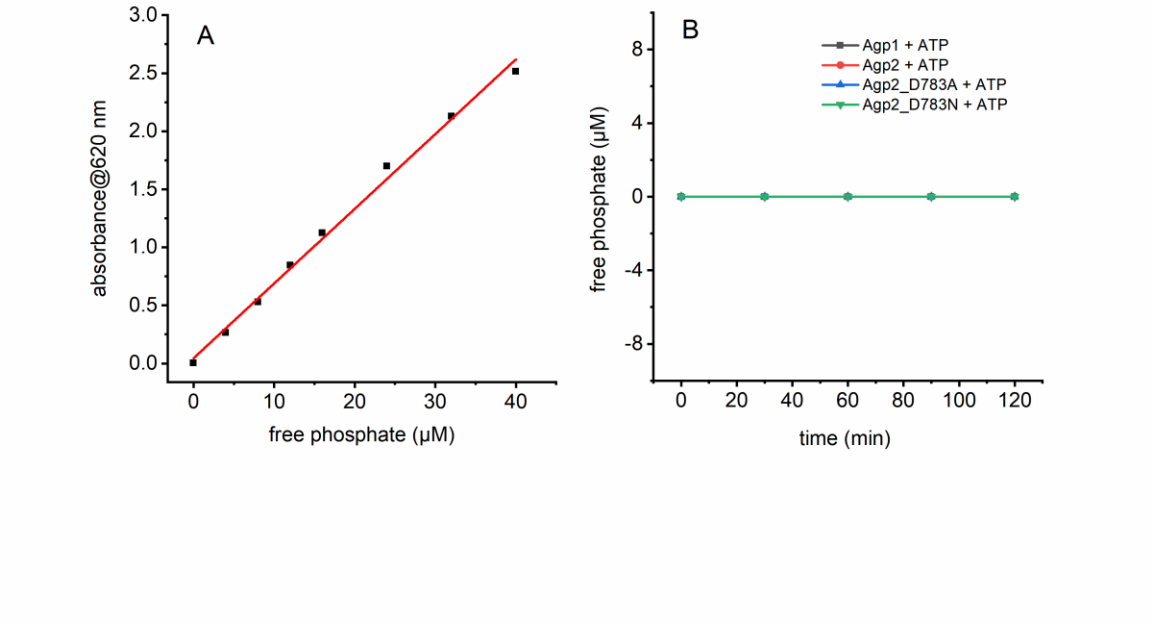

Figure 19. Free phosphate determination with the malachite green phosphate assay. (A) The standard curve of free phosphate. (B) Variations in amounts of free phosphate in the mixture of Agp1 (Pr), Agp2 (Pfr), Agp2_D783A (Pfr) or Agp2_D783N (Pfr) with ATP after different incubation times (0, 30, 60, 90 or 120 min). The absorbance was recorded at 620 nm. Three biological replicates were performed.

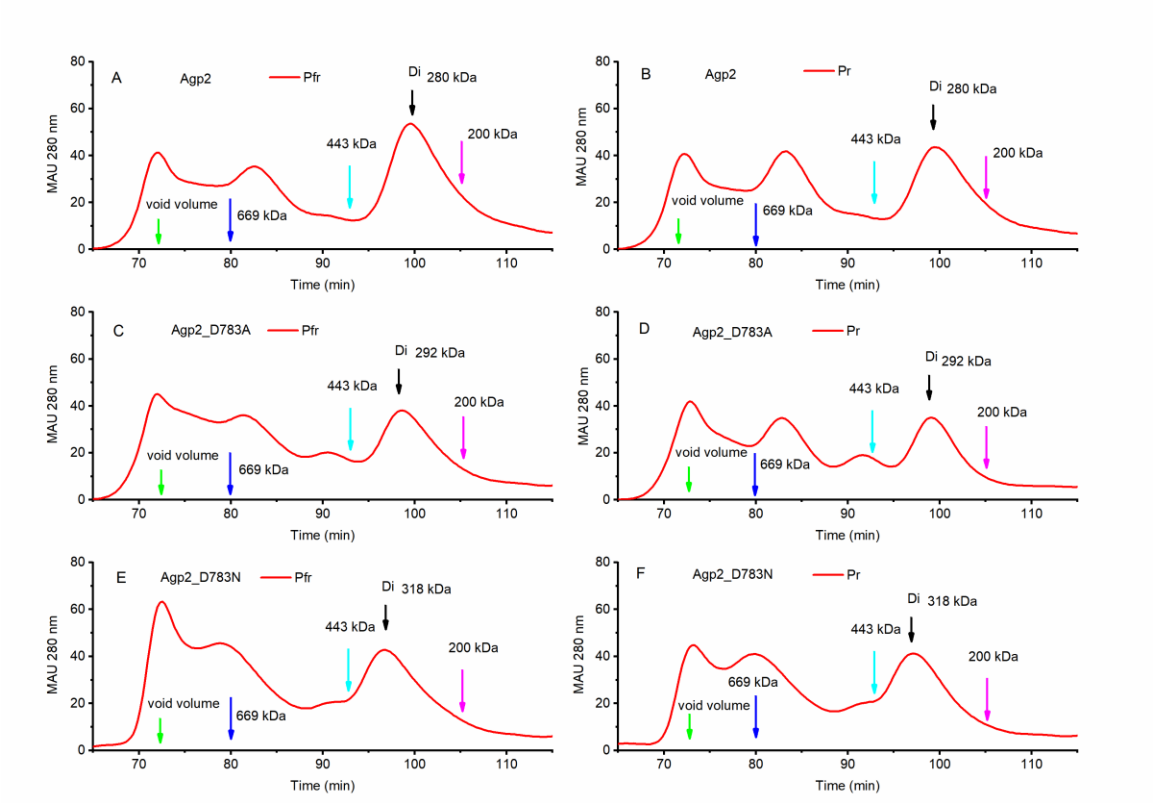

Figure 20. Size exclusion chromatography analysis of Pr and Pfr forms of Agp2 (A, B), Agp2_D783A (C, D) and Agp2_D783N (E, F). All protein concentrations were always 4 μM. The SEC elution profile was recorded at 280 nm. The dimer (Di) positions of Agp1 and Agp2 and the positions of four marker proteins are indicated by different color arrows, respectively.

I analyzed all forms combinations of Agp1 and Agp2 in the phosphorylation of mixture of Agp1 / Agp2 proteins and compared them with Agp1 or Agp2 alone, respectively. There was no visible phosphorylation of Agp2 when all ammonium sulfate was eliminated. Therefore, I just could know the effect of Agp2 on the Agp1 autophosphorylation. For Agp1 in the Pr form, the relative phosphorylation signal decreased significantly from 72 ± 1 (Agp1 alone) to 52 ± 3 (mixed with Pfr Agp2) or 55 ± 2 (mixed with Pr Agp2), respectively. Agp1 in the Pfr form had a lower signal than the Pr form, which was similar to earlier studies (Lamparter et al., 2002; Njimona and Lamparter, 2011). However, for Agp1 in the Pfr form, the signal was not influenced by Agp2 in the Pfr form or Pr form (Figure 21A). The mutant protein Agp2_D783N had high phosphorylation activity, and was therefore used to study the influence of Agp1 on the Agp2 phosphorylation activity. The effect of Agp2_D783N on the Agp1 activity in the Pr form was similar to wild type Agp2, the phosphorylation of Agp1 always decreased. In contrast to wild type Agp2, the Pfr activity of Agp1 could be inhibited by the mutant Agp2_D783N. The Pfr and Pr signals of Agp2_D783N, when mixed with Pr or Pfr of Agp1, was reduced from 38 ± 1 to 32 ± 2 and from 39 ± 3 to 30 ± 3, respectively. After incubation with Agp1-Pfr or Agp1-Pr, the Pr signal of Agp2_D783N was decreased to 31 ± 1 and increased to 44 ± 4, respectively. These results showed that Agp1 and Agp2 protein can slightly influence phosphorylation activities of Agp2 and those of Agp1, respectively. The influence of Pfr or Pr Agp2 on the Pr Agp1 was most obvious (Figure 21B). Because the concentration of ATP and each phytochromes was ca. 50 µM and 2.5 µM, respectively, I concluded that there was no competition influence between phytochromes Agp1 and Agp2.

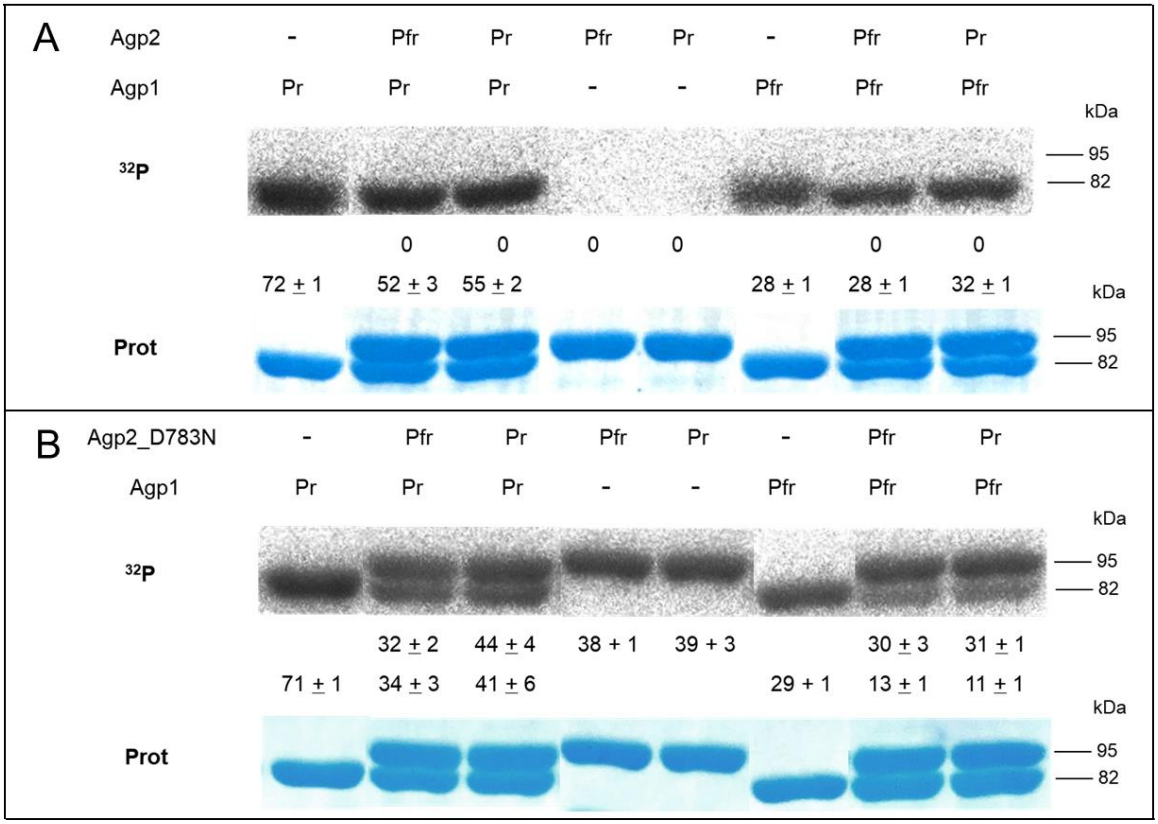

Figure 21. Change in phosphorylation of wild type Agp1 / wild type Agp2 assay (A) or wild type Agp1 / mutant Agp2_D783N assay (B). Typical autoradiogram images and Coomassie stained bands were shown on upper panels and below panels, respectively. For Agp1-Pr and Agp2-Pfr, we directly used dark states of them. For Agp1-Pfr and Agp2-Pr, the Agp1 and Agp2 of dark states were irradiated by red and far-red light before mixing, respectively. All proteins were always incubated with ATPγ^{32}P for 20 minutes and films were exposed for 20 hours. The positions at 82 kDa and 95 kDa refer to Agp1 and Agp2, respectively. In the rectangle area including a stained band, the relative staining intensities without background was expressed as mean values of 5 replicas ± SE. The sum of relative staining intensities of both Pr form of Agp1 and Pfr form of Agp1 set to value of 100.

3.4 Chromophore assembly

I also checked the influence of Agp1 and Agp2 on the chromophore assembly of each other. In the control experiments, after apo-proteins apo-Agp1 or apo-Agp2 was mixed with BV, their absorbance kinetics were measured by photometer at 700 nm or 750 nm, respectively. The spectra between 300 nm and 850 nm was also measured. In the mixture, the holo-Agp2 / BV sample was mixed with apo-Agp1 or the holo-Agp1 / BV sample mixed with apo-Agp2. The BV assembly of apo-Agp1 or apo-Agp2 was significantly effected by the other holo-protein. Earlier studies showed that the assembly of apo-Agp1 were always finished during ca. 2 min (Lamparter et al., 2002), whereas it could apparently finish after 40 min in the presence of holo-Agp2 (Figure 22). However, the time of apo-Agp2 assembly was reduced from 1 h (Karniol and Vierstra, 2003) to 25 min by holo-Agp1 (Figure 23). I speculate that the changes of BV assembly time might be due to the possible interaction between Agp1 and Agp2. The apo-Agp1 conformation could be altered by holo-Agp2, therefore the BV accession is influenced.

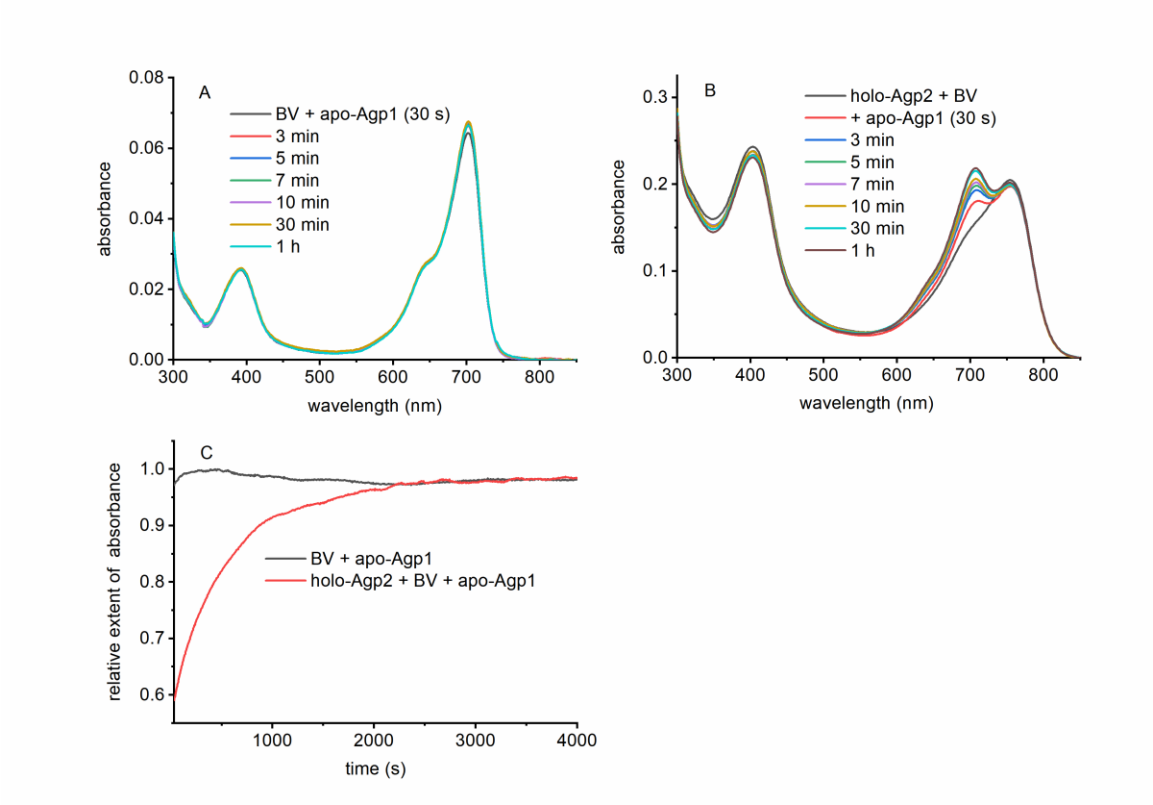

Figure 22. (A) Absorbance spectra during BV assembly of apo-Agp1. (B) Absorbance during BV assembly of apo-Agp1 with holo-Agp2. (C) Changes of the absorbance at 700 nm during apo-Agp1 assembly, black line: BV and apo-Agp1, red line: BV, apo-Agp1 and holo-Agp2 (the holo-Agp2 absorbance was set to value of 0). For both lines, the final absorbance value was scaled to 1.

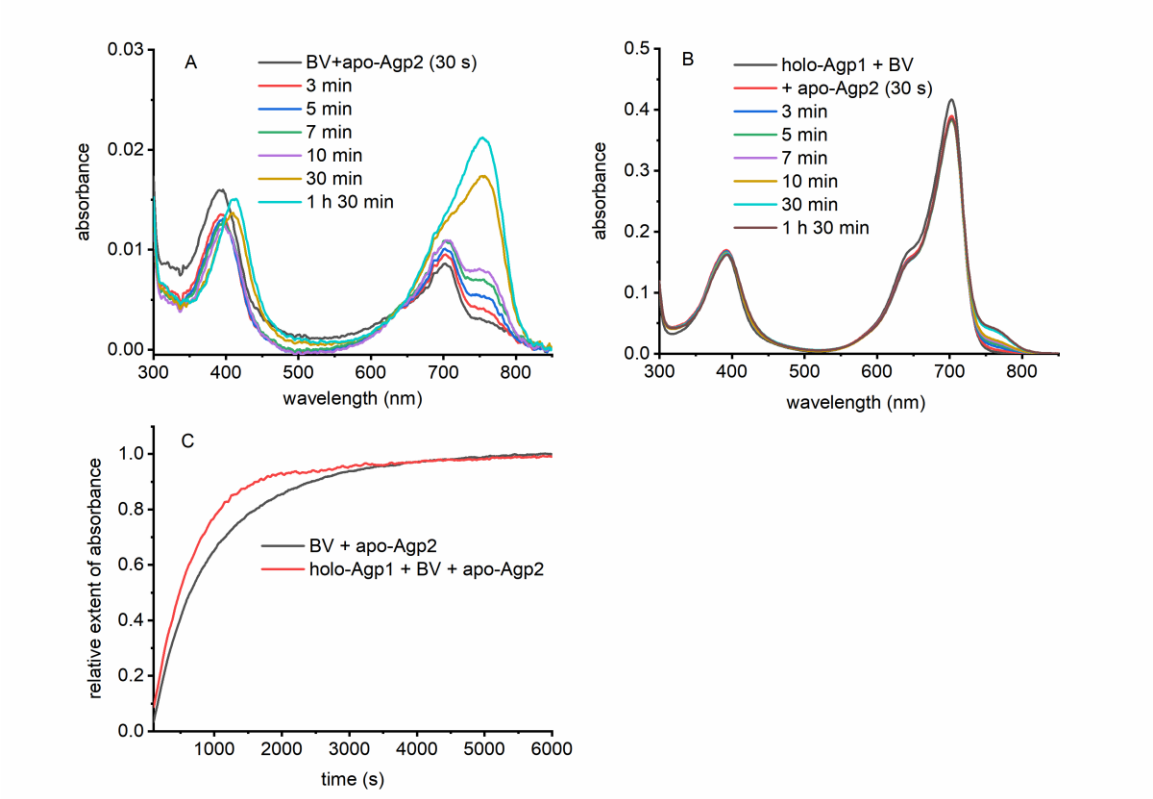

Figure 23. (A) Absorbance spectra during BV assembly of apo-Agp2. (B) Absorbance during BV assembly of apo-Agp2 with holo-Agp1. (C) Changes of the absorbance at 750 nm during apo-Agp1 assembly, black line: BV and apo-Agp2, red line: BV, apo-Agp2 and holo-Agp1 (the holo-Agp1 absorbance was set to value of 0). For both lines, the final absorbance value was scaled to 1.

4 Quantitative proteomics

4.1 Protein identification and distribution of differentially expressed proteins

In order to explore the molecular mechanism of the biological function of phytochromes in *A. fabrum*, experiment of TMT based quantitative proteomics was performed at the company of MtoZ-Biolabs Inc (United States). In this way, 2812 out of 5400 proteins were identified in the dark and light samples of *A. fabrum* WT and double mutant *agp1/2*$^{-}$. Compared with dark samples of *A. fabrum* WT, 8 up-regulated proteins and 16 down-regulated proteins were found in white light samples of *A. fabrum* WT and also 41 up-regulated proteins and 111 down-regulated proteins were observed in dark samples of *A. fabrum* double mutant *agp1/2*$^{-}$. 108 up-regulated proteins and 195 down-regulated proteins were detected in light samples of *A. fabrum* mutant as compared to those of *A. fabrum* WT. Compared to dark samples of *A. fabrum* mutant, only 26 up-regulated proteins and 4 down-regulated proteins were found in light samples of *A. fabrum* mutant. Moreover, no matter dark or white light, 16 up-regulated and 38 down-regulated proteins were always observed in mutant samples as compared to WT samples, indicating that phytochromes Agp1 and Agp2 could have white light independent regulation on those proteins in *A. fabrum* (Figure 24).

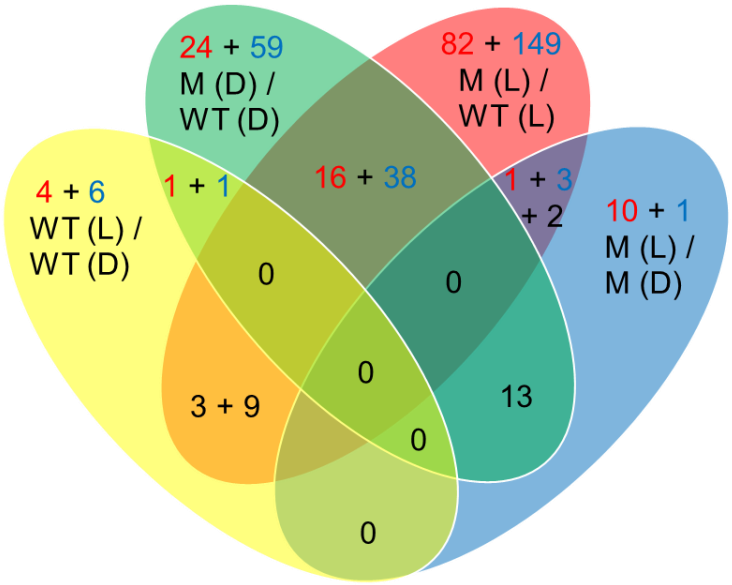

Figure 24. Distribution of differentially expressed proteins. WT (D): wild type (darkness); WT (L): wild type (white light); M (D): mutant *agp1/2*$^{-}$ (darkness); M (L): mutant *agp1/2*$^{-}$ (white light). Ratio (treated samples / control samples) > 1.5 ($P < 0.05$) and < 0.67 ($P < 0.05$) were set as significantly up-regulated (red numbers) and down-regulated (blue numbers) in treated samples, respectively. Black color number (3 + 9) means that 3 proteins were up-regulated in WT (L) samples as compared to WT (D) samples, but down-regulated in M (L) samples as compared to WT (L) samples and 9 proteins were down-regulated in WT (L) samples as compared to WT (D) samples but up-regulated in M (L) samples as compared to WT (L) samples. Black color number 2 means that up-regulated in M (L) samples as compared to M (D) samples, however down-regulated in M (L) samples as compared to WT (L) samples. Black color number 13 means that up-regulated in M (L) samples as compared to M (D) samples whereas down-regulated in M (D) samples as compared to WT (D) samples. The sum of differentially expressed proteins is 422 and that of identified protein is 2812. 353 and 134 proteins were only observed in both WT (L) and M (L) samples and both WT (D) and M (D) samples, respectively.

4.2 Analysis for differentially expressed proteins

In *A. fabrum*, phytochromes play positive roles in the movement (unpublished data from Dr. Yingnan Bai), conjugation (Bai et al., 2016) and plant infection which were directly regulated by motility proteins, conjugation proteins and virulence proteins, respectively. Of the 28 chemotaxis proteins of flagellar system of bacterial motility proteins of *A. fabrum*, cheB (Atu0519), cheW (Atu2075), cheW (Atu2617), cheY (Atu0516), cheY (Atu0520), mcpA (Atu0646), mcpC (Atu0872) and mcpV (Atu1027) were detected (Table 3). Of the 34 flagellar assembly proteins of flagellar system of bacterial motility proteins of *A. fabrum*, fla (Atu0542), flaA (Atu0545), flaB (Atu0543), flaD (Atu0567), flgE (Atu0574), flgK (Atu0575), flgL (Atu0576), fliN (Atu0562), fliP (Atu0546), motB (Atu3746) and motC (Atu0570) were detected (Table 4). Of the 10 proteins of pilus system of bacterial motility proteins of *A. fabrum*, ctpA (Atu0224), ctpC (Atu0222), ctpD (Atu0221), ctpE (Atu0220) and Atu4732 were detected (Table 5). Of the 22 conjugation proteins, only 4 were detected, traC (Atu6126), traD (Atu5109), mobC (Atu4857) and the AT-plasmid encoded traA (Atu5111) (there are 3 different traA genes in *A. fabrum*) (Table 6). Of the 26 proteins of T4SS of *A. fabrum*, avhB1 (Atu5162), avhB4 (Atu5165), avhB5 (Atu5166), avhB7 (Atu5168), virB7 (Atu6173), avhB8 (Atu5169), avhB9 (Atu5170) and avhB10 (Atu5171) were detected (Table 7). Of 26 virulence proteins without a protein of type IV secretion system of *A. fabrum*, only 2 virulence proteins virH1 (Atu6187) and acvB (Atu2522) were found (Table 8). However, proteins that regulate the infection of plant tissue such as VirA, VirG, VirD or VirE were lacking. Also, both phytochromes were not detected. Lack of detection is most likely due to low expression levels of proteins with regulatory functions or with rapid turnover.

After analysis of differentially expressed proteins, changes in mcpC (Atu0872) of chemotaxis protein (Table 3), motC (Atu0570) of flagellar assembly (Table 4) and ctpE (Atu0220) of pilus system (Table 5) were closely related to changes of *A. fabrum* movement regulated by the phytochromes. I also found that decrease in the expression of AT-plasmid encoded conjugation protein traA (Atu5111) in *A. fabrum agp1/2*$^{-}$ mutant (darkness) as compared to *A. fabrum* WT (darkness) (Table 6) was consistent with the

reduced rate of conjugation, indicating that phytochromes could influence the expression of traA (Atu5111) to regulate the conjugation in *A. fabrum*. In addition, all compounds of T6SS and three toxin-immunity pairs playing an important role in the interbacterial competition (Ma et al., 2014) were also detected. Of the 5 proteins of T6SS, vgrG (Atu4348), hcp (Atu4345), impL (Atu4332), impK (Atu4333) and clpB (Atu4334) were detected. Of three toxin-immunity pairs of T6SS, Atu4350 (1-toxin), Atu4351 (1-immunity), Atu3640 (2-toxin), Atu3639 (2-immunity), Atu4347 (3-toxin) and Atu4346 (3-immunity) were detected. No matter in dark or white light, there was always a significant reduction of hcp (Atu4345) in *A. fabrum agp1/2*$^{-}$ mutant as compared to WT. Moreover, under white light, the decrease of Atu4347 (3-toxin) protein was obvious in *A. fabrum* mutant as compared to WT (Table 9). These revealed that phytochromes of *A. fabrum* could control the interbacterial competition.

Table 3. The list of detected proteins of chemotaxis proteins of flagellar system of bacterial motility proteins of *Agrobacterium fabrum*. cheA (Atu0517), Atu0515, cheD (Atu0521), cheR (Atu0518), Atu4805, cheD (Atu2618), mcpA (Atu3094), mcpA (Atu6132), mcpG (Atu0738), mcpA (Atu2360), Atu0514, mcpA (Atu2173), Atu0373, mclA (Atu1912), mclA (Atu0526), mcpA (Atu0387), mcpA (Atu2223), Atu5442, Atu4736 and Atu3725 were not detected. WT (D): wild type (darkness); WT (L): wild type (white light); M (D): mutant *agp1/2*$^{-}$ (darkness); M (L): mutant *agp1/2*$^{-}$ (white light); Mean values of 3 biological replicates ± SE.

Protein	Abundances				Fold change >1.5 or < 0.67; $P < 0.1$ (*) or $P < 0.05$ (**)
	WT (D)	WT (L)	M (D)	M (L)	
cheB (Atu0519)	117 ± 40	115 ± 15	106 ± 28	85 ± 8	
cheW (Atu2075)	114 ± 5		100 ± 25		
cheW (Atu2617)	99 ± 10	118 ± 8	84 ± 2	82 ± 10	
cheY (Atu0516)	95 ± 8	102 ± 6	112 ± 25	98 ± 10	
cheY (Atu0520)	114 ± 2	113 ± 11	80 ± 3	87 ± 8	
mcpA (Atu0646)		133 ± 36		67 ± 10	
mcpC (Atu0872)	118 ± 24		47 ± 10		M(D) / WT(D)=0.40 *
mcpV (Atu1027)	83 ± 9	65 ± 6	112 ± 22	135 ± 57	

Table 4. The list of detected proteins of flagellar assembly proteins of flagellar system of bacterial motility proteins of *Agrobacterium fabrum*. flaF (Atu0577), flbT (Atu0578), flgA (Atu0551), flgB (Atu0555), flgC (Atu0554), flgD (Atu0579), flgF (Atu0558), flgG (Atu0552), flgH (Atu0548), flgI (Atu0550), flhA (Atu0581), flhB (Atu0564), fliE (Atu0553), fliF (Atu0523), fliG (Atu0563), fliI (Atu0557), fliL (Atu0547), fliM (Atu0561), fliQ (Atu0580), fliR (Atu0582), motA (Atu0560), motB (Atu0569) and motD (Atu0571) were not detected. WT (D): wild type (darkness); WT (L): wild type (white light); M (D): mutant *agp1/2*$^{-}$ (darkness); M (L): mutant *agp1/2*$^{-}$ (white light); Mean values of 3 biological replicates ± SE.

Protein	Abundances				Fold change >1.5 or < 0.67; $P < 0.1$ (*) or $P < 0.05$ (**)
	WT (D)	WT (L)	M (D)	M (L)	
fla (Atu0542)	103 ± 3	85 ± 6	99 ± 9	115 ± 17	
flaA (Atu0545)	82 ± 6	71 ± 2	131 ± 16	129 ± 25	M(D) / WT(D)=1.60 **; M(L) / WT(L)=1.82 **
flaB (Atu0543)	81 ± 8	72 ± 4	133 ± 8	129 ± 21	M(D) / WT(D)=1.64 **; M(L) / WT(L)=1.80 *
flaD (Atu0567)	105 ± 4	122 ± 21	93 ± 12	79 ± 4	
flgE (Atu0574)	106 ± 8	107 ± 12	98 ± 8	93 ± 4	
flgK (Atu0575)	104 ± 8	114 ± 16	105 ± 27	86 ± 2	
flgL (Atu0576)		91 ± 10		109 ± 11	
fliN (Atu0562)	99 ± 8	86 ± 2	134 ± 36	114 ± 5	
fliP (Atu0546)		93 ± 17		107 ± 19	
motB (Atu3746)	88 ± 20	81 ± 3	114 ± 38	120 ± 16	
motC (Atu0570)	148 ± 42	157 ± 53	29 ± 2	43 ± 2	M(D) / WT(D)=0.20 **; M(L) / WT(L)=0.27 *

Table 5. The list of detected proteins of pilus system of bacterial motility proteins of *Agrobacterium fabrum*. pilA (Atu3514), ctpB (Atu0223), ctpF (Atu0219), ctpG (Atu0218) and Atu4731 were not detected. WT (D): wild type (darkness); WT (L): wild type (white light); M (D): mutant *agp1/2*$^{-}$ (darkness); M (L): mutant *agp1/2*$^{-}$ (white light); Mean values of 3 biological replicates ± SE.

Protein	Abundances				Fold change >1.5 or < 0.67; $P < 0.1$ (*) or $P < 0.05$ (**)
	WT (D)	WT (L)	M (D)	M (L)	
ctpA (Atu0224)	94 ± 5	79 ± 7	111 ± 33	121 ± 9	M(L) / WT(L)=1.53 **
ctpC (Atu0222)	82 ± 20	118 ± 13	78 ± 6	82 ± 5	
ctpD (Atu0221)	99 ± 6	97 ± 6	135 ± 24	103 ± 10	M (D) / WT (D)=0.33 **; M (L) / WT (L)=0.54 **
ctpE (Atu0220)	175 ± 23	130 ± 13	58 ± 15	70 ± 3	
Atu4732	93 ± 12	99 ± 4	101 ± 3	101 ± 14	

Table 6: The list of detected proteins of conjugation of *Agrobacterium fabrum*. traA (Atu4855), traA (Atu6127), traB (Atu6129), traC (Atu5110), traF (Atu6128), traG (Atu5108), traG (Atu6124), traH (Atu6130), trbB (Atu6041), trbC (Atu6040), trbD (Atu6039), trbE (Atu6038), trbF (Atu6034), trbG (Atu6033), trbH (Atu6032), trbI (Atu6031), trbJ (Atu6037), trbL (Atu6035) were not detected. WT (D): wild type (darkness); WT (L): wild type (white light); M (D): mutant *agp1/2*$^{-}$ (darkness); M (L): mutant *agp1/2*$^{-}$ (white light); Mean values of 3 biological replicates ± SE.

Protein	Abundances				Fold change >1.5 or < 0.67; $P < 0.1$ (*) or $P < 0.05$ (**)
	WT (D)	WT (L)	M (D)	M (L)	
mobC (Atu4857)	87 ± 9	96 ± 6	138 ± 15	104 ± 11	M (D) / WT (D)=1.59 **
traA (Atu5111)	147 ± 22		49 ± 15		M (D) / WT (D)=0.33 **
traC (Atu6126)	69 ± 6	67 ± 6	161 ± 13	133 ± 13	M (D) / WT (D)=2.34 **; M (L) / WT (L)=2 **
traD (Atu5109)	85 ± 13	87 ± 1	133 ± 14	113 ± 5	M (D) / WT (D)=1.56 *

Table 7. The list of detected proteins of type IV secretion system of *Agrobacterium fabrum*. virB1 (Atu6167), avhB2 (Atu5163), virB2 (Atu6168), avhB3 (Atu5164), virB3 (Atu6169), virB4 (Atu6170), virB5 (Atu6171), avhB6 (Atu5167), virB6 (Atu6172), virB8 (Atu6174), virB9 (Atu6175), virB10 (Atu6176), avhB11 (Atu5172), virB11 (Atu6177), Atu4858 (traG), Atu5108 (traG), Atu6124 (traG) and virD4 (Atu6184) of type IV secretion system were not detected. WT (D): wild type (darkness); WT (L): wild type (white light); M (D): mutant *agp1/2*$^-$ (darkness); M (L): mutant *agp1/2*$^-$ (white light); Mean values of 3 biological replicates ± SE.

Protein	Abundances				Fold change >1.5 or < 0.67; $P < 0.1$ (*) or $P < 0.05$ (**)
	WT (D)	WT (L)	M (D)	M (L)	
avhB1 (Atu5162)	59 ± 4	88 ± 9	145 ± 19	112 ± 3	WT (L) / WT (D)=1.50 **; M (D) / WT (D)=2.46 **
avhB4 (Atu5165)	78 ± 3	69 ± 5	133 ± 29	131 ± 23	M (L) / WT (L)=1.89 *
avhB5 (Atu5166)	69 ± 1	100 ± 2	132 ± 57	100 ± 5	
avhB7 (Atu5168)	82 ± 11	79 ± 11	121 ± 23	121 ± 4	M (L) / WT (L)=1.52 **
virB7 (Atu6173)	100 ± 5		133 ± 21		
avhB8 (Atu5169)	89 ± 19	96 ± 13	100 ± 20	104 ± 9	
avhB9 (Atu5170)	74 ± 4	81 ± 9	137 ± 2	119 ± 7	M (D) / WT (D)=1.85 **
avhB10 (Atu5171)	74 ± 5	66 ± 5	136 ± 1	134 ± 4	M (D) / WT (D)=1.84 **; M (L) / WT (L)=2.01 **

Table 8. The list of detected proteins of virulence proteins without a protein of type IV secretion system of *Agrobacterium fabrum*. virA (Atu6166), virC1 (Atu6180), virC2 (Atu6179), virD1 (Atu6181), virD2 (Atu6182), virD3 (Atu6183), avhD4 (Atu4858), virD4 (Atu6184), virD5 (Atu6185), virE0 (Atu6188), virE1 (Atu6189), virE2 (Atu6190), virE3 (Atu6191), virE3 (Atu6186), virF (Atu6154), virG (Atu6178), virK (Atu6156), mviN (Atu0347), trlR (Atu6192), Atu6193, Atu6194, Atu6195, Atu6196 and Atu6197 were not detected. WT (D): wild type (darkness); WT (L): wild type (white light); M (D): mutant *agp1/2*$^{-}$ (darkness); M (L): mutant *agp1/2*$^{-}$ (white light); Mean values of 3 biological replicates ± SE.

Protein	Abundances				Fold change >1.5 or < 0.67; $P < 0.1$ (*) or $P < 0.05$ (**)
	WT (D)	WT (L)	M (D)	M (L)	
virH1 (Atu6187)	105 ± 10	115 ± 2	97 ± 3	85 ± 5	
acvB (Atu2522)	104 ± 3	111 ± 3	98 ± 9	89 ± 5	

Table 9. The list of detected proteins of Type VI secretion system and three toxin-immunity pairs - *Agrobacterium fabrum*. WT (D): wild type (darkness); WT (L): wild type (white light); M (D): mutant *agp1/2*$^{-}$ (darkness); M (L): mutant *agp1/2*$^{-}$ (white light); Mean values of 3 biological replicates ± SE.

Protein	Abundances				Fold change >1.5 or < 0.67; $P < 0.1$ (*) or $P < 0.05$ (**)
	WT (D)	WT (L)	M (D)	M (L)	
Type VI secretion system					
vgrG (Atu4348)	87 ± 2	81 ± 7	146 ± 82	119 ± 20	
hcp (Atu4345)	114 ± 9	126 ± 9	76 ± 1	74 ± 4	M (D) / WT (D)=0.67 **; M (L) / WT (L)=0.59 **
impL (Atu4332)	86 ± 4	84 ± 4	115 ± 12	116 ± 12	
impK (Atu4333)	96 ± 5	86 ± 6	96 ± 7	114 ± 11	
clpB (Atu4334)	107 ± 7	89 ± 4	85 ± 8	111 ± 11	
Effectors of three toxin-immunity pairs of type VI secretion system					
Atu4350 (1-toxin)	105 ± 5	101 ± 1	98 ± 9	99 ± 8	
Atu4351 (1-immunity)	101 ± 4	117 ± 3	103 ± 5	83 ± 9	
Atu3640 (2-toxin)	93 ± 7	103 ± 14	106 ± 24	97 ± 3	
Atu3639 (2-immunity)	94 ± 11	97 ± 2	113 ± 15	103 ± 8	
Atu4347 (3-toxin)	114 ± 2	123 ± 7	85 ± 1	77 ± 3	M (L) / WT (L)=0.63 **
Atu4346 (3-immunity)	90 ± 8	99 ± 5	121 ± 7	101 ± 8	

5 The effect of Agp1 and Agp2 on the interbacterial competition

Here TMT-based quantitative proteomics results showed that there was a significant reduction of the T6SS haemolysin-coregulated protein (Au4345) and putative peptidoglycan amidase effector (Atu4347) in *A. fabrum agp1/2*$^{-}$ double mutant as compared with *A. fabrum* WT (Table 9). Earlier reports indicated that *A. fabrum* could inject DNase effectors into the *E. coli* DH10B to finally kill the cells through T6SS (Ma et al., 2014). Therefore, I tested the competition between *A. fabrum* WT, *agp1*$^{-}$, *agp2*$^{-}$, or *agp1/2*$^{-}$ mutant and *E. coli* DH5α on LB agar. Surprisingly, there was no different survival numbers of *E. coli* DH5α among control (*E. coli* DH5α), WT (*E. coli* DH5α + *A. fabrum* WT) and *agp1/2*$^{-}$ (*E. coli* DH5α + *A. fabrum agp1/2*$^{-}$) assays. *A. fabrum agp1*$^{-}$ mutant could kill *E. coli* DH5α in darkness but the red or far-red light suppressed the attack. In contrast, *E. coli* DH5α could not be killed by *A. fabrum agp2*$^{-}$ in darkness, whereas in red light condition *E. coli* DH5α was killed (Figure 25).

To investigate whether phytochromes Agp1 and Agp2 regulates the competition between *A. fabrum* and other soil bacterium, interbacterial competition was performed by inoculating *A. fabrum* WT or *agp1/2*$^{-}$ mutant with other soil bacterium in LB for a given time. The quantitative proteomics results showed that abundance of hcp (Atu4345) of T6SS in *A. fabrum agp1/2*$^{-}$ mutant was decreased to 67 % as compared with that of wild type (Table 6). To know whether the mutant could compensate for the protein reduction by increasing the amount of bacteria, the initial amount ratio of *A. fabrum* WT / *A. fabrum* mutant *agp1/2*$^{-}$ was 0.67, 50 ml *A. fabrum* WT (OD_{600}=2) or 50 ml *A. fabrum* mutant *agp1/2*$^{-}$ (OD_{600}=3) to mix with 50 ml other soil bacterium (OD_{600}=2). After quantitatively sequencing the hypervariable region V2 of 16S rRNA gene, composition of WT or *agp1/2*$^{-}$ mutant *A. fabrum* in the competition assay was obtained (Figure 26). Yuanyuan Ma from Zoological Institute, Kiel University (Germany), contributed to the 16S rRNA experiment. For WT *A. fabrum*, the percentage was stable at 57 % after 12 h incubation under darkness or white light as compared with initial assay. However, the *agp1/2*$^{-}$ mutant *A. fabrum* decreased significantly from 65 % to 56% (darkness) and from 65 % to 44 % (white light) during the 12 h competition (Figure 27). Alone, the growth

rate of *agp1/2*$^{-}$ mutant *A. fabrum* was higher than that of WT *A. fabrum* (Figure 7 and 8). Here an obvious reduction of *A. fabrum agp1/2*$^{-}$ mutant in the competition assay was detected. These data suggested that phytochromes improved the competition ability in the *A. fabrum*.

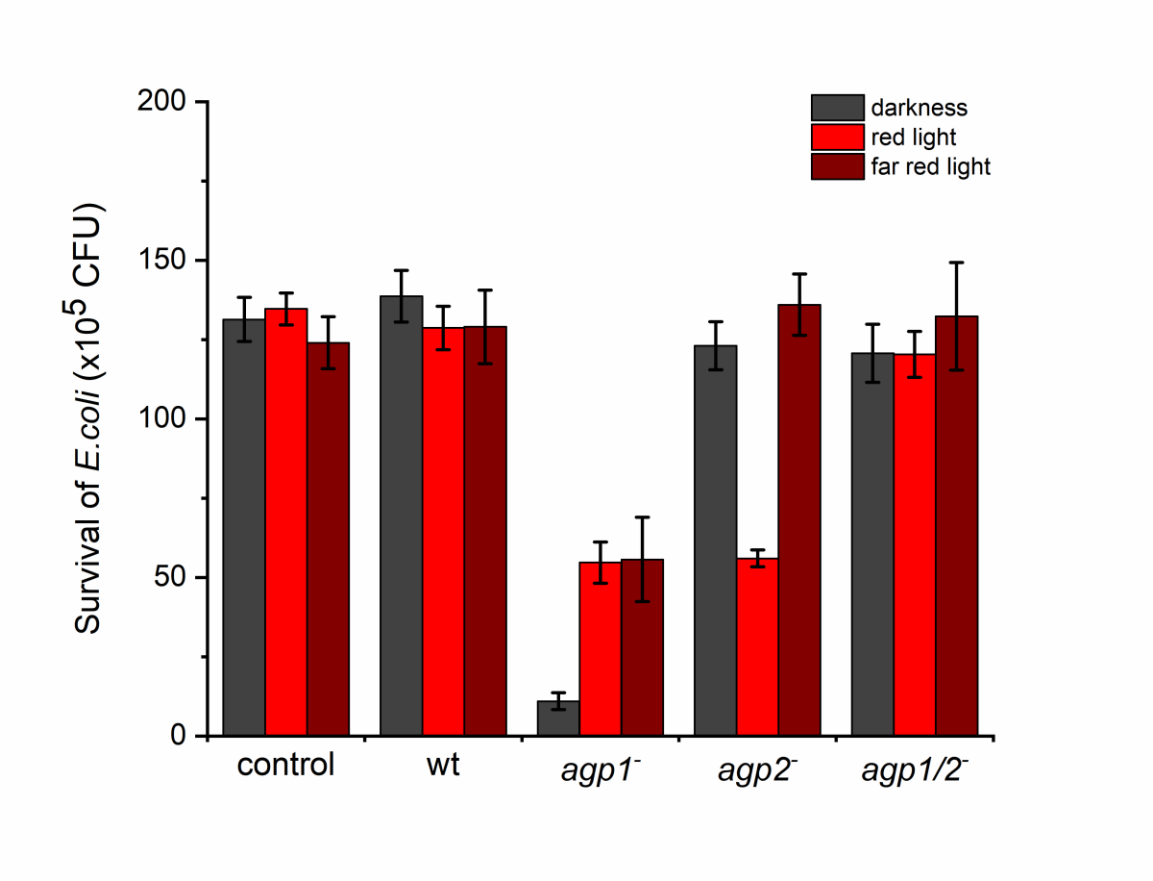

Figure 25. Competition assays of *A. fabrum-E.coli*. For each treatment, there are 3 biological replicates.

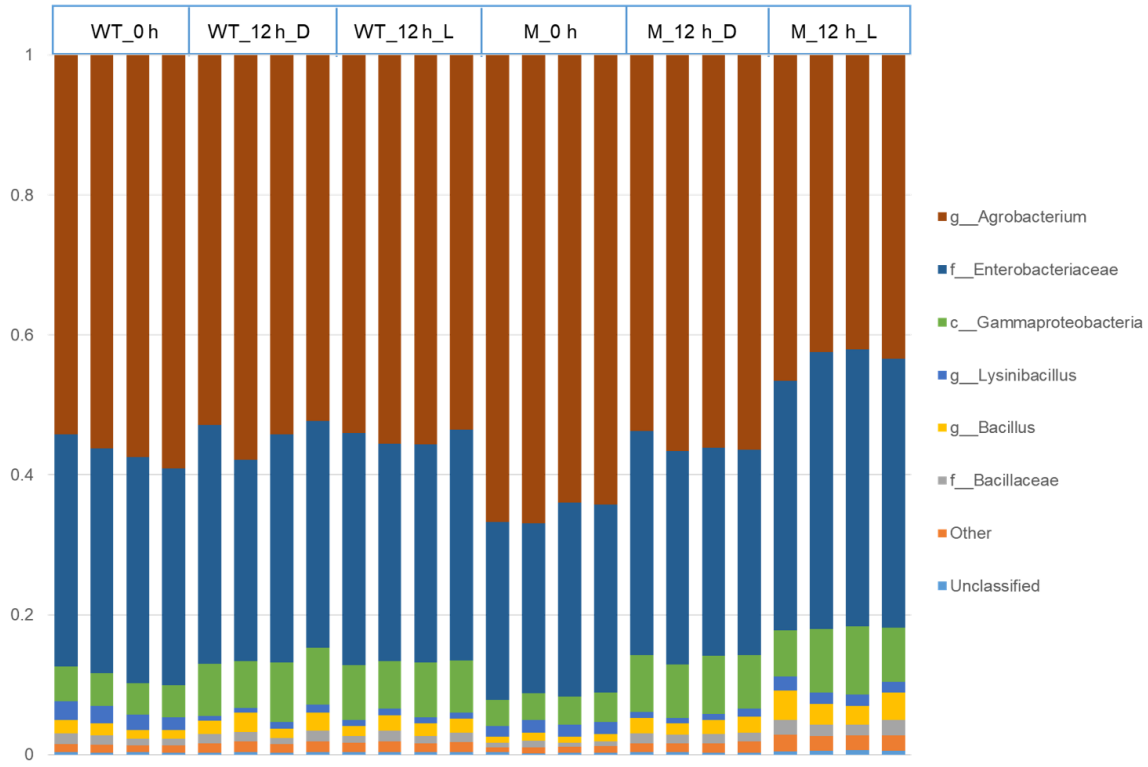

Figure 26. Changes in bacterial composition. *A. fabrum* WT and *agp1/2*$^{-}$ mutant (M) competitive activity against other soil bacterium. There are 4 biological replicates for each treatment showed on the top of graph. The numbers between 0 and 1 of bar left mean the relative abudance of bacteria in each competition assay. WT_0 h: wild type_0 hour; M_0 h: mutant_0 hour; WT_12 h_D: wild type_0 hour_darkness; M_0 h_D: mutant_0 hour_darkness; WT_12 h_L: wild type_0 hour_white light; M_0 h_L: mutant_0 hour_white light; g: genus; f: family; c: class

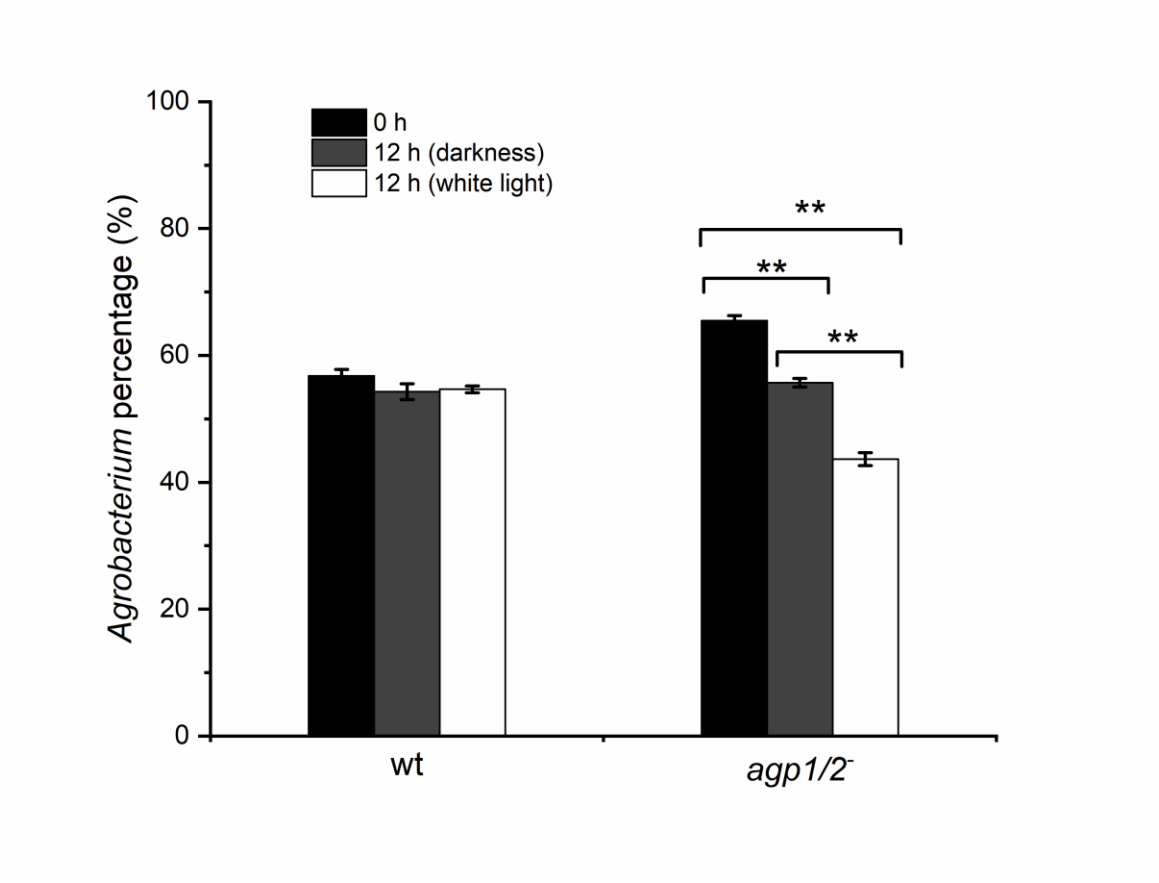

Figure 27. Changes in percentage of *A. fabrum* WT or *agp1/2*$^{-}$ mutant in the competition assays under darkness or white light. Mean values of 4 biological replicates ± SE. **=*P* <0.01.

Discussion

1 Importance of the phytochromes Agp1, Agp2 and their homologues in *Agrobacterium* species

Two phytochromes termed Agp1 and Agp2 or AtBphP1 and AtBphP2 were discovered in *A. fabrum* (Goodner et al., 2001; Karniol and Vierstra, 2003; Lamparter et al., 2002; Wood et al., 2001). For a long time, the role of these photoreceptors has been unclear. Recently, it was described that the conjugation (Bai et al., 2016) and movement (unpublished data from Dr. Yingnan Bai) were under these two phytochromes control. The root infection assay of *Arabidopsis thaliana* with *A. fabrum* wild type and *agp1/2*$^{-}$ double knockout mutant indicated that plant infection could be under phytochromes Agp1 and Agp2 control (Rottwinkel, 2011). Here I show by mutant studies that also *A. fabrum* growth (Figure 7, 8, 9 and 10), plant stem or leaf infection (Figure 11, 12 and 13) and interbacterial competition (Figure 25, 26 and 27) are effected by these phytochromes.

In order to know which phytochrome is more important for survival or evolution, I investigated the distribution of phytochromes Agp1, Agp2 and their homologues in genus *Agrobacterium*. This indicated that Agp2 could be more important than Agp1 (Table 1). Moreover, the growth results implied that the high temperature tolerance in *A. fabrum* could be positively regulated by Agp2 (Figure 9). Therefore, Agp2 may be more important for survival as compared with Agp1 in *Agrobacterium* species. Maybe all *Agrobacterium* bacterium have a common ancestor with two phytochromes and in some strains either one of phytochromes was lost during evolution.

Agp2 is a bathy phytochrome which dark state is Pfr and absorb maximally in the 750 nm wavelength range (Karniol and Vierstra, 2003; Rottwinkel et al., 2010), whereas Agp1 has a Pr dark state and absorb maximally in the 700 nm wavelength range (Lamparter et al., 2002). Together these data show that the detection of the long wavelength red light seems to be more relevant for living and evolution of *Agrobacterium*.

2 Signal transduction of phytochromes Agp1 and Agp2

In the process of conjugation, the TraA protein plays a central role. This relaxase (Figure 28) cleaves firstly a single strand DNA in plasmid, and then binds covalently to the end of DNA and finally separates the two strands (Fuqua et al., 1995; Garcillan-Barcia et al., 2009; Smillie et al., 2010). Both codistribution of phytochromes Agp1/2 and TraA (Figure 29) and Ti-plasmid mutant studies of *A. fabrum* indicated that those phytochromes may directly or indirectly interact with TraA protein to control the conjugation in *A. fabrum* (Bai et al., 2016; Lamparter, 2006). Analogously, the results of TMT-based quantitative proteomics also showed that phytochromes could influence the expression of TraA protein to regulate the conjugation.

For the signal transduction of the plant infection controlled by phytochromes Agp1 and Agp2, there was no positive information from the results of quantitative proteomics. The process of plant infection is initiated by a relaxase termed VirD2 (Atu6182) (Figure 30), which nicks the pTi plasmid at *oriT* position and covalently binds to single stranded T-DNA (Yanofsky et al., 1986). However, the VirD2 protein was not detected by quantitative proteomics. The VirD2 function in the plant infectionis similar with TraA in conjugation. Therefore, I assume that phytochromes may interact with VirD2 protein to regulate the plant infection in *A. fabrum*.

According to the quantitative proteomics results, I also found that phytochromes of *A. fabrum* could affect the hcp (Atu4345) and Atu4347 (3-toxin) proteins of T6SS which plays an important role interbacterial competition. Therefore, it was tested by the interbacterial competition assays between *A. fabrum* WT or mutant *agp1/2*$^{-}$ and other soil bacterium. Finally, the speculation of interbacterial competition controlled by phytochromes in *A. fabrum* was proved. Other methods such as western blotting to verify quantitative proteomics were not tested. However, experiment of interbacterial competition could indicate that the results of differentially expressed proteins were reliable.

In summary, our results helps understanding the role of phytochromes and their signal transduction in *A. fabrum*.

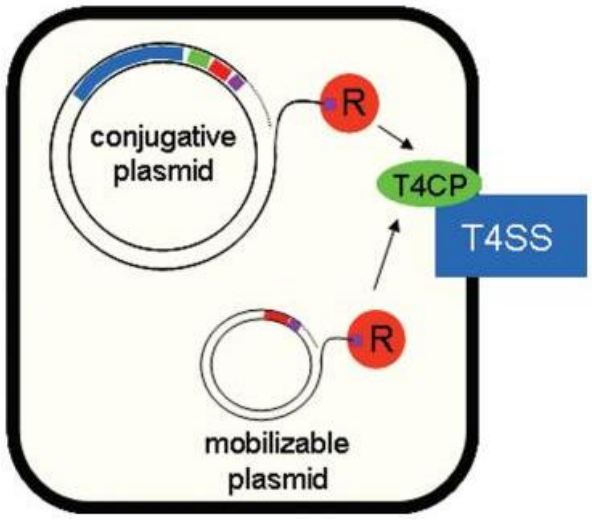

Figure 28. Schematic view of the process of bacterial conjugation. R: a relaxase; T4CP: a type IV coupling protein; T4SS: type IV secretion system. Figure from (Smillie et al., 2010).

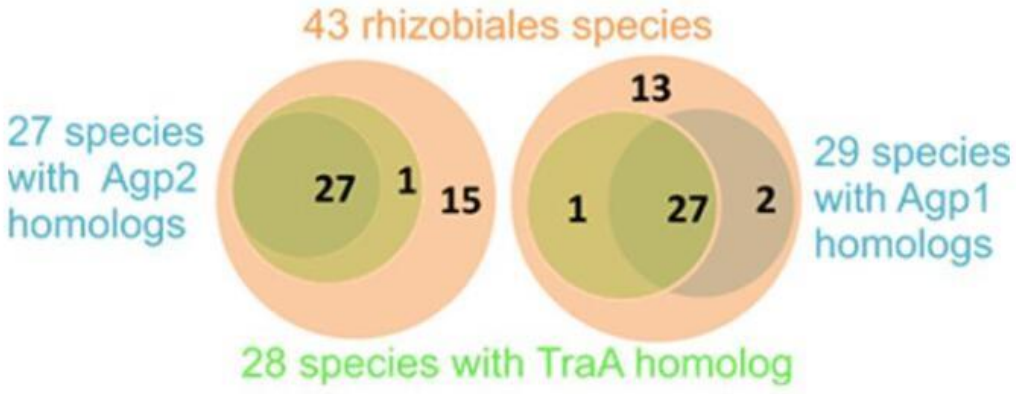

Figure 29. Codistribution of phytochromes Agp1 / Agp2 and conjugaton protein TraA in Rhizobiales. Figure from (Bai et al., 2016).

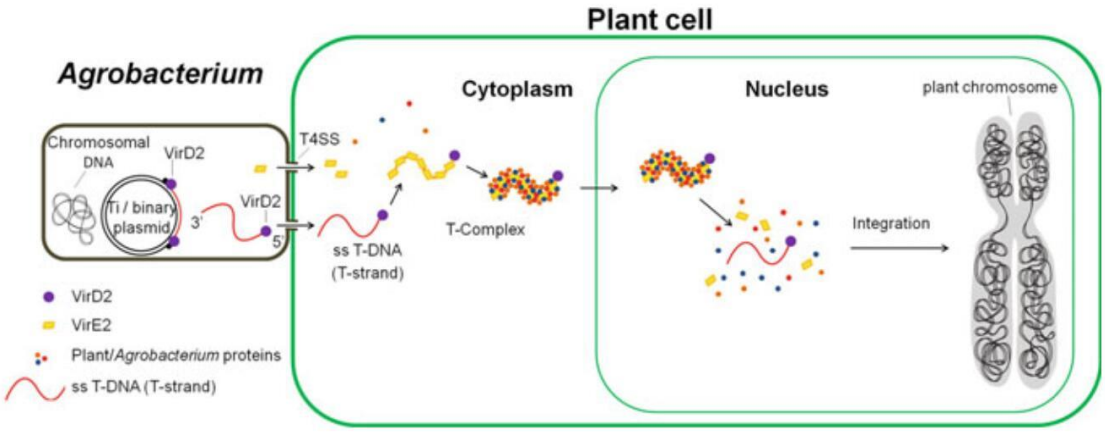

Figure 30. Schematic view of Ti-DNA transfer from *Agrobacterium* plasmid to plant chromosome in the process of plant infection. Figure from (Singer, 2018; Singer, 2013).

3 Interaction between phytochromes Agp1 and Agp2

Light controls the conjugation of *A. fabrum* via phytochromes Agp1 and Agp2. The contribution of Agp1 in the conjugation is similar with that of Agp2 (Bai et al., 2016). Therefore, the possible interaction between both phytochrome proteins was tested *in vitro*. For protein-protein interaction, one standard assay, SEC, was firstly used. When proteins enter the gel matrix of SEC, they will be quickly diluted. Therefore, there is a change in elution maxima of interacting proteins. Moreover, experiments of UV-vis spectra, dark conversion, autophosphorylation and BV assembly proved the theory. The one phytochrome protein could slightly change the properties of the other protein.

In our researches, no phosphorylation signal was observed in Agp2 protein. The result conflicts with previous studies (Karniol and Vierstra, 2003) that observed a clear phosphorylation signal in Pr and Pfr forms of Agp2. There was a strong autophosphorylation signal in phytochrome FphA, which was a fungal phytochrome with

response regulator at the C-terminal. However, there was no obvious difference between Pfr and Pr forms (Brandt et al., 2008). In our researches of Agp2, I only obtained weak and strong autophosphorylation in mutants Agp2_D783A and Agp2_D783N, respectively, where the aspartic acid (putative receiver amino acid) of the Agp2 response regulator was mutated. I initially thought that there could be a rapid dephosphorylation in the response regulator, resulting in the missing Agp2 autophosphorylation signal. For many response regulators, dephosphorylation activity is reported (Immormino et al., 2016). In the Agp2 sample incubated with ATP, no free phosphate was detected, therefore, the guess of rapid turnover of phosphate was rejected. SEC results showed that there was an obvious conformational shift between Agp2 WT and mutants. This conformational change is most probably dependent on the presence or absence of a charge at position 783 of Agp2. The relative extent of SEC mobility shifts of mutants Agp2_D783A and Agp2_D783N were closely related to their increased phosphorylation activities. Therefore, the increased autophosphorylation of the two mutants are probably caused by their conformational change. In the wild type Agp2, the conserved histidine of the HWE histidine kinase domain could be covered by response regulator which also block the autophosphorylation. Ionic interactions relating to Asp783 could stabilize this structure. Positive charge at the position as caused by mutagenesis could lead to a more open conformation, which could allow autophosphorylation. To test whether Agp1 has an effect on the Agp2 autophosphorylation, the mutants Agp2_D783A and Agp2_D783N were generated. As side impact, the Agp2 phosphorylation mechanism also was partly explained by the mutants. There was no significant phosphorylation difference between Pfr and Pr of Agp2_D783N, and also no phosphotransfer from domain of HWE histidine kinase to domain of response regulator. However, I observed significant conformational changes of the mutant as caused by charge or the Asp783 loss of domain of response regulator. Therefore, there may be no signal pathway through the HWE His kinase domain of Agp2 to response regulator domain. Combined physiological / molecular and structural researches (Schmidt et al., 2018) experiments should be performed to unravel details of Agp2 signal transduction.

In the BV assembly researches, a strong impact between Agp1 and Agp2 was found in the mixture samples. To prevent competition impacts, only holo-proteins were used to test for an influence on the BV assembly. Chromophore assembly of phytochrome has been studied through time resolved spectroscopy (Borucki et al., 2003), however, the structural details are still unclear. Based on the protein structure, there is no access from the outside in the holo-protein chromophore pocket which likes a close container (Nagano et al., 2016). Although the apo-protein structure is still unknown, the chromophore pocket of holo-protein must be not the same as that of apo-protein which should have an open conformation to allow the chromophore entering from outside. The different assembly kinetics among Agp1, Agp2 and other phytochromes is found (Li et al., 1995; Nagano et al., 2016; Remberg et al., 1998). These differences should be based on distinct openings of the apo-protein chromophore pockets. The obvious slow rate of apo-Agp1 assembly in the presence of holo-Agp2 might be caused by the closure of the Agp1 open chromophore pocket. As mentioned above, the weak interaction between phytochromes Agp1 and Agp2 shows that they can switch rapidly between the non-bound state (preferred state) and the bound state. However, other hypotheses are still necessary for the strong influence of Agp1 – Agp2 interaction on the BV assembly. If such as proteins Agp1 and Agp2 combine to each other for half the time, and also if in the Agp1 bound state the chromophore pocket is shut, but switched on the Agp1 non-bound state, BV assembly could be half as quick as for Agp1 alone. Therefore, I must consider the possibility of BV assembly of Agp1 influenced in the Agp1 / Agp2 non-bound and in the bound state and of the BV pocket remaining shut for a period of time upon separation of both proteins. Similarly, the effect of holo-Agp1 on the apo-Agp2 assembly may also be discussed, even though the impact goes to the reverse direction: the addition of holo-Agp1 quickens the apo-Agp2 assembly. BV pocket of Agp2 could be opened by Agp1, which caused a more fast BV incorporation. Three states of Agp2 chromophore pocket may be necessary: first stage-open BV pocket (apo-Agp2 when interaction with holo-Agp1), second stage-partly open BV pocket (apo-Agp2) and third stage-closed BV pocket (holo-Agp2, as shown in the crystal structure (Schmidt et al., 2018)). It is quite

interesting to observe that the rapid apo-Agp1 assembly is decelerated by holo-Agp2 and the slow apo-Agp2 assembly is accelerated by holo-Agp1.

In summary, there is a weak Agp1-Agp2 proteins interaction according to the results gotten by several different ways. As far as I know, it is the first research of this type for bacterial phytochromes. For plant phytochromes, heterodimers formed between them are another case for phytochromes interaction. However, the previous studies showed that tight homodimers were formed by recombinant Agp1 that do probably not separate (Noack et al., 2007) and Agp1 Agp2 heterodimers may be not easily formed in solution. I could assume either interactions between Agp1 dimers / Agp2 monomers or complexes formed between dimers of Agp1 and those of Agp2. *In vivo*, another interaction with conjugation protein TraA maybe stabilize the interaction between phytochromes Agp1 and Agp2.

Materials and methods

1 Growth tests

Strains of *A. fabrum* C58 WT, single mutant *agp1*$^{-}$ or *agp2*$^{-}$ and double mutant *agp1/2*$^{-}$ harbouring Ti plasmid and pBIN-GUS plasmid (kanamycin resistance cassette) were used in the research (Bai et al., 2016; Oberpichler et al., 2006; Vancanneyt et al., 1990). Bacteria was inoculated in 100 ml LB medium with 86 μM Kanamycin (Kan) to OD_{600}=0.05, which was grown in darkness, white light (40 μmol $m^{-2}s^{-1}$), red light (40 μmol $m^{-2}s^{-1}$) or blue light (40 μmol $m^{-2}s^{-1}$) at different temperature (20 °C, 25 °C, 28 °C, 32 °C or 37 °C) conditions for 51 h with shaking at 110 rpm. The concentrations were measured at OD_{600}.

2 Infection of *Nicotiana benthamiana* with *A. fabrum*

The infection was performed using 6-week-old *N. benthamiana* and the four genotypes of *A. fabrum* harvested from LB agar plates or liquid LB. The plant stems and leaves were used as infected sites in the study.

2.1 Stem

The superficial sections (1-2 cm long) on stem of *N. benthamiana* was cut by sterile scalpel. Bacteria from the agar was applied directly onto the wound of plants with a pipette tip. The infected plants were then placed at room temperature in red light (0.8 μmol $m^{-2}s^{-1}$), or with aluminium foil covering the wound for darkness treatment. The bacterial growth was terminated by 220 μM cefotaxime (few drop on each cut) after 24 h. Finally, the plants without aluminium foil were grown at room temperature under natural light conditions. After 6 weeks, tumors of the wound were observed and then the photographs were taken.

2.2 Leaf

Bacteria was inoculated in liquid LB medium over night at 28 °C till OD_{600}=2. After centrifugation at 5000 g for 15 min at room temperature, the supernatant was removed and then the pellet was resuspended in 11 mM MES, 10 mM $MgCl_2$, pH 7 to the final OD_{600} of 0.8. After incubation in sterile bench for 2 h at room temperature, the solution containing bacteria was infiltrated into the plant leaves by 2 ml syringe. The infected plants were then incubated at room temperature for 24 h in red light (0.8 μmol $m^{-2}s^{-1}$) or in darkness. After transformation, the GUS activity of leaves was measured by staining and fluorometric assays.

2.2.1 GUS staining

5-bromo-4-chloro-3-indolyl glucuronide (X-Gluc, Thermo Fisher) assay with minor modifications (Jefferson et al., 1987) was used to examine the expression of GUS gene in infected leaves. The leaves were cut off and placed into X-Gluc stain solution containing 200 mM sodium phosphate (pH 7), 2 mM X-Gluc and 0.01 % (v/v) Triton X-100 at 37 °C for 17 h in darkness. After decolorization of the leaves by successively soaking in 70% (v/v), 80% (v/v), 90% (v/v), 100% (v/v) ethanol, the blue GUS stains were observed and photographed.

2.2.2 GUS fluorometric assays

The quantitative GUS activity in the leaves was determined by 4-Methylumbelliferyl-β-D-glucuronide hydrate (4-MUG, Sigma) assay (Blázquez, 2007; Jefferson, 1987; Jefferson et al., 1987). The leaves were incubated in reaction mix containing 50 mM sodium phosphate, 10 mM EDTA, 0.1 % (w/v) SDS, 0.1 % (v/v) Triton X-100, 1 mM 4-MUG, pH 7 for 17 h at 37 °C in darkness. The reaction was stopped by the addition of 1 M Na_2CO_3 to final concentrations of 0.99 M. The fluorescence was measured with a Jasco FP 8300 fluorimeter. The excitation and emission wavelength was 365 nm and 455 nm, respectively. Normalization of the GUS activity calculated as nmol of 4-MU per minute per leaf was performed using four 4-MU standards (0.5 nM, 5 nM, 50 nM, and 500 nM).

3 Interaction between Agp1 and Agp2

3.1 Protein preparation

4.1.1 Expression vectors and site-directed mutagenesis of Agp2

Expression plasmids pAG1 (Lamparter et al., 2002) and pSA2 (Lamparter and Michael, 2005) were used for Agp1 and Agp2, respectively. After expression, all proteins contain 6xHis affinity tags at their C-terminal. For the point mutation of Agp2, I used the pSA2 expression vector as template. According the protocol of Quik Change Kit (Agilent), the construct of Agp2_D783A and Agp2_D783N mutants was performed. Primers used for each Agp2 mutant were shown in Table 10.

Table 10. Primer sequences for site-directed mutagenesis of Agp2. FP: Forward primer; RP: Reverse primer

Purpose	Gene	Primer sequence (5' to 3')
Site-directed mutagenesis	*Agp2_D783A*	FP: GGAACCAAGATTGATG**G**CGAGAATGGCGACGTC
		RP: GACGTCGCCATTCTCG**C**CATCAATCTTGGTTCC
	Agp2_D783N	FP: GGAACCAAGATTGATGT**T**GAGAATGGCGACGTCAG
		RP: CTGACGTCGCCATTCTC**A**ACATCAATCTTGGTTCC

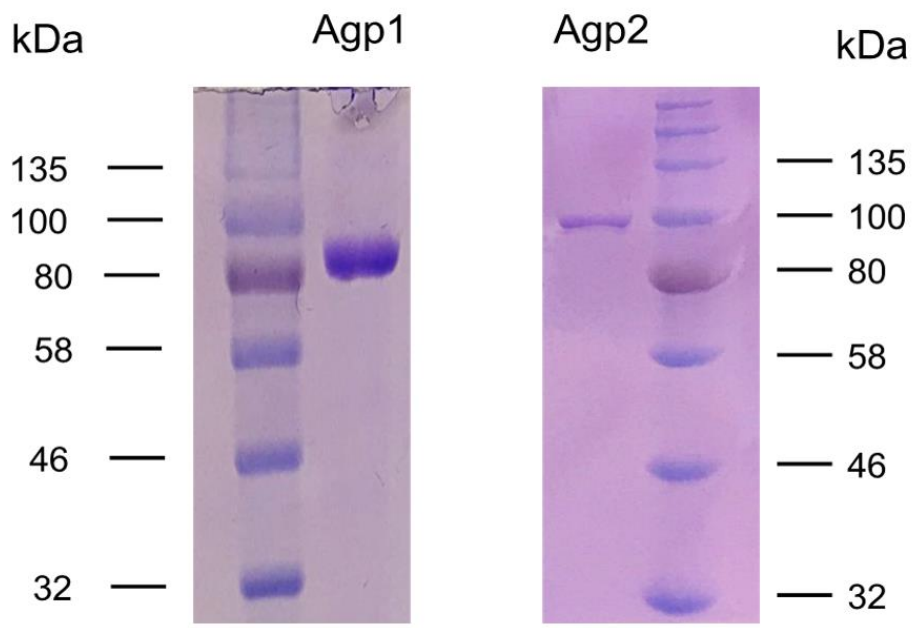

Figure 31. SDS-PAGE gels of purified protein Agp1 (left) or Agp2 (right) after coomassie stain. For marker proteins, the positions are shown on the right side or left side.

4.1.2 Protein expression and purification, and holo-protein assembly

Agp1 and Agp2 (apo-protein) were expressed with a His tag and purified as described previously in more detail (Inomata et al., 2006; Lamparter and Michael, 2005; Lamparter et al., 2002). The proteins were induced with IPTG at 18 °C over night, followed by French pressure. After centrifugation at 9000 g for 30 min, protein precipitation from supernatant was performed with 50 % ammonium sulfate. The pellet was then dissolved in 50 mM Tris/HCl, 10 mM Imidazol, 1 M NaCl, 100 mg/l cholic acid, pH 7.8. The Ni-affinity chromatography was used to purify the proteins from mixture. Finally, collected protein, containing the fractions, was again performed with 50% ammonium sulfate precipitation, and dissolved in basic buffer (50 mM Tris/Cl, 300 mM NaCl, 5 mM EDTA, pH 7.8). After checking by SDS / PAGE, pure Agp1 and Agp2 was proved (Figure 31). After measurement by electric conductivity, I found that the concentration of ammonium sulfate was ca. 50 mM in the purified protein sample. At this stage of purification, typical protein concentrations were 20 µM. For the BV (Sigma) purification, BV in aqueous

solution was loaded to 1 ml Sep-Pak C18 cartridges (Waters), washed with ultra-pure water and eluted in methanol, and then evaporated to dryness, and cooled to room temperature. Finally, the purified BV was dissolved in DMSO at 2-10 mM concentrations. To get holo-protein, apo-protein was mixed with 2-fold molar excess concentration of BV and incubated at room temperature for 2 h. Ammonium sulfate and free BV could be removed by NAP 10 columns (GE healthcare). For the experiments of phosphorylation and assembly, residual ammonium sulfate in apo-protein was also removed by the NAP separation.

To evaluate the assembly of apo-Agp1 or apo-Agp2 kinetically with BV, the apo-protein was directly incubated with BV in a photometer cuvette. And then, the cuvette, containing 1 µM protein and 1 µM BV, was directly measured by photometer and the absorbance at 700 nm or 750 nm was recorded at 1-second intervals. Moreover, the mixture (1 µM apo-Agp1, 1 µM BV and 5 µM holo-Agp2) or (1 µM apo-Agp2, 1 µM BV and 5 µM holo-Agp1) were also measured by the same method. The concentrations of protein and biliverdin were evaluated by measuring at 280 nm in basic buffer and by measuring at 696 nm in methanic / HCl (0.8 $mM^{-1}cm^{-1}$ extinction coefficient was used), respectively (McDonagh, 1979).

3.2 Irradiation and photometry

To obtain the Agp1 at Pr form, the protein was incubated in dark during BV assembly or holo-protein was kept in dark for 2 h at room temperature. After dark incubation, more than 90 % Agp1 would be converted from Pfr form to Pr from. Similarly, the Agp2 and mutants at Pfr form were also achieved by this way. After dark incubation, Agp2 was almost entirely in the Pfr form. For the Pfr from of Agp1 or Pr form of Agp2 (also mutants), the protein was irradiated with emitting diodes of red light (λmax = 644 nm, 20 µmol $m^{-2}s^{-1}$ or λmax = 655 nm, 32 µmol $m^{-2}s^{-1}$) or emitting diodes of far-red light (λmax = 780 nm, 1500 µmol $m^{-2}s^{-1}$) for 2 min, respectively (Karniol and Vierstra, 2003). UV/vis spectra (1000 nm min^{-1} scan speed) were always measured at 18 °C with a photometer (Jasco V550) (Krieger et al., 2008). Final volumes and concentrations of Agp1 or Agp2 were 1 mL and 5 µM, respectively.

3.3 Size exclusion chromatography

I used a Superdex 200 10/300GL column (GE Healthcare) in the experiments of size exclusion chromatography (SEC). The running buffer (50 mM Tris/HCl, 150 mM NaCl and 5 mM EDTA, pH 7.8) was used and the samples were separated at 0.1 ml/min flow rate in cold room (4 °C). Marker proteins blue dextran (2000 kDa), thyroglobulin (669 KDa), apoferritin (443 KDa), β−amylase (200 KDa), alcoholdehydrogenase (150 KDa), bovine serum albumin (66 KDa) and carboanhydrase (29 KDa) (Sigma) were applied. 200 µl samples with 4 µM concentration for each protein was added into the column. Protein elution was recorded at 280 nm.

3.4 Phosphorylation

Agp1 and Agp2 (also the mutants) autophosphorylation were performed and analyzed using the method of earlier experiments (Lamparter et al., 2002). In green light, the samples of phytochrome were added into phosphorylation buffer (final concentration 2.5 µM phytochrome for each, 25 mM Tris-HCl, 4 mM ß-mercaptoethanol, 5 mM $MgCl_2$, 50 mM KCl, 5% ethylene glycol, ca. 50 µM ATP containing 0.37 MBq [γ^{-32}P]ATP, pH 7.8) or with $(NH_4)_2SO_4$ (final concentration 50 mM) and incubated in darkness for 20 min at room temperature. For the determination of free phosphate, I used the malachite green phosphate assay kit (Sigma) (Altmann et al., 1971). 80 µl test sample, 150 µl 'Working Reagent' and 780 µl water were added into 1.5 ml tube. After incubation at room temperature for 30 min, the color development was finished and then the mixtures were measured at 620 nm.

3.5 Computer analyses

The analysis of triexponential decay and figures were performed by Origin 2018. For calculations such as standard error calculations, mean values, and subtraction and addition of different spectra, Excel was used.

4 Proteome analysis

4.1 Bacteria preparation

The single colony of *A. fabrum* C58 WT or double mutant *agp1/2*$^{-}$ from LB agar plate was inoculated and grown in 100 ml LB with 86 μM Kan at 28 °C and 110 rpm over night. The WT and mutant cells from preculture were diluted with LB for final OD_{600} of 0.6 and volume of 100 ml, respectively. After 24 h incubation at 28 °C and 110 rpm in darkness achieved by aluminium foil or white light (40 μmol $m^{-2}s^{-1}$), the 2 ml culture were centrifuged 12000 g for 5 minutes at 4 °C and then the cell pellet was washed thrice with cold 10 mM Tris, 1.4 mM PMSF, 1 mM EDTA, pH 7.5. The cells were stored at -80 °C.

4.2 Protein extraction and digestion

Frozen cells (about 80 mg) were resuspended and homogenized in 0.3 ml lysis buffer (50 mM Tris, 5% SDS, 0.1 mM EDTA, 150 mM NaCl, 1 mM $MgCl_2$, 50 mM dithiothreitol, pH 8) (Chourey et al., 2010). The supernatant was collected after centrifugation at 10000 g for 5 minutes at 4 °C. The protein concentration was measured with Pierce™ BCA Protein Assay Kit (Thermo Fisher Scientific). Sample from the supernatant (Table 11) was diluted with 50 mM triethylammonium bicarbonate (TEAB) (pH 8.5) for a final protein concentration of 1 μg/μl and volume of 100 μl and then reduced by 10 mM tris(2-carboxyethyl)phosphine (TCEP) (pH 7) at 56°C for 1 h and alkylated by 20 mM iodoacetamide (IAA) in darkness for 1h at room temperature. After the addition of 600 μl pre-cooled (-20 °C) acetone and freeze at -20 °C, the mixture was centrifuged at 8000 g for 10 min at 4 °C. The acetone was removed and the pellet was dried for 2-3 min. Finally, the protein pellet was reconstitute with 100 μl 50 mM TEAB (pH 8.5) and then digested overnight at 37 °C by adding 2.5 μg trypsin (Madison, WI, USA).

Table 11. Concentration of different protein samples. WT_D: wild type_darkness; WT_L: wild type_white light; M_D: mutant_darkness; M_L: mutant_white light

Group ID	Sample Name	Concentration (μg/μl)
D	M_D1	1.58
D	M_D2	1.97
D	M_D3	2.38
D	WT_D1	1.76
D	WT_D2	1.77
D	WT_D3	2.48
L	M_L1	2.8
L	M_L2	2.24
L	M_L3	2.48
L	WT_L1	2.91
L	WT_L2	2.21
L	WT_L3	2.45

4.3 Peptide labeling

After labeling with TMT reagents as Table 12 (Thermo Fisher Scientific Inc.), six samples from darkness group (group ID: D) were mixed together for nanoscale liquid chromatography coupled to tandem mass spectrometry (nano LC-MS / MS) analysis. For white light group (group ID: L), it was similar with darkness group.

Table 12. Labeling information of different protein samples. D: darkness; L: white light; WT_D: wild type_darkness; WT_L: wild type_white light; M_D: mutant_darkness; M_L: mutant_white light

Group ID	Sample Name	Label Reagent
D	M_D1	TMT10-126
D	M_D2	TMT10-127N
D	M_D3	TMT10-127C
D	WT_D1	TMT10-128N
D	WT_D2	TMT10-128C
D	WT_D3	TMT10-130N
L	M_L1	TMT10-126
L	M_L2	TMT10-129N
L	M_L3	TMT10-129C
L	WT_L1	TMT10-130N
L	WT_L2	TMT10-130C
L	WT_L3	TMT10-131

4.4 Nano LC - MS / MS analysis

The nano liquid chromatography (LC) - mass spectrum (MS) / MS analysis was performed by a Dionex Ultimate 3000 Nano liquid chromatography (LC) system with Obitrap Q Exactive™ mass spectrometer (Thermo Fisher Scientific, USA) with an electrospray ionization nanospray source. Nanoflow ultra high-performance liquid chromatography (UPLC): Easy-nLC1000 (ThermoFisher Scientific, USA) with nanocolumn: 100 μm×10 cm in-house made column packed with a reversed-phase ReproSil-Pur C18-AQ resin (3 μm, 120 Å, Dr. Maisch GmbH, Germany) was used in fractionation experiment. 5 μl sample was loaded into nanocolumn. Mobile phase was 0.1% formic acid in water (A) and 0.1% formic acid in acetonitrile (B). The peptides were separated at a flow rate of 600 nl/min with LC linear gradient: 15 min, from 6% to 9% B; 20 min, from 9% to 14% B; 60 min, from 14% to 30% B; 15 min, from 30% to 40% B; 3 min, from 40% to 95% B; 7 min, 95% B. For the mass spectrometry (MS) parameters, MS resolution and MS precursor m/z range were 60000 and 300-1650, respectively. 15 most intense peptide ions from the MS scan were fragmented by collision-induced dissociation (40% normalized collision energy). We used the Orbitrap with a resolution of 15000 for MS / MS scan.

4.5 Data analysis

The raw MS dates were analyzed and searched with Proteome Discover 2.1 software (Thermo Fisher Scientific) against protein database of *A. fabrum*. The carbamidomethylation and oxidation were selected as fixed and variable modifications, respectively. The enzyme specificity, maximum missed cleavages, precursor ion mass tolerance and MS / MS tolerance were set to trypsin, 2, 10 ppm and 20 ppm, respectively. For identification analysis of downstream protein, only peptides with high confident identification were considered.

5 Bacterial competition

5.1 Competition assays

The competition assay between *A. fabrum* and *E. coli* DH5α was performed according to the method of (Ma et al., 2014). Before mixing, overnight culture of *A. fabrum* WT, *agp1*$^{-}$, *agp2*$^{-}$, or *agp1/2*$^{-}$ mutant and *E. coli* DH5α were sub-cultured at 28 °C and 37 °C for 5 h, respectively. In the mixture, the ratio was 10 (final OD_{600} of *A. fabrum* = 0.1) : 1 (final OD_{600} of *E. coli* = 0.01). After spot of 10 µl mixture on plates of LB agar, the plates were incubated under different light condition at 25 °C for 16 h. The bacterial cells were collected from agar, followed by strongly vortexing for 3 minutes in 1ml LB, and then serially diluted by LB. After being plated in LB agar, the mixture cells were grown at 37 °C for 16 h. Finally, the colony forming units (CFU) of plates were scored.

For competition assay between *A. fabrum* and other soil bacterium, *A. fabrum* WT, double mutant *agp1/2*$^{-}$ (harbouring Ti plasmid) and other soil bacterium collected from the soil of forest soils at Karlsruhe (49° 0′ N, 8° 24′ E) (Figure 32) were cultured in LB at 28 °C over night, respectively. *A. fabrum* WT (OD_{600} = 2) and double mutant (OD_{600} = 3) was mixed with same volume soil bacterium (OD_{600} = 2) at a 1:1 ratio and 1.5:1 ratio, respectively, and grown at 28 °C for 12 h with shaking at 110 rpm under darkness or white light (40 µmol $m^{-2}s^{-1}$).

Figure 32. Site of soil collection. Soil was collected from forest at Karlsruhe (49° 0′ N, 8° 24′ E).

5.2 Genomic DNA extraction and sequencing of 16S rRNA

Total genomic DNA was extracted from microbial cells using NucleoSpin® Microbial DNA kit (Macherey-Nagel). Forward primer 27 FP (AGAGTTTGATCMTGGCTCAG) and reverse primer 338 RP (TGCTGCCTCCCGTAGGAGT) were used for amplification of hypervariable region V2 of the 16S rRNA gene. The PCR was performed with 25 µl reactions containing Phusion High Fidelity DNA Polymerase (Thermo Fisher Scientific, Waltham, USA) and 15 ng of template DNA. The PCR parameters were: 1 cycle (98°C, 180 s), 35 cycles (98°C, 10 s; 58°C, 30 s; 72°C, 60 s), 1 cycle (72°C, 300 s). After reaction, the 2 % agarose gel was used to check PCR products. If the amplified bands were correct and clear, the genomic DNA samples were used for sequencing of 16S ribosomal RNA gene. The sequencing of V2 region was performed on a MiSeq platform (Illumina).

5.3 Analysis of 16S rRNA sequencing data

The QIIME package (1.9.0 version) was used to analyze the sequencing data (Caporaso et al., 2010). Assembly of paired end reads and identification of chimeric sequences were performed with SeqPrep and Chimera Slayer, respectively (Haas et al., 2011). Operational taxonomic unit (OUT) picking was conducted at 97% similarity level and UCLUST algorithm against GreenGenes (13.8 version) reference sequences was used to perform the annotation (DeSantis et al., 2006; Edgar, 2010). To avoid misinformation, I just kept the OTUs with at least 50 reads in the dataset (Faith et al., 2013). For the analysis, normalized 10000 reads was used and then the alpha-diversity was calculated with Chao1 metric.

References

Al-Sady, B., Ni, W., Kircher, S., Schäfer, E., and Quail, P.H. (2006). Photoactivated phytochrome induces rapid PIF3 phosphorylation prior to proteasome-mediated degradation. Molecular cell *23*, 439-446.

Altmann, H., E, F., A, G., and Scholz, L. (1971). Photometric determination of small amounts of ortho phosphate with malachite green. Fresen Z Anal Chem *256*, 274-275.

Alvarez-Martinez, C.E., and Christie, P.J. (2009). Biological diversity of prokaryotic type IV secretion systems. Microbiol. Mol. Biol. Rev. *73*, 775-808.

Aravind, L., and Ponting, C.P. (1997). The GAF domain: an evolutionary link between diverse phototransducing proteins. Trends in biochemical sciences *22*, 458-459.

Aravind, L., and Ponting, C.P. (1999). The cytoplasmic helical linker domain of receptor histidine kinase and methyl-accepting proteins is common to many prokaryotic signalling proteins. FEMS microbiology letters *176*, 111-116.

Ashby, A.M. (1988). Agrobacterium tumefaciens: chemotaxis and crop protection. (Durham University).

Atmakuri, K., Cascales, E., and Christie, P.J. (2004). Energetic components VirD4, VirB11 and VirB4 mediate early DNA transfer reactions required for bacterial type IV secretion. Molecular microbiology *54*, 1199-1211.

Averbukh, E. (2018). Lichteffekte bei Infektionen mit Agrobacterium fabrum in Pflanzen. In Masterarbeit from Karlsruher Institut für Technologie.

Bai, Y., Rottwinkel, G., Feng, J., Liu, Y., and Lamparter, T. (2016). Bacteriophytochromes control conjugation in Agrobacterium fabrum. Journal of Photochemistry and Photobiology B: Biology *161*, 192-199.

Bayram, Ö., Braus, G.H., Fischer, R., and Rodriguez-Romero, J. (2010). Spotlight on Aspergillus nidulans photosensory systems. Fungal Genetics and Biology *47*, 900-908.

Beattie, G.A., Hatfield, B.M., Dong, H.L., and McGrane, R.S. (2018). Seeing the Light: The Roles of Red- and Blue-Light Sensing in Plant Microbes. In Annual Review of Phytopathology, Vol 56, J.E. Leach, and S.E. Lindow, eds. (Palo Alto: Annual Reviews), pp. 41-66.

Beijersbergen, A., Smith, S.J., and Hooykaas, P.J. (1994). Localization and topology of VirB proteins of Agrobacterium tumefaciens. Plasmid *32*, 212-218.

Bhoo, S.-H., Davis, S.J., Walker, J., Karniol, B., and Vierstra, R.D. (2001). Bacteriophytochromes are photochromic histidine kinases using a biliverdin chromophore. Nature *414*, 776.

Blázquez, M. (2007). Quantitative GUS activity assay in intact plant tissue. Cold Spring Harbor Protocols *2007*, pdb. prot4688.

Borucki, B., Otto, H., Rottwinkel, G., Hughes, J., Heyn, M.P., and Lamparter, T. (2003). Mechanism of Cph1 phytochrome assembly from stopped-flow kinetics and circular dichroism. Biochemistry *42*, 13684-13697.

Brandt, S., von Stetten, D., Günther, M., Hildebrandt, P., and Frankenberg-Dinkel, N. (2008). The Fungal Phytochrome FphA from Aspergillus nidulans. J. Biol. Chem *283*, 34605-34614.

Buchberger, T., and Lamparter, T. (2015). Streptophyte phytochromes exhibit an N-terminus of cyanobacterial origin and a C-terminus of proteobacterial origin. BMC research notes *8*, 144.

Caporaso, J.G., Kuczynski, J., Stombaugh, J., Bittinger, K., Bushman, F.D., Costello, E.K., Fierer, N., Pena, A.G., Goodrich, J.K., and Gordon, J.I. (2010). QIIME allows analysis of high-throughput community sequencing data. Nature methods *7*, 335.

Castillon, A., Shen, H., and Huq, E. (2007). Phytochrome interacting factors: central players in phytochrome-mediated light signaling networks. Trends in plant science *12*, 514-521.

Chesnokova, O., Coutinho, J.B., Khan, I.H., Mikhail, M.S., and Kado, C.I. (1997). Characterization of flagella genes of Agrobacterium tumefaciens, and the effect of a bald strain on virulence. Molecular microbiology *23*, 579-590.

Chilton, M.-D., Drummond, M.H., Merlo, D.J., Sciaky, D., Montoya, A.L., Gordon, M.P., and Nester, E.W. (1977). Stable incorporation of plasmid DNA into higher plant cells: the molecular basis of crown gall tumorigenesis. Cell *11*, 263-271.

Cho, H., and Winans, S.C. (2007). TraA, TraC and TraD autorepress two divergent quorum‐regulated promoters near the transfer origin of the Ti plasmid of Agrobacterium tumefaciens. Molecular microbiology *63*, 1769-1782.

Choi, G., Yi, H., Lee, J., Kwon, Y.-K., Soh, M.S., Shin, B., Luka, Z., Hahn, T.-R., and Song, P.-S. (1999). Phytochrome signalling is mediated through nucleoside diphosphate kinase 2. Nature *401*, 610.

Chourey, K., Jansson, J., VerBerkmoes, N., Shah, M., Chavarria, K.L., Tom, L.M., Brodie, E.L., and Hettich, R.L. (2010). Direct cellular lysis/protein extraction protocol for soil metaproteomics. Journal of proteome research *9*, 6615-6622.

Davis II, E.W., Weisberg, A.J., Tabima, J.F., Grunwald, N.J., and Chang, J.H. (2016). Gall-ID: tools for genotyping gall-causing phytopathogenic bacteria. PeerJ *4*, e2222.

DeSantis, T.Z., Hugenholtz, P., Larsen, N., Rojas, M., Brodie, E.L., Keller, K., Huber, T., Dalevi, D., Hu, P., and Andersen, G.L. (2006). Greengenes, a chimera-checked 16S rRNA gene database and workbench compatible with ARB. Appl. Environ. Microbiol. *72*, 5069-5072.

Dillen, W., De Clercq, J., Kapila, J., Zambre, M., Van Montagu, M., and Angenon, G. (1997). The effect of temperature on Agrobacterium tumefaciens‐mediated gene transfer to plants. The Plant Journal *12*, 1459-1463.

Edgar, R.C. (2010). Search and clustering orders of magnitude faster than BLAST. Bioinformatics *26*, 2460-2461.

English, G., Trunk, K., Rao, V.A., Srikannathasan, V., Hunter, W.N., and Coulthurst, S.J. (2012). New secreted toxins and immunity proteins encoded within the Type VI secretion system gene cluster of S erratia marcescens. Molecular microbiology *86*, 921-936.

Esteban, B., Carrascal, M., Abian, J., and Lamparter, T. (2005). Light-induced conformational changes of cyanobacterial phytochrome Cph1 probed by limited proteolysis and autophosphorylation. Biochemistry *44*, 450-461.

Faith, J.J., Guruge, J.L., Charbonneau, M., Subramanian, S., Seedorf, H., Goodman, A.L., Clemente, J.C., Knight, R., Heath, A.C., and Leibel, R.L. (2013). The long-term stability of the human gut microbiota. Science *341*, 1237439.

Fankhauser, C., Yeh, K.-C., Clark, J., Zhang, H., Elich, T.D., and Chory, J. (1999). PKS1, a substrate phosphorylated by phytochrome that modulates light signaling in Arabidopsis. Science *284*, 1539-1541.

Franco, J.A.V., Collier, R., Wang, Y., Huo, N., Gu, Y., Thilmony, R., and Thomson, J.G. (2016). Draft genome sequence of Agrobacterium rhizogenes strain NCPPB2659. Genome announcements *4*.

Fuqua, C., Burbea, M., and Winans, S.C. (1995). Activity of the Agrobacterium Ti plasmid conjugal transfer regulator TraR is inhibited by the product of the traM gene. Journal of bacteriology *177*, 1367-1373.

Garcillan-Barcia, M.P., Francia, M.V., and de la Cruz, F. (2009). The diversity of conjugative relaxases and its application in plasmid classification. Fems Microbiology Reviews *33*, 657-687.

Gelvin, S.B. (2000). Agrobacterium and plant genes involved in T-DNA transfer and integration. Annual review of plant biology *51*, 223-256.

Gelvin, S.B. (2003). Agrobacterium-mediated plant transformation: the biology behind the “gene-jockeying” tool. Microbiol. Mol. Biol. Rev. *67*, 16-37.

Giraud, E., Fardoux, J., Fourrier, N., Hannibal, L., Genty, B., Bouyer, P., Dreyfus, B., and Verméglio, A. (2002). Bacteriophytochrome controls photosystem synthesis in anoxygenic bacteria. Nature *417*, 202.

Giraud, E., Zappa, S., Jaubert, M., Hannibal, L., Fardoux, J., Adriano, J.M., Bouyer, P., Genty, B., Pignol, D., and Vermeglio, A. (2004). Bacteriophytochrome and regulation of the synthesis of the photosynthetic apparatus in Rhodopseudomonas palustris: pitfalls of using laboratory strains. Photochemical & Photobiological Sciences *3*, 587-591.

Goodner, B., Hinkle, G., Gattung, S., Miller, N., Blanchard, M., Qurollo, B., Goldman, B.S., Cao, Y., Askenazi, M., and Halling, C. (2001). Genome sequence of the plant pathogen and biotechnology agent Agrobacterium tumefaciens C58. Science *294*, 2323-2328.

Hübschmann, T., Börner, T., Hartmann, E., and Lamparter, T. (2001). Characterization of the Cph1 holo‐phytochrome from Synechocystis sp. PCC 6803. European journal of biochemistry *268*, 2055-2063.

Haas, B.J., Gevers, D., Earl, A.M., Feldgarden, M., Ward, D.V., Giannoukos, G., Ciulla, D., Tabbaa, D., Highlander, S.K., and Sodergren, E. (2011). Chimeric 16S rRNA sequence formation and detection in Sanger and 454-pyrosequenced PCR amplicons. Genome research *21*, 494-504.

Holmes, R., and Jobling, M. (1996a). Genetics: conjugation. Barons medical microbiology *4*.

Holmes, R., and Jobling, M. (1996b). Genetics: exchange of genetic information. (Univ of Texas Medical Branch).

Hughes, J., Lamparter, T., Mittmann, F., Hartmann, E., Gärtner, W., Wilde, A., and Börner, T. (1997). A prokaryotic phytochrome. Nature *386*, 663.

Igbalajobi, O., Yu, Z., and Fischer, R. (2019). Red-and Blue-Light Sensing in the Plant Pathogen Alternaria alternata Depends on Phytochrome and the White-Collar Protein LreA. mBio *10*, e00371-00319.

Immormino, R.M., Silversmith, R.E., and Bourret, R.B. (2016). A Variable Active Site Residue Influences the Kinetics of Response Regulator Phosphorylation and Dephosphorylation. Biochemistry *55*, 5595-5609.

Inomata, K., Noack, S., Hammam, M.A., Khawn, H., Kinoshita, H., Murata, Y., Michael, N., Scheerer, P., Krauss, N., and Lamparter, T. (2006). Assembly of synthetic locked chromophores with Agrobacterium phytochromes Agp1 and Agp2. Journal of Biological Chemistry *281*, 28162-28173.

Jaubert, M., Zappa, S., Fardoux, J., Adriano, J.-M., Hannibal, L., Elsen, S., Lavergne, J., Verméglio, A., Giraud, E., and Pignol, D. (2004). Light and Redox Control of Photosynthesis Gene Expression in Bradyrhizobium dual roles of two PpsR. Journal of Biological Chemistry *279*, 44407-44416.

Jefferson, R.A. (1987). Assaying chimeric genes in plants: the GUS gene fusion system. Plant molecular biology reporter *5*, 387-405.

Jefferson, R.A., Kavanagh, T.A., and Bevan, M.W. (1987). GUS fusions: beta‐glucuronidase as a sensitive and versatile gene fusion marker in higher plants. The EMBO journal *6*, 3901-3907.

Kajala, K., Coil, D.A., and Brady, S.M. (2014). Draft genome sequence of Rhizobium rhizogenes strain ATCC 15834. Genome Announc. *2*, e01108-01114.

Kami, C., Hersch, M., Trevisan, M., Genoud, T., Hiltbrunner, A., Bergmann, S., and Fankhauser, C. (2012). Nuclear phytochrome A signaling promotes phototropism in Arabidopsis. The Plant Cell, tpc. 111.095083.

Karniol, B., and Vierstra, R.D. (2003). The pair of bacteriophytochromes from Agrobacterium tumefaciens are histidine kinases with opposing photobiological properties. Proceedings of the National Academy of Sciences *100*, 2807-2812.

Karniol, B., and Vierstra, R.D. (2004). The HWE histidine kinases, a new family of bacterial two-component sensor kinases with potentially diverse roles in environmental signaling. Journal of bacteriology *186*, 445-453.

Kendrick, R.E., and Kronenberg, G.H.M. (1994). Photomorphogenesis in Plants, 2nd edition, 2 edn (Dordrecht: Kluwer Academic Publishers).

Kircher, S., Kozma-Bognar, L., Kim, L., Adam, E., Harter, K., Schäfer, E., and Nagy, F. (1999). Light quality–dependent nuclear import of the plant photoreceptors phytochrome A and B. The Plant Cell *11*, 1445-1456.

Krieger, A., Molina, I., Oberpichler, I., Michael, N., and Lamparter, T. (2008). Spectral properties of phytochrome Agp2 from Agrobacterium tumefaciens are specifically modified by a compound of the cell extract. Journal of Photochemistry and Photobiology B: Biology *93*, 16-22.

Kuzmanović, N., Puławska, J., Prokić, A., Ivanović, M., Zlatković, N., Gašić, K., and Obradović, A. (2015). Draft genome sequences of Agrobacterium nepotum strain 39/7T and Agrobacterium sp. strain KFB 330. Genome Announc. *3*, e00331-00315.

Lamparter, T. (2004). Evolution of cyanobacterial and plant phytochromes. FEBS letters *573*, 1-5.

Lamparter, T. (2006). A computational approach to discovering the functions of bacterial phytochromes by analysis of homolog distributions. BMC bioinformatics *7*, 141.

Lamparter, T., Carrascal, M., Michael, N., Martinez, E., Rottwinkel, G., and Abian, J. (2004). The biliverdin chromophore binds covalently to a conserved cysteine residue in the N-terminus of Agrobacterium phytochrome Agp1. Biochemistry *43*, 3659-3669.

Lamparter, T., Krauß, N., and Scheerer, P. (2017). Phytochromes from Agrobacterium fabrum. Photochemistry and photobiology *93*, 642-655.

Lamparter, T., and Michael, N. (2005). Agrobacterium phytochrome as an enzyme for the production of ZZE bilins. Biochemistry *44*, 8461-8469.

Lamparter, T., Michael, N., Mittmann, F., and Esteban, B. (2002). Phytochrome from Agrobacterium tumefaciens has unusual spectral properties and reveals an N-terminal chromophore attachment site. Proceedings of the National Academy of Sciences *99*, 11628-11633.

Lariguet, P., Schepens, I., Hodgson, D., Pedmale, U.V., Trevisan, M., Kami, C., de Carbonnel, M., Alonso, J.M., Ecker, J.R., and Liscum, E. (2006). Phytochrome kinase substrate 1 is a phototropin 1 binding protein required for phototropism. Proceedings of the National Academy of Sciences *103*, 10134-10139.

Lassalle, F., Campillo, T., Vial, L., Baude, J., Costechareyre, D., Chapulliot, D., Shams, M., Abrouk, D., Lavire, C., and Oger-Desfeux, C. (2011). Genomic species are

ecological species as revealed by comparative genomics in Agrobacterium tumefaciens. Genome Biology and Evolution *3*, 762-781.

Li, J., Li, G., Wang, H., and Deng, X.W. (2011). Phytochrome signaling mechanisms. The Arabidopsis book/American Society of Plant Biologists *9*.

Li, L., Murphy, J.T., and Lagarias, J.C. (1995). Continuous fluorescence assay of phytochrome assembly in vitro. Biochemistry *34*, 7923-7930.

Lin, J.-S., Ma, L.-S., and Lai, E.-M. (2013). Systematic dissection of the agrobacterium type VI secretion system reveals machinery and secreted components for subcomplex formation. PloS one *8*, e67647.

Ma, L.-S., Hachani, A., Lin, J.-S., Filloux, A., and Lai, E.-M. (2014). Agrobacterium tumefaciens deploys a superfamily of type VI secretion DNase effectors as weapons for interbacterial competition in planta. Cell host & microbe *16*, 94-104.

McDonagh, A. (1979). The porphyrins. The Porphyrins *6*, 243-491.

Moore, L.W., Chilton, W.S., and Canfield, M.L. (1997). Diversity of opines and opine-catabolizing bacteria isolated from naturally occurring crown gall tumors. Appl. Environ. Microbiol. *63*, 201-207.

Morris, J.W., and Morris, R.O. (1990). Identification of an Agrobacterium tumefaciens virulence gene inducer from the pinaceous gymnosperm Pseudotsuga menziesii. Proceedings of the National Academy of Sciences *87*, 3614-3618.

Nagano, S., Scheerer, P., Zubow, K., Michael, N., Inomata, K., Lamparter, T., and Krauss, N. (2016). The crystal structures of the N-terminal photosensory core module of Agrobacterium phytochrome Agp1 as parallel and anti-parallel dimers. J Biol. Chem *291*, 20674-20691.

Nester, E.W. (2015). Agrobacterium: nature's genetic engineer. Frontiers in plant science *5*, 730.

Ni, M., Tepperman, J.M., and Quail, P.H. (1998). PIF3, a phytochrome-interacting factor necessary for normal photoinduced signal transduction, is a novel basic helix-loop-helix protein. Cell *95*, 657-667.

Njimona, I., and Lamparter, T. (2011). Temperature effects on Agrobacterium phytochrome Agp1. Plos One *6*, e25977.

Njimona, I., Yang, R., and Lamparter, T. (2014). Temperature effects on bacterial phytochrome. PloS one *9*, e109794.

Noack, S., Michael, N., Rosen, R., and Lamparter, T. (2007). Protein conformational changes of Agrobacterium phytochrome Agp1 during chromophore assembly and photoconversion. Biochemistry *46*, 4164-4176.

Oberpichler, I., Molina, I., Neubauer, O., and Lamparter, T. (2006). Phytochromes from Agrobacterium tumefaciens: difference spectroscopy with extracts of wild type and knockout mutants. FEBS letters *580*, 437-442.

Oberpichler, I., Pierik, A.J., Wesslowski, J., Pokorny, R., Rosen, R., Vugman, M., Zhang, F., Neubauer, O., Ron, E.Z., and Batschauer, A. (2011). A photolyase-like protein from Agrobacterium tumefaciens with an iron-sulfur cluster. PLoS One *6*, e26775.

Oberpichler, I., Rosen, R., Rasouly, A., Vugman, M., Ron, E.Z., and Lamparter, T. (2008). Light affects motility and infectivity of Agrobacterium tumefaciens. Environmental microbiology *10*, 2020-2029.

Pan, S.Q., Jin, S., Boulton, M.I., Hawes, M., Gordon, M.P., and Nester, E.W. (1995). An Agrobacterium virulence factor encoded by a Ti plasmid gene or a chromosomal gene is required for T‐DNA transfer into plants. Molecular microbiology *17*, 259-269.

Parke, D., Ornston, L., and Nester, E. (1987). Chemotaxis to plant phenolic inducers of virulence genes is constitutively expressed in the absence of the Ti plasmid in Agrobacterium tumefaciens. Journal of bacteriology *169*, 5336-5338.

Penfold, R.J., and Pemberton, J.M. (1994). Sequencing, chromosomal inactivation, and functional expression in Escherichia coli of ppsR, a gene which represses carotenoid and bacteriochlorophyll synthesis in Rhodobacter sphaeroides. Journal of bacteriology *176*, 2869-2876.

Purschwitz, J., Müller, S., Kastner, C., Schöser, M., Haas, H., Espeso, E.A., Atoui, A., Calvo, A.M., and Fischer, R. (2008). Functional and physical interaction of blue-and red-light sensors in Aspergillus nidulans. Current Biology *18*, 255-259.

Rüdiger, W., and Thümmler, F. (1994). The phytochrome chromophore. In Photomorphogenesis in plants (Springer), pp. 51-69.

Ray, C.G., and Ryan, K.J. (2004). Sherris medical microbiology: an introduction to infectious diseases (McGraw-Hill).

Remberg, A., Ruddat, A., Braslavsky, S.E., Gärtner, W., and Schaffner, K. (1998). Chromophore incorporation, Pr to Pfr kinetics, and Pfr thermal reversion of recombinant N-Terminal fragments of phytochrome A and B chromoproteins. Biochemistry *37*, 9983-9990.

Ripoll-Rozada, J., Zunzunegui, S., de la Cruz, F., Arechaga, I., and Cabezón, E. (2013). Functional interactions of VirB11 traffic ATPases with VirB4 and VirD4 molecular motors in type IV secretion systems. Journal of bacteriology *195*, 4195-4201.

Rockwell, N.C., Su, Y.-S., and Lagarias, J.C. (2006). Phytochrome structure and signaling mechanisms. Annu. Rev. Plant Biol. *57*, 837-858.

Rottwinkel, G. (2011). Studien zu Verbreitung, Charakteristika und Funktionen der Bakteriophytochrome in Rhizobiales (Mensch und Buch Verlag).

Rottwinkel, G., Oberpichler, I., and Lamparter, T. (2010). Bathy phytochromes in rhizobial soil bacteria. Journal of bacteriology *192*, 5124-5133.

Ryu, J.S., Kim, J.I., Kunkel, T., Kim, B.C., Cho, D.S., Hong, S.H., Kim, S.H., Fernández, A.P., Kim, Y., and Alonso, J.M. (2005). Phytochrome-specific type 5 phosphatase

controls light signal flux by enhancing phytochrome stability and affinity for a signal transducer. Cell *120*, 395-406.

Schepens, I., Boccalandro, H.E., Kami, C., Casal, J.J., and Fankhauser, C. (2008). Phytochrome kinase substrate 4 modulates phytochrome-mediated control of hypocotyl growth orientation. Plant physiology *147*, 661-671.

Schmidt, A., Sauthof, L., Szczepek, M., Lopez, M.F., Escobar, F.V., Qureshi, B.M., Michael, N., Buhrke, D., Stevens, T., Kwiatkowski, D.*, et al.* (2018). Structural snapshot of a bacterial phytochrome in its functional intermediate state. Nature Communications *9*, 4912.

Sharrock, R.A., and Clack, T. (2004). Heterodimerization of type II phytochromes in Arabidopsis. Proceedings of the National Academy of Sciences *101*, 11500-11505.

Shaw, C., Loake, G., Brown, A., Garrett, C., Deakin, W., Alton, G., Hall, M., Jones, S., O'Leary, M., and Primavesi, L. (1991). Isolation and characterization of behavioural mutants and genes of Agrobacterium tumefaciens. Microbiology *137*, 1939-1953.

Shen, Y., Kim, J.-I., and Song, P.-S. (2005). NDPK2 as a signal transducer in the phytochrome-mediated light signaling. Journal of Biological Chemistry *280*, 5740-5749.

Shirasu, K., Morel, P., and Kado, C. (1990). Characterization of the virB operon of an Agrobacterium tumefaciens Ti plasmid: nucleotide sequence and protein analysis. Molecular microbiology *4*, 1153-1163.

Singer, K. (2018). The mechanism of T-DNA integration: some major unresolved questions. In Agrobacterium Biology (Springer), pp. 287-317.

Singer, K.K. (2013). T-DNA Integration during Agrobacterium-Mediated Transformation of Plants.

Slater, S.C., Goldman, B.S., Goodner, B., Setubal, J.C., Farrand, S.K., Nester, E.W., Burr, T.J., Banta, L., Dickerman, A.W., and Paulsen, I. (2009). Genome sequences of three Agrobacterium biovars help elucidate the evolution of multichromosome genomes in bacteria. Journal of bacteriology *191*, 2501-2511.

Smillie, C., Garcillán-Barcia, M.P., Francia, M.V., Rocha, E.P., and de la Cruz, F. (2010). Mobility of plasmids. Microbiol. Mol. Biol. Rev. *74*, 434-452.

Smith, E.F., and Townsend, C.O. (1907). A plant-tumor of bacterial origin. Science *25*, 671-673.

Tanaka, N., Ogura, T., Noguchi, T., Hirano, H., Yabe, N., and Hasunuma, K. (1998). Phytochrome-mediated light signals are transduced to nucleoside diphosphate kinase in Pisum sativum L. cv. Alaska. Journal of Photochemistry and Photobiology B: Biology *45*, 113-121.

Trimble, W.L., Phung, L.T., Meyer, F., Gilbert, J.A., and Silver, S. (2012). Draft genome sequence of Agrobacterium albertimagni strain AOL15. (Am Soc Microbiol).

van Thor, J.J., Borucki, B., Crielaard, W., Otto, H., Lamparter, T., Hughes, J., Hellingwerf, K.J., and Heyn, M.P. (2001). Light-induced proton release and proton

uptake reactions in the cyanobacterial phytochrome Cph1. Biochemistry *40*, 11460-11471.

Vancanneyt, G., Schmidt, R., O'Connor-Sanchez, A., Willmitzer, L., and Rocha-Sosa, M. (1990). Construction of an intron-containing marker gene: splicing of the intron in transgenic plants and its use in monitoring early events in Agrobacterium-mediated plant transformation. Molecular and General Genetics MGG *220*, 245-250.

Ward, J., Akiyoshi, D., Regier, D., Datta, A., Gordon, M., and Nester, E. (1988). Characterization of the virB operon from an Agrobacterium tumefaciens Ti plasmid. Journal of Biological Chemistry *263*, 5804-5814.

Wood, D.W., Setubal, J.C., Kaul, R., Monks, D.E., Kitajima, J.P., Okura, V.K., Zhou, Y., Chen, L., Wood, G.E., and Almeida, N.F. (2001). The genome of the natural genetic engineer Agrobacterium tumefaciens C58. science *294*, 2317-2323.

Wu, H.Y., Chung, P.C., Shih, H.W., Wen, S., and Lai, E. (2008). Secretome analysis uncovers an Hcp-family protein secreted via a type VI secretion system in Agrobacterium tumefaciens. Journal of bacteriology *190*, 2841-2850.

Wu, S.H., McDowell, M.T., and Lagarias, J.C. (1997). Phycocyanobilin is the natural precursor of the phytochrome chromophore in the green alga Mesotaenium caldariorum. Journal of Biological Chemistry *272*, 25700-25705.

Yanofsky, M.F., Porter, S.G., Young, C., Albright, L.M., Gordon, M.P., and Nester, E.W. (1986). The virD operon of Agrobacterium tumefaciens encodes a site-specific endonuclease. Cell *47*, 471-477.

Yu, Z., Armant, O., and Fischer, R. (2016). Fungi use the SakA (HogA) pathway for phytochrome-dependent light signalling. Nature microbiology *1*, 16019.

Yu, Z., and Fischer, R. (2018). Light sensing and responses in fungi. Nature Reviews Microbiology, 1.

Zahradník, J., Kyslíková, E., and Kyslík, P. (2016). Draft genome sequence of Agrobacterium sp. strain R89-1, a morphine alkaloid-biotransforming bacterium. Genome Announc. *4*, e00196-00116.

Zhang, F., Scheerer, P., Oberpichler, I., Lamparter, T., and Krauß, N. (2013). Crystal structure of a prokaryotic (6-4) photolyase with an Fe-S cluster and a 6, 7-dimethyl-8-ribityllumazine antenna chromophore. Proceedings of the National Academy of Sciences *110*, 7217-7222.

Zienicke, B., Molina, I., Glenz, R., Singer, P., Ehmer, D., Escobar, F.V., Hildebrandt, P., Diller, R., and Lamparter, T. (2013). Unusual spectral properties of bacteriophytochrome Agp2 result from a deprotonation of the chromophore in the red-absorbing form Pr. Journal of Biological Chemistry, jbc. M113. 479535.

Appendix

Table 13. The list of differentially expressed proteins (FC>1.5 or < 0.67 and $P < 0.05$). WT (D): *A. fabrum* wild type (darkness); WT (L): *A. fabrum* wild type (white light); M (D): *A. fabrum* double mutant *agp1/2*$^-$ (darkness); M (L): *A. fabrum* double mutant *agp1/2*$^-$ (white light); FC: fold change.

Protein	Accession	FC = WT (L) / WT (D)	Function	MW [kDa]	calc. pI	Score Sequest
Up-regulated						
cobL	Q7CW86	1.5	Precorrin-6y methyltransferase	44.6	5.5	32.26
avhB1	Q7D3S2	1.5	Type IV secretion protein	24.6	5.03	12.05
Atu2197	A9CI69	1.98	Uncharacterized protein	34.7	6.02	9.22
Atu8154	Q8U5C1	1.52	Plasmid stabilization system protein	14	9.09	6.78
Atu4555	Q7CV91	1.82	Uncharacterized protein	27.8	5.16	5.9
Atu3117	A9CEP8	1.95	Uncharacterized protein	42.6	5.85	3.84
Atu4876	A9CHA0	1.74	Putative oxidoreductase	38.2	6.19	3.58
Atu6114	A9CKV5	1.59	Uncharacterized protein	8.7	10.81	1.96
Down-regulated						
Atu0946	A9CJP4	0.61	Dehydrogenase	39.5	5.47	173.94
rho	A9CHB1	0.64	Transcription termination factor	47	6.19	126.29
clpP	Q8UFY6	0.65	ATP-dependent Clp protease proteolytic subunit 2	23.3	6.23	96.02
nuoI	Q8UFW9	0.63	NADH-quinone oxidoreductase subunit I	18.8	7.58	54.72
rpsI	Q8UFZ8	0.65	30S ribosomal protein S9	16.7	11.21	51.1
yajC	A9CIX5	0.49	Preprotein tranlocase protein	12.6	9.13	36.43
rpsL	Q8UE13	0.55	30S ribosomal protein S12	14	11.49	27.8

rpmG	Q8UFU8	0.66	50S ribosomal protein L33	6.3	10.07	24.52
cox15	Q7CZN9	0.64	Heme A synthase	40.9	8.72	13.56
atpI	A9CK04	0.54	ATP synthase protein I	12.9	5.31	12.74
Atu4600	A9CGV8	0.57	ABC transporter, nucleotide binding/ATPase protein	64	8.5	12.23
cyoC	A9CKN5	0.59	Cytochrome o ubiquinol oxidase subunit III	23	6.6	10.96
soxD	A9CG07	0.53	Sarcosine oxidase delta subunit	11.9	5.27	10.86
Atu6048	A9CL00	0.64	Uncharacterized protein	91.9	7.06	6.74
napE	A9CGL2	0.59	Periplasmic nitrate reductase protein	6.6	9.54	6.29
Atu8036	Q8U4Y5	0.47	Protein YBGT-related protein	4.7	5.02	0

Protein	Accession	FC = M (D) / WT (D)	Function	MW [kDa]	calc. pI	Score Sequest
Up-regulated						
ileS	Q8UHJ6	1.60	Isoleucine--tRNA ligase	108.4	5.66	508.79
Atu5296	A9CLE5	3.51	Arylester hydrolase	32.6	6.96	455.2
rpmE	Q8U9I5	1.53	50S ribosomal protein L31	8.1	8.56	220.9
flaA	Q7D187	1.59	Flagellin	31.6	4.97	214.31
flaB	Q7D188	1.65	Flagellin	33	4.88	212.65
Atu3372	A9CF36	1.78	ABC transporter, substrate binding protein (Sugar)	32.8	4.98	206.39
Atu3032	A9CEK4	1.75	Uncharacterized protein	14.1	9.77	132.8
iolB	A9CGR8	1.54	Uncharacterized protein	30	5.49	120.79
Atu5287	A9CLF0	3.34	Uncharacterized protein	19.9	4.89	119.67

rpmD	P68995	1.73	50S ribosomal protein L30	7.7	11.28	105.43
Atu8119	Q8U5M3	1.54	Uncharacterized protein	15.5	4.89	103.26
Atu5297	A9CLE4	2.51	Hydrolase	34.6	6.67	90.64
Atu8118	Q8U5M6	1.50	Putative universal stress protein	17.7	4.94	76.99
Atu3114	Q7CRM8	1.76	ABC transporter, substrate binding protein (Sugar)	46.3	7.94	76.97
Atu2014	A9CIE2	1.66	ABC transporter, substrate binding protein	34.5	6.05	73.8
Atu3095	Q7CRK9	1.58	Uncharacterized protein	17.1	5.2	73.4
avhB9	Q7D3R4	1.85	Type IV secretion protein AvhB9	31.3	7.43	65.59
Atu5336	Q7D3B8	2.52	Uncharacterized protein	12.3	4.59	63.71
Atu4744	A9CH25	1.63	ABC transporter, substrate binding protein (Sugar)	29.9	5.78	62.99
bkdA2	A9CF98	1.69	2-oxoisovalerate dehydrogenase beta subunit	36.8	5.31	51.94
traC	A9CLN4	2.34	Conjugal transfer protein	10.3	6.13	40.32
Atu4596	A9CGV5	1.61	Uncharacterized protein	34.2	8.15	39.82
Atu5281	A9CLF3	2.78	Uncharacterized protein	8.5	6.11	36.57
ugpA	A9CKE7	1.51	ABC transporter, substrate binding protein (Sn-glycerol 3-phosphate)	47.4	7.83	36.21
Atu5288	A9CLE9	3.79	Uncharacterized protein	14.3	8.37	33.24
mobB	A9CIR4	1.50	Molybdopterin-guanine dinucleotide biosynthesis protein B	18.8	6.34	32.14
avhB10	Q7D3R3	1.84	Type IV secretion protein	42.7	5.69	28.28
Atu0886	A9CJS5	1.57	Uncharacterized protein	19.4	5.19	27.71
Atu4027	A9CFY9	2.02	Cytochrome c2	18.1	9.63	25.15
cinA	A9CJ26	1.59	Competence/damage-inducible protein CinA	17.6	7.52	21.97
Atu8124	Q8U5L4	1.81	Uncharacterized protein	14.6	4.88	21.49
Atu1501	Q7CZ41	1.70	Uncharacterized protein	12.6	10.4	18.85

					5	
rctB	A9CLN1	1.78	Transcriptional regulator protein	11.5	5.4	13.64
mobC	A9CH85	1.59	Mobilization protein C	12.4	9.25	12.25
avhB1	Q7D3S2	2.46	Type IV secretion protein AvhB1	24.6	5.03	12.05
Atu2313	A9CI12	1.51	Uncharacterized protein	12.9	5.72	10.24
Atu5278	A9CLF5	2.76	Uncharacterized protein	18.3	5.67	6.23
Atu8206	Q8U5T0	3.38	Uncharacterized protein	10.3	9.74	4.39
Atu5324	A9CLD1	2.46	Zinc-binding oxidoreductase	35.2	5.47	2.91
proX	A9CLJ7	3.47	ABC transporter, nucleotide binding/ATPase protein (Glycine betaine/L-proline)	37	5.95	2.64
Atu5239	Q7D3K0	3.01	Transcriptional regulator, LacI family	39.5	7.23	0
Down-regulated						
dnaK	P50019	0.60	Chaperone protein DnaK	68	4.98	979.41
groES	P30780	0.46	10 kDa chaperonin	10.5	5.57	596.92
serA	A9CFK0	0.63	D-3-phosphoglycerate dehydrogenase	56.5	5.62	472.46
gntZ	A9CIZ2	0.65	6-phosphogluconate dehydrogenase, decarboxylating	51.2	5.68	321.13
Atu4345	A9CGG8	0.67	Uncharacterized protein	17.3	5.27	285.88
fabG	A9CJ78	0.66	3-oxoacyl-(Acyl carrier protein) reductase	24.8	6.6	234.71
serS	Q8UEQ2	0.63	Serine--tRNA ligase	47.6	5.78	202.46
hutU	Q8U8Z9	0.60	Urocanate hydratase	61	6.37	199.47
ndk	Q8UGB6	0.60	Nucleoside diphosphate kinase	15.3	5.57	184.85
dapD	Q8UIC6	0.52	2,3,4,5-tetrahydropyridine-2,6-dicarboxylate N-succinyltransferase	30.5	5.57	162.66

Atu3585	Q7CSU6	0.55	Glutathione S-transferase	32.9	6.35	161.14
Atu2424	A9CHV5	0.36	ABC transporter, nucleotide binding/ATPase protein	26.5	9.39	161.1
typA	A9CHI8	0.62	GTP-binding tyrosin phosphorylated protein	66.6	5.49	130.44
Atu2053	Q7CXZ7	0.66	FAD dependent oxidoreductase	50.2	5.39	108.57
secB	Q8UJC2	0.63	Protein-export protein	17.3	4.79	106.89
Atu3493	A9CFA9	0.65	Non-heme haloperoxidase	30.3	6.47	101.48
Atu0333	A9CKD9	0.63	ABC transporter, nucleotide binding/ATPase protein	29.2	9.2	92.24
Atu0983	Q7D077	0.61	Uncharacterized protein	11	6.52	89.61
Atu1993	Q7CY44	0.57	tRNA/rRNA metyltransferase	31.8	9.2	87.29
Atu3406	Q7CSD9	0.52	Uncharacterized protein	29.6	5.53	83.27
cobW	A9CHC1	0.65	Cobalamin synthesis protein	37.2	4.82	79.81
Atu2336	A9CHZ5	0.64	Uncharacterized protein	22.6	10.1	73.55
Atu1132	A9CJG4	0.47	Glutathione S-transferase related protein	22.1	7.12	71.21
bgl	Q7CV27	0.65	Beta-glucosidase	51.3	5.67	69.01
traM	Q44452	0.50	Transcriptional repressor TraM	11.2	6.15	64.55
tgt	Q8UES8	0.60	Queuine tRNA-ribosyltransferase	41.9	6.67	62.72
minC	Q8UAW8	0.51	Probable septum site-determining protein MinC	25.7	5.38	60.51
Atu1473	A9CJ14	0.67	Uncharacterized protein	29.2	4.86	53.47
Atu2026	Q7CY17	0.64	Exodeoxyribonuclease V	42	6.47	50.76
Atu4318	Q8U7Y1	0.59	Putative D-xylulose reductase	36.8	5.67	49.03
bioA	Q7CVT0	0.49	Adenosylmethionine-8-amino-7-oxononanoate aminotransferase	50.5	6.6	43.55
Atu1856	A9CIJ1	0.66	Inositol monophosphatase family protein	29.8	4.79	41.59

pdxH	Q8UHC2	0.54	Pyridoxine/pyridoxamine 5'-phosphate oxidase	23.7	7.5	37.63
hflx	Q8U5B2	0.66	GTPase	49.3	6.13	36.57
glmS	Q8UEH1	0.65	Glutamine--fructose-6-phosphate aminotransferase [isomerizing]	66.1	5.83	31.2
gmk	Q8UGD7	0.49	Guanylate kinase	25.3	5.9	31.03
dxr	Q8UC86	0.55	1-deoxy-D-xylulose 5-phosphate reductoisomerase	42.3	5.14	29.91
Atu3026	A9CEK0	0.65	Short chain dehydrogenase	25.7	7.4	29.39
nifS	Q7CYG4	0.61	Cysteine desulfurase	44.9	6.24	27.98
Atu1827	Q8UED3	0.63	Anhydro-N-acetylmuramic acid kinase	39.3	6.25	27.58
minE	Q8UAX0	0.43	Cell division topological specificity factor	9.7	7.06	25.77
cysI	A9CJ21	0.52	Sulfite reductase (NADPH) hemoprotein beta-component	61.7	6.11	25.18
mutA	A9CFE8	0.57	Methylmalonyl-CoA mutase	77.3	5.39	24.43
bdhA	Q7CXD5	0.51	D-beta-hydroxybutyrate dehydrogenase	27.4	6.15	24.19
rfbD	A9CGW6	0.41	dTDP-4-dehydrorhamnose reductase	31.9	6.62	24.15
Atu2186	A9CI74	0.60	Transcriptional regulator, LysR family	34	6.8	22.97
aglA	A9CI23	0.47	Alpha-glucosidase	62.3	5.72	21.51
Atu3861	Q7CTH0	0.59	Acyl-CoA hydrolase	14.3	6.57	20.33
cycH	A9CJN0	0.57	CycH protein	41.9	5.21	19.65
Atu0240	A9CKI6	0.44	Uncharacterized protein	15	7.58	19.39
Atu2574	Q7CWR2	0.56	Uncharacterized protein	24.2	6.93	18.87
Atu1181	Q7CZT4	0.59	Uncharacterized protein	19.6	7.43	18.47
Atu0797	A9CJV8	0.60	Hydrolase	23.4	5.71	18.13
Atu0903	Q7D0E4	0.56	Uncharacterized protein	30.9	6.21	16.7

Atu1192	Q8U5D3	0.21	Transcriptional regulator, MarR family	17.5	9.58	16.46
Atu8198	Q8U500	0.55	Uncharacterized protein	13.6	9.2	15.98
alr	P58737	0.64	Alanine racemase, catabolic	40.6	6.23	14.64
Atu0073	Q8UJ65	0.44	DNA replication and repair protein	40.8	6.16	14.62
minD	A9CEX2	0.55	Site-determining protein	29.4	7.39	13.64
cox15	Q7CZN9	0.63	Heme A synthase	40.9	8.72	13.56
papS	Q7CXI6	0.61	Poly(A) polymerase	45.6	6.84	13.25
Atu1166	Q8UG74	0.65	Transcriptional repressor	18.2	7.77	13.02
argE	A9CF54	0.41	Acetylornithine deacetylase	39.1	5.16	12.8
glsA	Q8UEA1	0.59	Glutaminase	32.9	7.06	11.6
Atu3140	Q8UB77	0.47	Probable 5-dehydro-4-deoxyglucarate dehydratase	32.5	5.91	10.28
Atu2060	Q7CXZ0	0.56	ABC transporter, substrate binding protein (Glycine betaine)	34.1	5.24	9.83
hupX	A9CLN8	0.46	DNA binding protein	8	10.08	9.51
Atu5086	Q7D3Y2	0.59	Uncharacterized protein	52.4	6.29	9.04
Atu0300	A9CKE9	0.60	Methyltransferase	21.9	9.58	8.06
lpxK	Q8UHI5	0.63	Tetraacyldisaccharide 4'-kinase	37.7	9.45	7.25
Atu0437	A9CK99	0.62	Uncharacterized protein	25.6	6.1	5.86
lrp	Q7CSE6	0.60	Transcriptional regulator, AsnC family	18	7.37	5.71
Atu2451	A9CHU0	0.66	Uncharacterized protein	22	9.8	5.51
Atu3835	A9CFR4	0.33	Uncharacterized protein	29.6	5.2	5.36
cfa	A9CIF7	0.59	Cyclopropane-fatty-acyl-phospholipid synthase	39	6.28	5.1
Atu3527	Q7CSP4	0.44	Uncharacterized protein	30.8	5.67	5.09
Atu1766	Q7CYK9	0.47	Uncharacterized protein	8.4	10.78	5.07
Atu1814	A9CIL2	0.28	Epoxide hydrolase	38.7	6.25	4.61

Atu3392	A9CF50	0.48	Methyltransferase	30.3	7.66	4.46
Atu6113	A9CKV6	0.64	Uncharacterized protein	21	5.69	4.3
fabG	A9CL71	0.54	3-oxoacyl-(Acyl-carrier protein) reductase	25	5.43	4.11
Atu3842	A9CFR5	0.43	Uncharacterized protein	21.9	8.25	3.95
Atu1030	Q7D045	0.52	GTP pyrophosphohydrolase/synthetase, RelA/SpoT family	83.8	6.43	3.71
Atu3074	A9CEM5	0.48	Short chain dehydrogenase	26.8	5.97	3.48
ctpE	A9CKJ6	0.33	Components of type IV pilus	20.4	6.55	3.46
Atu3833	A9CFR2	0.40	Uncharacterized protein	20	5.9	3.4
Atu5199	Q7D3N8	0.58	Oxidoreductase	38.3	6.35	3.4
Atu0722	Q7D0U4	0.62	Uncharacterized protein	19	7.46	3.13
exoP	A9CFZ9	0.30	Exopolysaccharide polymerization/transport protein	86.9	6.71	2.84
Atu4375	A9CGI9	0.14	Uncharacterized protein	41.2	5.82	2.66
Atu3980	Q7CTS4	0.44	Hydrolase	25.3	6.29	2.57
kgtP	Q7CTV4	0.26	MFS permease	48.2	9.28	2.39
aat	Q8UFR8	0.55	Leucyl/phenylalanyl-tRNA--protein transferase	22.7	6.54	2.33
Atu5498	A9CL42	0.58	Oxidoreductase with iron-sulfur subunit	18.8	4.81	2.29
Atu4529	Q7CV67	0.59	Uncharacterized protein	69.7	5.22	2.28
Atu3834	A9CFR3	0.45	Uncharacterized protein	25.6	4.93	2.25
Atu4477	A9CGQ4	0.40	Transcriptional regulator, TetR family	25.3	5.69	2.24
socR	Q7D446	0.49	Santhopine-responsive transcriptional repressor	38.2	7.62	2.18
kdpB	Q8U9D9	0.35	Potassium-transporting ATPase ATP-binding subunit	72.9	5.71	2.16
Atu4238	A9CGA0	0.12	Hydrolase	30.2	5.66	2.13

dhaS	A9CLJ0	0.20	Aldehyde dehydrogenase	54.6	5.72	2.09
traA	Q7D3W2	0.33	Conjugal transfer protein	171.1	8.9	2.04
mutS	Q8UIF2	0.13	DNA mismatch repair protein	98.1	5.63	1.97
Atu0215	A9CKJ9	0.66	Uncharacterized protein	29.7	9.48	1.95
apaG	Q8UI68	0.31	Protein ApaG	14.7	4.34	1.93
Atu0570	Q7D176	0.20	Chemotaxis protein	45.6	5.6	1.93
pssN	Q7CS19	0.45	Exopolysaccharide export protein	42.5	7.33	1.9
Atu4122	A9CG37	0.31	Transcriptional regulator, LysR family	34.7	8.19	1.79
rpoN	Q8U5M8	0.22	RNA polymerase sigma-54 factor	56.7	4.86	1.64
Atu0869	A9CJT2	0.67	Uncharacterized protein	13.2	5.39	0
Atu2320	A9CI06	0.48	Transcriptional regulator, TetR family	21.1	6.95	0

Protein	Accession	FC = M (L) / WT (L)	Function	MW [kDa]	calc. pI	Score Sequest
Up-regulated						
Atu2469	A9CHT0	2.04	Uncharacterized protein	32.4	5.24	603.99
ileS	Q8UHJ6	1.58	Isoleucine--tRNA ligase	108.4	5.66	508.79
Atu5296	A9CLE5	3.44	Arylester hydrolase	32.6	6.96	455.2
frcB	A9CKR7	1.57	ABC transporter, substrate binding protein (Sugar)	35.2	5.29	384.91
dctP	A9CLG5	3.81	ABC transporter, substrate binding protein	40.4	6.8	324.49
rplA	Q8UE05	1.85	50S ribosomal protein L1	24.2	9.45	285.33
Atu5118	A9CLN0	2.20	Aminotransferase, class II	44.8	7.02	262.52
Atu3891	A9CFT2	1.51	Uncharacterized protein	63.9	5.94	246.7

rplJ	Q8UE06	1.84	50S ribosomal protein L10	18.2	9.61	223.78
trpE(G)	A9CI26	1.67	Anthranilate synthase component I and II	80.5	5.86	221.22
rpmE	Q8U9I5	1.62	50S ribosomal protein L31	8.1	8.56	220.9
fixP	A9CIY8	1.86	Cbb3-type cytochrome c oxidase subunit	30.9	4.88	214.71
Atu3372	A9CF36	1.56	ABC transporter, substrate binding protein (Sugar)	32.8	4.98	206.39
rpsJ	Q8UE17	1.81	30S ribosomal protein S10	11.5	10.18	201.13
ilvI	Q7CY08	2.04	Acetolactate synthase	65.4	5.88	198.66
Atu5117	Q7D3V8	2.00	Uncharacterized protein	36	6.71	198.54
ugpB	Q8UB32	1.61	sn-glycerol-3-phosphate-binding periplasmic protein	47.2	6.71	187.72
Atu0946	A9CJP4	3.04	Dehydrogenase	39.5	5.47	173.94
hflK	Q7CY01	1.54	Protein HflK	40.2	5	126.08
rplL	Q8UE07	1.74	50S ribosomal protein L7/L12	12.7	4.86	125.18
clpP	Q8UD57	2.07	ATP-dependent Clp protease proteolytic subunit 3	22.3	5.49	122.31
rplD	Q8UE19	1.88	50S ribosomal protein L4	22.4	10.26	119.88
Atu3772	A9CFM5	1.80	Uncharacterized protein	37.6	5.62	119.75
Atu5287	A9CLF0	3.54	Uncharacterized protein	19.9	4.89	119.67
xylF	A9CFE7	1.73	ABC transporter, substrate binding protein (Xylose)	36	6.33	117.24
rpsE	Q8UE35	1.91	30S ribosomal protein S5	20.5	10.52	113.25
rplM	Q8UFZ7	1.60	50S ribosomal protein L13	17.3	10.13	104.23
Atu4577	Q7CVB1	1.64	ABC transporter, substrate binding protein	35.3	5.02	102.42

Atu3253	A9CEX5	1.56	ABC transporter, substrate binding protein	36	7.18	101.69
Atu1971	Q7CY63	2.05	Uncharacterized protein	15.9	9.11	101.27
Atu1885	A9CIH8	1.52	Transcriptional regulator, AsnC family	18.7	6.24	100.82
rnpO	Q8UGK8	1.61	DNA-directed RNA polymerase subunit omega	14.3	4.26	95.28
Atu2656	Q7CWJ5	1.74	Uncharacterized protein	58.6	7.97	94.4
Atu5297	A9CLE4	1.58	Hydrolase	34.6	6.67	90.64
hemH	Q8U9F7	1.60	Ferrochelatase	39.4	6.8	81.2
dnaJ	P50018	1.83	Chaperone protein	40.9	7.59	77.27
Atu2014	A9CIE2	1.56	ABC transporter, substrate binding protein	34.5	6.05	73.8
rplC	Q8UE18	1.77	50S ribosomal protein L3	22.6	10.35	73.56
atpH	Q7CWL8	1.85	ATP synthase subunit delta	19.8	5.66	73.35
rpmA	Q8UBR6	2.55	50S ribosomal protein L27	9.4	11.03	67.42
Atu5336	Q7D3B8	2.92	Uncharacterized protein	12.3	4.59	63.71
Atu4744	A9CH25	1.67	ABC transporter, substrate binding protein (Sugar)	29.9	5.78	62.99
gyrB	A9CKT5	1.61	DNA gyrase subunit B	88.8	5.77	61.26
Atu3151	A9CER5	1.53	ABC transporter, substrate binding protein (Sugar)	45.5	4.82	54.3
glnA	Q7D146	1.61	Glutamine synthetase	53.1	5.33	52.87
Atu0008	Q7D2D0	1.94	Uncharacterized protein	24.2	4.94	52.09
yidC	Q8UIB3	1.94	Membrane protein insertase	67.1	7.64	51.61
rpsI	Q8UFZ8	2.43	30S ribosomal protein S9	16.7	11.21	51.1
rpmI	Q8UIN8	2.40	50S ribosomal protein L35	7.3	11.25	43.36
rpmF	Q8UJ26	2.42	50S ribosomal protein L32	6.9	10.73	42.86
Atu1222	A9CJC7	1.81	Uncharacterized protein	27.3	10.1	41.2

traC	A9CLN4	2.00	Conjugal transfer protein	10.3	6.13	40.32
Atu5265	A9CLG7	1.71	Sugar binding protein	46.2	4.75	39.78
fixN	Q7CZ11	2.01	Cytochrome-c oxidase, FixN chain	60.8	8.84	36.9
Atu5281	A9CLF3	2.06	Uncharacterized protein	8.5	6.11	36.57
yajC	A9CIX5	2.99	Preprotein tranlocase protein	12.6	9.13	36.43
Atu5288	A9CLE9	2.22	Uncharacterized protein	14.3	8.37	33.24
blcC	Q7D3U0	1.52	N-acyl homoserine lactonase AttM	29.3	6.21	31.92
rluB	A9CK15	1.85	Pseudouridine synthase	72.5	10.26	30.27
avhB10	Q7D3R3	2.01	Type IV secretion protein AvhB10	42.7	5.69	28.28
Atu5270	A9CLG3	2.02	Permease component of C4 dicarboxylate transporter	19.9	7.97	24.93
rpmG	Q8UFU8	1.95	50S ribosomal protein L33	6.3	10.07	24.52
Atu5359	Q8UJW6	3.26	UPF0339 protein Atu5359	6.9	9.13	21.92
ctpA	Q7D1X1	1.53	Components of type IV pilus, pilin subunit	6.4	9.25	19.89
secG	Q7CYV5	1.50	Protein-export membrane protein SECG	15.3	9	19.37
Atu5299	A9CLE3	1.60	Uncharacterized protein	40.2	7.14	17.31
deaD	A9CG67	1.51	Cold-shock dead-box protein A	67.9	9.03	16.24
Atu5383	Q8U5S9	1.66	Transcriptional regulator, TetR family	22.5	6.4	12.97
Atu0643	Q7D114	2.15	Uncharacterized protein	68.4	8.53	12.8
Atu4600	A9CGV8	2.24	ABC transporter, nucleotide binding/ATPase protein	64	8.5	12.23
Atu8099	Q8U5X6	2.21	Uncharacterized protein	6.6	9.63	11.47
Atu5212	Q7D3M5	1.64	Uncharacterized protein	24.4	7.06	11.32

Atu3641	A9CFH3	2.07	Uncharacterized protein	41.7	5.12	11.06
cyoC	A9CKN5	2.39	Cytochrome o ubiquinol oxidase subunit III	23	6.6	10.96
soxD	A9CG07	2.34	Sarcosine oxidase delta subunit	11.9	5.27	10.86
nuoA	A9CJB3	1.94	NADH-quinone oxidoreductase subunit A	13.7	4.56	10.49
nuoL	A9CJA3	2.29	NADH ubiquinone oxidoreductase chain L	73.2	7.77	10.41
nuoM	A9CJA2	2.76	NADH dehydrogenase I chain M	55.4	7.5	8.35
avhB7	Q7D3R6	1.52	Type IV secretion protein AvhB7	9.7	7.08	8.06
aroQ	Q8UFR5	1.53	3-dehydroquinate dehydratase 1	15.6	6.95	7.54
impM	Q7CUN2	1.65	Serine/threonine phosphoprotein phosphatase	51.7	6.86	7.32
Atu0638	A9CK42	1.74	Uncharacterized protein	7.3	9.17	7.21
Atu5343	A9CLC1	2.04	ABC transporter, substrate binding protein (Oligopeptide)	56.8	6.34	7.2
dfp	Q7D1P8	1.75	Coenzyme A biosynthesis bifunctional protein CoaBC	42.3	6.9	6.41
napE	A9CGL2	2.36	Periplasmic nitrate reductase protein	6.6	9.54	6.29
Atu5278	A9CLF5	2.47	Uncharacterized protein	18.3	5.67	6.23
Atu2286	A9CI29	4.03	UPF0114 protein	19.3	5.96	5.79
Atu3758	Q8U9H0	2.37	UPF0335 protein	9.7	4.86	5.79
Atu3763	Q7CT90	2.13	Uncharacterized protein	61.4	9.1	5.61
Atu0730	Q7D0T7	1.60	Uncharacterized protein	19.7	9.79	5.31
Atu5039	A9CLS2	1.68	Uncharacterized protein	44.3	6.47	5.24

Atu8206	Q8U5T0	3.22	Uncharacterized protein	10.3	9.74	4.39
panB	Q8UA91	1.80	3-methyl-2-oxobutanoate hydroxymethyltransferase	29.7	6.34	4.06
Atu1967	Q7CY65	2.46	Uncharacterized protein	22.5	5.73	3.99
ureB	Q8UCS8	2.18	Urease subunit beta	11.1	8.59	3.96
Atu2352	A9CHY7	1.68	Uncharacterized protein	9.4	5.01	3.67
hutH	A9CFP1	1.51	Histidine ammonia-lyase	52.4	5.72	3.63
aglG	A9CK58	1.84	ABC transporter, membrane spanning protein	41.6	9.19	2.78
proX	A9CLJ7	2.26	ABC transporter, nucleotide binding/ATPase protein (Glycine betaine/L-proline)	37	5.95	2.64
Atu1107	A9CJH1	2.44	Uncharacterized protein	39.5	9.52	2.55
Atu4602	Q7CVD5	2.19	IS 426 transposase	14.8	9.8	2.44
dgk	A9CIH6	1.76	Diacylglycerol kinase	14.8	7.52	2.38
Atu5269	A9CLG4	2.51	Permease component of C4 dicarboxylate transporter	51.8	8.72	2.25
mtbA	Q7CWX7	1.62	MFS permease	65.6	8.88	1.91
Atu0925	Q8UGW0	2.13	Uncharacterized protein	19.9	5.54	1.89
exoX	Q7CTZ5	1.65	Exopolysaccharide production repressor protein	10.3	9.31	1.88
Atu8036	Q8U4Y5	2.60	Protein YBGT-related protein	4.7	5.02	0
mnhF	A9CJQ9	2.00	Na+/H+ antiporter	13.8	10.43	0
Down-regulated						
glyA	Q8UG75	0.63	Serine hydroxymethyltransferase 1	46.5	6.55	666.08
groES	P30780	0.49	10 kDa chaperonin	10.5	5.57	596.92

serC	A9CFK1	0.61	Phosphoserine aminotransferase	42.5	5.68	524.46
greA	Q8UDE5	0.53	Transcription elongation factor	17.3	4.92	323.06
Atu4345	A9CGG8	0.59	Uncharacterized protein	17.3	5.27	285.88
Atu4610	A9CGW4	0.63	Sugar nucleotide epimerase/dehydratase	38.5	6.61	254.68
kdgA	Q7CV35	0.59	Keto-hydroxyglutarate-aldolase/keto-deoxy-phosphogluconate aldolase	21.5	5.63	251.66
adh	Q7CY20	0.57	NADP-dependent alcohol dehydrogenase	37.6	5.64	246.09
cysK	A9CKE4	0.61	Cysteine synthase	33.6	5.83	245.06
aspB	Q7D196	0.61	Aminotransferase	42.3	5.35	234.85
fabG	A9CJ78	0.66	3-oxoacyl-(Acyl carrier protein) reductase	24.8	6.6	234.71
sodBI	A9CJS9	0.62	Superoxide dismutase	22.6	6.1	207.04
hpcE	A9CKT3	0.60	2-hydroxyhepta-2,4-diene-1,7-dioate isomerase	29.7	5.36	204.23
hutU	Q8U8Z9	0.66	Urocanate hydratase	61	6.37	199.47
ndk	Q8UGB6	0.64	Nucleoside diphosphate kinase	15.3	5.57	184.85
prfC	A9CKE3	0.65	Peptide chain release factor 3	58.8	5.68	182.31
Atu1093	Q7D001	0.61	Aldo/keto reductase	37.8	5.85	165.46
dapD	Q8UIC6	0.65	2,3,4,5-tetrahydropyridine-2,6-dicarboxylate N-succinyltransferase	30.5	5.57	162.66
Atu2424	A9CHV5	0.28	ABC transporter, nucleotide binding/ATPase protein	26.5	9.39	161.1
lysA	A9CFF5	0.65	Diaminopimelate decarboxylase	45.6	6.05	160.84
Atu2455	Q8UCM8	0.57	Uracil-DNA glycosylase	26.7	7.11	157.55
scrK	Q7D1J1	0.62	Fructokinase	32.8	5.64	157.3

rsmC	Q7D284	0.65	Ribosomal RNA small subunit methyltransferase	36.6	6.57	155.2
rfbA	Q7CVE5	0.66	Glucose-1-phosphate thymidylyltransferase	31.5	5.49	143.29
Atu3982	A9CFW6	0.57	Uncharacterized protein	72.7	6.15	138.69
Atu4347	Q7CUP8	0.63	Uncharacterized protein	18.3	8.88	133.4
hpt	A9CFF7	0.64	Hypoxanthine phosphoribosyltransferase	19.8	5.19	130.98
gst	A9CJU4	0.56	Glutathione-S-transferase	24.1	6.39	126.59
queA	Q8UES7	0.52	S-adenosylmethionine: tRNA ribosyltransferase-isomerase	40.7	5.59	111.46
Atu1136	A9CJG2	0.65	Reductase	78.3	6.51	108.5
secB	Q8UJC2	0.66	Protein-export protein SecB	17.3	4.79	106.89
bcp	A9CIK6	0.63	Bacterioferritin comigratory protein	16.7	6.8	101.57
Atu3493	A9CFA9	0.66	Non-heme haloperoxidase	30.3	6.47	101.48
Atu2761	A9CHD9	0.67	Exodeoxyribonuclease III	30.6	8.28	94.56
hutI	Q8U8Z6	0.67	Imidazolonepropionase	44.4	5.26	94.07
Atu0211	A9CKK1	0.61	Uncharacterized protein	31.2	5.57	93.26
Atu3331	A9CF08	0.65	Uncharacterized protein	28.4	8.37	91.74
Atu0983	Q7D077	0.61	Uncharacterized protein	11	6.52	89.61
Atu3726	A9CFK5	0.67	Flavin dependant oxidoreductase	36.6	6.27	87.35
fabZ	A9CIV8	0.62	(3R)-Hydroxymyristoyl-(Acyl carrier protein)-Dehydratase	17.1	5.54	87.11
Atu2144	A9CI91	0.65	Uncharacterized protein	28	5.6	84.42
Atu3406	Q7CSD9	0.41	Uncharacterized protein	29.6	5.53	83.27
glpK	Q8U940	0.65	Glycerol kinase	54.6	5.54	82.4
Atu0813	A9CJV2	0.62	Uncharacterized protein	14.7	9.52	78

Atu2336	A9CHZ5	0.66	Uncharacterized protein	22.6	10.1	73.55
traM	Q44452	0.32	Transcriptional repressor	11.2	6.15	64.55
Atu4121	Q7CU40	0.65	Monooxygenase	37.8	5.59	64.32
tgt	Q8UES8	0.62	Queuine tRNA-ribosyltransferase	41.9	6.67	62.72
minC	Q8UAW8	0.59	Probable septum site-determining protein	25.7	5.38	60.51
Atu0690	A9CK14	0.58	Uncharacterized protein	20.2	7.14	58.86
Atu2614	A9CHK6	0.64	Uncharacterized protein	8.2	9.33	57.14
Atu1372	A9CJ63	0.53	Uncharacterized protein	16.2	5.48	57
kdgK	Q7CXE6	0.65	2-dehydro-3-deoxygluconokinase	31.4	5.4	55.08
blcR	Q7D3U3	0.65	Transcriptional repressor of the blcABC operon	29.7	6.54	52.64
Atu4019	A9CFY5	0.64	Two component response regulator	23.9	5.85	49.9
recR	Q8UJ45	0.66	Recombination protein	21.3	6.68	49.33
Atu5430	A9CL77	0.63	Uncharacterized protein	15.5	4.91	48.21
Atu1441	A9CJ27	0.56	Uncharacterized protein	17.6	6.8	45.59
bioA	Q7CVT0	0.66	Adenosylmethionine-8-amino-7-oxononanoate aminotransferase	50.5	6.6	43.55
gidB	Q8UBM1	0.61	Ribosomal RNA small subunit methyltransferase G	23	8.63	42.93
Atu1325	A9CJ86	0.64	Acetyltransferase	18.4	5.63	42.14
hadL	Q7CSD8	0.63	Haloalkanoic acid dehalogenase	24.9	6.21	41.87
Atu0479	Q7D1E1	0.67	ABC transporter, substrate binding protein (Amino acid)	27.7	5.36	32.42
Atu1989	Q7CY46	0.57	Two component response regulator	16.7	5.05	31.72

gmk	Q8UGD7	0.60	Guanylate kinase	25.3	5.9	31.03
gidA	Q8UET6	0.63	Methylenetetrahydrofolate --tRNA-(uracil-5-)-methyltransferase	51.8	5.81	30.77
dxr	Q8UC86	0.63	1-deoxy-D-xylulose 5-phosphate reductoisomerase	42.3	5.14	29.91
rluA	A9CFZ5	0.64	Ribosomal large subunit pseudouridine synthase A	24.8	8.19	29.73
Atu3409	A9CF60	0.58	ABC transporter, substrate binding protein (Oligopeptide)	57.9	7.56	29.41
Atu3026	A9CEK0	0.59	Short chain dehydrogenase	25.7	7.4	29.39
Atu3407	A9CF58	0.48	Aminotransferase, class III	48.8	6.06	28.66
ordL	A9CHN2	0.66	Oxidoreductase	45.9	6.62	28.02
nifS	Q7CYG4	0.54	Cysteine desulfurase	44.9	6.24	27.98
rctA	A9CLM1	0.47	Transcriptional regulator protein	13.1	9.52	27.15
murI	Q8UE93	0.61	Glutamate racemase	30	5.39	26.09
lspL	A9CG55	0.57	UDP-glucuronic acid epimerase	37.4	6.7	25.77
minE	Q8UAX0	0.58	Cell division topological specificity factor	9.7	7.06	25.77
Atu0397	Q7D1J3	0.61	Uncharacterized protein	47.6	9.06	25.58
Atu0606	Q7D143	0.47	Uncharacterized protein	9.1	7.66	24.68
Atu5487	Q7D2Y6	0.61	Uncharacterized protein	11.6	4.46	24.25
rfbD	A9CGW6	0.57	dTDP-4-dehydrorhamnose reductase	31.9	6.62	24.15
Atu3908	Q7CTL4	0.63	Transcriptional regulator, GntR family	24.8	6.81	23.65
metA	Q7CWE8	0.65	Homoserine O-acetyltransferase	35.7	6.05	22.11
aglA	A9CI23	0.57	Alpha-glucosidase	62.3	5.72	21.51

phoB	A9CKA3	0.62	Two component response regulator	26	6.43	21.01
Atu1343	Q7CZG7	0.44	Uncharacterized protein	16.8	6.27	20.86
Atu2275	A9CI35	0.59	Uncharacterized protein	15.3	5.17	20.37
uxuA	Q8UA46	0.60	Mannonate dehydratase 2	43.6	5.77	20.33
Atu3861	Q7CTH0	0.64	Acyl-CoA hydrolase	14.3	6.57	20.33
Atu0781	Q8UHA2	0.67	UPF0301 protein	21.9	4.92	19.88
Atu0240	A9CKI6	0.65	Uncharacterized protein	15	7.58	19.39
Atu5516	A9CL33	0.60	Uncharacterized protein	50.7	5.52	19.34
myg1	A9CFP3	0.63	Uncharacterized protein	33.9	5.33	18.7
nasT	Q7CTL3	0.67	Two component response regulator	21.8	5.74	18.63
rluD	Q7CX17	0.31	Pseudouridine synthase	37.5	6.07	18.62
Atu0792	A9CJW1	0.63	Uncharacterized protein	16.8	8.27	18.61
Atu2331	A9CHZ9	0.55	Uncharacterized protein	28	5.57	18.37
Atu4270	Q7CUH6	0.61	Uncharacterized protein	22.3	5.03	18.37
Atu1626	A9CIU6	0.63	NAD dependent epimerase/dehydratase family protein	32	6.33	18.36
dacF	Q7CSY9	0.64	Penicillin-binding protein dacf	41	9.7	17.88
Atu2811	Q7CW73	0.64	Uncharacterized protein	44.8	5.38	17.67
Atu1192	Q8U5D3	0.29	Transcriptional regulator, MarR family	17.5	9.58	16.46
Atu2673	Q7CWI1	0.60	Dual-specificity RNA methyltransferase RlmN	45.3	7.28	15.94
Atu4503	A9CGR4	0.61	Creatinine amidohydrolase	28.9	6.21	15.81
Atu3054	Q7CRH0	0.65	Uncharacterized protein	42.9	7.15	15.8
Atu0292	A9CKF3	0.65	Iron-sulfur cluster binding protein	36.2	6.46	15.53
rbsB	A9CKY3	0.64	ABC transporter, substrate binding protein (Ribose)	45.9	8.12	15.38

Atu0864	A9CJT4	0.65	Oxidoreductase	27	5.41	14.84
alr	P58737	0.67	Alanine racemase, catabolic	40.6	6.23	14.64
zur	A9CIZ4	0.62	Ferric uptake regulation protein	15.4	6.7	13.84
minD	A9CEX2	0.43	Site-determining protein	29.4	7.39	13.64
Atu0011	A9CKT6	0.64	Transcriptional regulator	13.4	8.15	13.25
Atu0907	A9CJR4	0.65	Phosphinothricin acetyltransferase	18.4	6.42	13.07
Atu2734	A9CHF9	0.67	Dehydrogenase	38.7	5.59	12.9
argE	A9CF54	0.39	Acetylornithine deacetylase	39.1	5.16	12.8
Atu2343	A9CHY9	0.66	Acetyltransferase	16.5	6.57	12.55
pcaR	Q7CV82	0.63	Transcriptional regulator, IclR family	27.4	7.12	12.47
Atu0796	Q7D0N2	0.55	Putative peptidase	26.7	7.62	12.45
Atu3164	A9CES4	0.41	Dehydrogenase	26.7	6.35	11.69
Atu5489	Q8UJI8	0.64	Uncharacterized protein	8.5	7.5	10.9
dnaJ	A9CIE5	0.64	Molecular chaperone, DnaJ family	22.7	5.3	10.57
sodBII	Q7CVB7	0.67	Superoxide dismutase	22.3	6.07	10.38
Atu4674	Q7CVJ9	0.47	Transcriptional regulator, GntR family	26.4	6.55	10.37
Atu0949	A9CJP3	0.63	Uncharacterized protein	29.4	5.35	10.21
Atu4416	A9CGL7	0.55	Phosphopantetheinyl transferase	25.7	6.06	10.05
Atu0072	A9CKR2	0.47	Uncharacterized protein	44.5	9.07	9.98
Atu2060	Q7CXZ0	0.51	ABC transporter, substrate binding protein (Glycine betaine)	34.1	5.24	9.83
aceA	A9CK53	0.61	Isocitrate lyase	46.8	6.16	9.42

Atu6117	A9CKV3	0.65	NTP pyrophosphohydrolase, MutT family	18	6.09	9.23
Atu4301	A9CGE2	0.50	Uncharacterized protein	26.8	6.42	9.1
attH	Q7D3U4	0.65	Uncharacterized protein	39.1	5.44	8.99
truA	Q8UIC9	0.64	tRNA pseudouridine synthase A	29.9	7.06	8.95
aroE	A9CGT0	0.64	Shikimate dehydrogenase (NADP(+))	31.3	6.6	8.47
gltX	A9CFE9	0.63	Glutamyl-tRNA Synthetase	33.2	6.2	8.32
Atu5064	Q7D402	0.66	Transcriptional regulator, MarR family	16.7	8.48	8.17
Atu1554	Q8UF45	0.67	Uncharacterized protein	6.9	7.36	7.34
Atu4874	A9CH98	0.61	Uncharacterized protein	16.2	4.88	6.78
Atu8154	Q8U5C1	0.52	Plasmid stabilization system protein	14	9.09	6.78
fadD	A9CIS6	0.43	Long-chain fatty acid-CoA ligase	55.3	6.61	6.26
Atu4141	Q7CU59	0.67	Uncharacterized protein	16	5.16	6.06
Atu4555	Q7CV91	0.54	Uncharacterized protein	27.8	5.16	5.9
Atu0675	A9CK21	0.67	Uncharacterized protein	8.9	5.07	5.83
ruvC	Q8U9K4	0.59	Crossover junction endodeoxyribonuclease	18.2	8.88	5.83
ipk	Q8UHP8	0.58	4-diphosphocytidyl-2-C-methyl-D-erythritol kinase	31.8	6.54	5.58
hemO	Q7CWX1	0.59	Heme oxygenase	22.3	5.21	5.55
Atu2451	A9CHU0	0.56	Uncharacterized protein	22	9.8	5.51
Atu3835	A9CFR4	0.21	Uncharacterized protein	29.6	5.2	5.36
nusG	Q7D1F8	0.60	Transcription antitermination protein	20.4	8.02	5.31
amaB	Q7CRI5	0.51	N-carbamoyl-beta-alanine amidohydrolase	44.6	4.96	5.25

Atu4384	A9CGJ5	0.52	Uncharacterized protein	19.5	4.73	5.07
Atu0839	Q7D0K2	0.53	Uncharacterized protein	36.2	6.47	4.95
Atu1059	A9CJI9	0.59	Putative SOS response-associated peptidase	28	6.13	4.86
Atu1814	A9CIL2	0.61	Epoxide hydrolase	38.7	6.25	4.61
nwsB	A9CJG9	0.65	Two component response regulator	21.9	5.85	4.56
Atu5188	Q7D3P9	0.64	Zinc-binding dehydrogenase	35.2	6.54	4.54
Atu3798	Q7CTC0	0.59	Transcriptional regulator, TetR family	23.4	8.85	4.53
bme3	Q7CVX9	0.33	Uncharacterized protein	46.3	9.42	4.53
Atu2466	Q7CWZ7	0.49	Two component response regulator	24.7	5.27	4.46
Atu0636	Q7D120	0.64	Uncharacterized protein	25.4	6.43	4.46
Atu4131	A9CG46	0.26	Hydroxybutyrate dehydrogenase	27.7	6.37	4.42
Atu2660	Q8UC38	0.58	UPF0235 protein	12.2	8.7	4.25
Atu1439	Q7CZ90	0.64	Uncharacterized protein	10.2	7.93	4.04
Atu1114	Q7CZY6	0.56	GGDEF family protein	71.3	6.86	4.01
Atu4398	A9CGK5	0.52	Uncharacterized protein	33.9	6.32	3.9
ocd	P09773	0.62	Ornithine cyclodeaminase	39	5.48	3.86
Atu3117	A9CEP8	0.56	Uncharacterized protein	42.6	5.85	3.84
Atu1553	A9CIX8	0.66	Uncharacterized protein	16.1	5.6	3.79
Atu4378	Q7CUS8	0.62	Uncharacterized protein	20.1	5.64	3.63
Atu3074	A9CEM5	0.56	Short chain dehydrogenase	26.8	5.97	3.48
ctpE	A9CKJ6	0.54	Components of type IV pilus	20.4	6.55	3.46
Atu5199	Q7D3N8	0.50	Oxidoreductase	38.3	6.35	3.4
Atu1326	A9CJ85	0.63	Acetyltransferase	17.2	6.95	3.22
moaA	Q8UER0	0.61	GTP 3',8-cyclase	39	7.11	3.17

Atu1872	A9CII6	0.49	Uncharacterized protein	14.8	5.31	3
nadD	Q8UBS2	0.50	Probable nicotinate-nucleotide adenylyltransferase	20.9	9.99	2.91
Atu3620	A9CFG5	0.57	Uncharacterized protein	36.6	5.58	2.77
speF	Q7CRV2	0.61	Ornithine decarboxylase	41.1	5.59	2.47
Atu1617	A9CIV0	0.66	Uncharacterized protein	33.4	8.72	2.27
Atu4420	Q7CUW8	0.57	Transcriptional regulator, LacI family	36.6	6.01	2.26
Atu2342	A9CHZ0	0.34	Uncharacterized protein	19.4	6.19	2.24
Atu5181	A9CLL6	0.56	Short chain dehydrogenase	25.1	5.29	2.11
deoR	A9CH78	0.49	Transcriptional regulator, DeoR family	26.5	6.99	2.01
Atu0215	A9CKJ9	0.38	Uncharacterized protein	29.7	9.48	1.95
Atu1819	A9CIL0	0.63	Uncharacterized protein	13.5	4.88	1.89
Atu0024	A9CKS9	0.47	Uncharacterized protein	115.9	5.52	1.85
Atu4122	A9CG37	0.45	Transcriptional regulator, LysR family	34.7	8.19	1.79
exsB	Q8UAM7	0.48	7-cyano-7-deazaguanine synthase	25.3	5.8	1.71
cbiP	Q8UBP3	0.37	Cobyric acid synthase	51.2	5.33	1.64
Atu3400	A9CF55	0.36	Uncharacterized protein	13	6.11	1.6
Atu3108	A9CEP3	0.66	Uncharacterized protein	69.2	6.62	0
int	Q8UG48	0.36	Phage-related integrase	43	9.16	0
Atu4867	A9CH92	0.57	Uncharacterized protein	20	6.34	0
Atu2524	A9CHP6	0.16	Uncharacterized protein	88	9.47	0
Atu2525	Q7CWU9	0.32	MFS permease	47.3	9.95	0
Atu1460	A9CJ19	0.56	Uncharacterized protein	17.5	10.9	0

Protein	Accession	FC = M (L) / M (D)	Function	MW [kDa]	calc. pI	Score Sequest
Up-regulated						
Atu1132	A9CJG4	1.59	Glutathione S-transferase related protein	22.1	7.12	71.21
Atu0436	A9CKA0	2.07	DNA helicase	80	5.69	69.4
bdhA	Q7CXD5	1.59	D-beta-hydroxybutyrate dehydrogenase	27.4	6.15	24.19
dapA	A9CHR2	1.55	Dihydrodipicolinate synthase	31.2	5.73	20.64
cycH	A9CJN0	1.58	CycH protein	41.9	5.21	19.65
fdhF	Q7CVN2	1.58	Formate dehydrogenase alpha subunit	105.2	5.87	17.35
ggt	A9CH16	4.21	Gamma-glutamyltranspeptidase	64.4	6	16.52
Atu0073	Q8UJ65	1.64	DNA replication and repair protein	40.8	6.16	14.62
Atu3572	A9CFE4	2.00	Transcriptional regulator	15.1	10.1	14.57
papS	Q7CXI6	1.59	Poly(A) polymerase	45.6	6.84	13.25
Atu4763	A9CH37	2.66	Transcriptional regulator, AsnC family	17.7	7.2	11.48
Atu0376	A9CKC2	2.11	Uncharacterized protein	9.5	5.15	11.38
Atu4674	Q7CVJ9	1.69	Transcriptional regulator, GntR family	26.4	6.55	10.37
Atu3140	Q8UB77	1.60	Probable 5-dehydro-4-deoxyglucarate dehydratase	32.5	5.91	10.28
Atu0300	A9CKE9	1.61	Methyltransferase	21.9	9.58	8.06
Atu0638	A9CK42	1.63	Uncharacterized protein	7.3	9.17	7.21
Atu1848	A9CIJ5	1.78	Transcriptional regulator, GntR family	51.5	5.66	7.02
Atu1814	A9CIL2	1.87	Epoxide hydrolase	38.7	6.25	4.61

fabG	A9CL71	1.55	3-oxoacyl-(Acyl-carrier protein) reductase	25	5.43	4.11
Atu1030	Q7D045	1.52	GTP pyrophosphohydrolase/synthetase, RelA/SpoT family	83.8	6.43	3.71
kdgR	A9CGQ1	2.28	Transcriptional regulator	28	6.7	3.58
Atu3147	A9CER3	3.33	Oxidoreductase	72.9	6	3.18
Atu3834	A9CFR3	1.73	Uncharacterized protein	25.6	4.93	2.25
Atu5181	A9CLL6	2.07	Short chain dehydrogenase	25.1	5.29	2.11
mutS	Q8UIF2	2.47	DNA mismatch repair protein	98.1	5.63	1.97
apaG	Q8UI68	2.27	Protein ApaG	14.7	4.34	1.93
Down-regulated						
Atu1475	A9CJ12	0.63	Uncharacterized protein	14.3	4.82	20
Atu3164	A9CES4	0.62	Dehydrogenase	26.7	6.35	11.69
ipk	Q8UHP8	0.59	4-diphosphocytidyl-2-C-methyl-D-erythritol kinase	31.8	6.54	5.58
Atu2342	A9CHZ0	0.54	Uncharacterized protein	19.4	6.19	2.24

Acknowledgement

I would like to thank my supervisor Prof. Dr. Tilman Lamparter for providing support and encouragement. For the topic selection of my Ph.D thesis, the progress of the experiment and the writing of the thesis, he provided a lot of help. His meticulous and diligent work attitudes deeply influence me. Whenever I have an experimental question to ask him, he can patiently explain. In the past four years, I have learned a lot from him, especially in terms of learning and being a nice person, which has benefited me a lot. These laid a solid foundation for my future life. On the completion of my thesis, I would like to express my heartfelt gratitude and most sincere respect to him.

Thanks to Dr. Norbert Krauß, Gero Kaeser, Afaf El Kurdi, Nadja Wunsch, Elisabetha Averbukh, Dr. Hongju Ma, Anja Kohler, Katharina Thoulass, Anna-Luise Kuppinger, Dr. Arin Ali, Prof. Dr. Reinhard Fischer for help. In addition, I am especially grateful to my parents, old sister, brother-in-law and girlfriend (Yuanyuan Ma) for their support and help in my study and life over the past four years.

Thanks to all the teachers, classmates, family and friends who have cared and helped me. Finally, I am especially grateful to the China Scholarship Council for my financial support.